THE REQUIREMENT FOR β1-INTEGRIN IN THE MUSCLE STEM CELL NICHE

By

Michelle Rozo

A dissertation submitted to The Johns Hopkins University in conformity with the requirements for the degree of Doctor of Philosophy

Baltimore, Maryland
May 1, 2015

ABSTRACT

Interactions between stem cells and their microenvironment, or niche, are essential for their maintenance and function. The adult muscle stem cell, i.e. the satellite cell (SC), is maintained in a quiescent state. Muscle damage, followed by release of numerous factors including fibroblast growth factor (FGF), leads to SC activation for muscle regeneration. Aged SCs have reduced regeneration capacity as they are insensitive to FGF for self-renewal, but what underlies this defect is unknown.

Utilizing a satellite cell specific Cre/loxP drive to ablate β1-integrin specifically in the adult SC, I show that β1-integrin is the sensor of the SC niche. β1-integrin deficient young SCs lose their quiescence and their ability to sustain muscle regeneration. Here I describe a phenotype reminiscent of the $Pax7^{-/-}$ mice, demonstrating the importance for β1-integrin in maintaining the stem cell fate. Satellite cells that have lost integrin commit to differentiation at the expense of renewal, and secondarily are deficient in fusion.

Interestingly, these properties are reminiscent of aged SCs. Noting these similarities, I further investigated the β1-integrin activity and function in aged satellite cells. I show that aged SCs display aberrant patterns of active β1-integrin and its effectors, revealing their dysregulation. By enhancing β1-integrin activation in aged SCs, self-renewal is restored by rescuing sensitivity to FGF *in vitro* and muscle regenerative capacity *in vivo*. These results show β1-integrin senses the SC niche to maintain responsiveness to FGF, and provides potential therapeutics for age-related muscle decline.

Advisor: Chen-Ming Fan, Ph.D.
Second Reader: Yixian Zheng, Ph.D.

ACKNOWLEDGEMENTS

First and foremost, I would like to thank Dr. Chen-Ming Fan. Under his guidance and tutelage, I have learned how to be critical of my data, how to design experiments, and how to constantly strive for knowledge and insight, as these make the best weapons against formidable opponents. Most importantly, I have gained confidence in my self: my opinion, my abilities, and my potential, through the balance of his criticism and approval. Above all, I immensely appreciate his understanding. First, of my ambition to leave academia, which he honored and supported throughout my graduate career. Second, and perhaps, more significantly, of the external challenges that I encountered during the last five years. There were many moments where the culmination of this journey seemed unobtainable, and it is only with his support that I was able to persevere.

Next, I would like to thank the members of my thesis committee, Drs Allan Spradling, Yixian Zheng, and Xin Chen for their advice and support. I would also like to thank the faculty, post-docs, and graduate students in Carnegie and the JHU Biology Department for feedback on progress reports, support, and generally creating a wonderful environment in which to develop as a scientist.

I also would like to thank the past and present members of the Fan Lab, including Christoph Lepper, Pete Lopez, Evan Siple, Hui Low, Lydia Li, Micah Webster, Tyler Harvey, Patrick Li, and Samantha Satchell for providing a great culture. Especially important for me has been the muscle community, Christoph for moving the lab in this direction, and Lydia, Micah, and Hui for continued support and discussion along the way.

Finally, I would like to thank the many great friends and family that have supported me during my years at Johns Hopkins. In particular, I want to thank my father

for instilling in me the drive and passion for exploration. My accomplishments in graduate school I owe in large part to him.

TABLE OF CONTENTS **PAGE**

INDEX OF FIGURES **PAGE**

CHAPTER 1

Introduction

Adult stem cells

Stem cells possess remarkable characteristics not only to generate an embryo from a single fertilized egg but also to regenerate adult tissue to maintain homeostasis. A cell is defined as a "stem cell" if it has the capacity to self-renew as well as to divide to give rise to differentiated cell types of one or many lineages. The gold standard stem cell is the embryonic stem cell (ESC), the undifferentiated stem cell capable of giving rise to any cell of the embryo. As the embryo develops, however, pluripotent ESCs are replaced by more committed somatic stem cells (SSCs), which produce tissues and organs. These cells either give rise to a single cell type (unipotent) or most likely multiple cell types (multipotent).

A subset of SSCs are maintained through adulthood to support tissues through regular replacement of cells that die through natural wear-and-tear or by more severe injury. Many adult stem cells are maintained in a quiescent state but can rapidly enter the cell cycle to produce amplifying and differentiating daughter cells as necessary. Stem cell quiescence is maintained by both intrinsic and extrinsic factors. The extrinsic cues provided to stem cells from their microenvironment, or niche, is one essential component required to sustain quiescence, as well as to stimulate activation when stressed. A niche can be comprised of other cells and/or the surrounding extracellular matrix (ECM), which secrete and organize diverse factors that allow stem cells to maintain their intrinsic properties. Identifying the components of the niche and how they influence their complementary stem cell are essential to harness the unique properties of adult stem cells for use in the treatment of degenerative diseases and after injury.

Skeletal muscle

The skeletal muscle system is supported by a dedicated stem cell, called the satellite cell. This adult stem cell is maintained in a quiescent state under the basal lamina and on top of each individual muscle fiber, or myofiber. Myofibers are in turn comprised of myofibrils, long, multinucleate cylinders that are bundled to connect bone to tendon in order to perform contractile movements. The functional unit of the muscle fiber is the sarcomere, which organizes the actin and myosin filaments (MacIntosh et al., 2006). The "sliding filament theory", published in 1954, first postulated how actin slides past myosin in order to generate tension for muscle contraction (Krans, 2010).

Given this mechanical nature of contraction, skeletal muscle is prone to injury, especially exercise-induced trauma. Most commonly is delayed onset muscle soreness (DOMS) that occurs with eccentric work, e.g. lengthening contracted muscles in downhill running or squatting with weights. DOMS is associated with a rise in serum creatine kinase levels, the presence of which demonstrates that a tear has formed in the muscle fiber plasma membrane, or sarcolemma (Järvinen et al., 2008). Yet, no necrosis of myofibers occurs with DOMS (Yu et al., 2004). Instead degeneration of the sarcomere structure is observed with smearing or disruption of the boundary between each unit, called the Z-line. Myofibril remodeling follows, leading to an increase in F-actin and desmin proteins and a concomitant growth of muscle size. The contribution of the satellite cell toward this type of injury has been debated – some experimental evidence displayed incorporation of a cell cycle marker into these stem cells following eccentric exercise demonstrating their

activation, however it is now generally agreed upon that the satellite cell does not contribute to general muscle remodeling (Äärimaa et al., 2004).

However, more severe damage to muscle – strains or contusions that shear the muscle – does result in satellite cell recruitment to drive repair. Muscle strains result from excessive tensile force placed upon myofibers that ruptures individual fibers and damages the surrounding basal lamina and vasculature. Healing of strain injury follows a consistent path, similar to muscle contusions or lacerations, with three phases:

1. Degenerative phase (1-3days) – characterized by degeneration via a necrosis pathway of the myofibers, after which a haematoma forms, and inflammatory cells can infiltrate the damaged area resulting in local swelling. Leukocytes mature into macrophages over the course of a few hours and release chemotactic signals. The ECM also contains numerous growth factors that are released upon its damage; fibroblast growth factor (FGF), insulin-like growth factor1 (IGF-1), transforming growth factor-β (TGF-β), hepatocyte growth factor (HGF), and interleukin-6 (IL-6), among others, have been shown to be released with mitogenic properties that activate the satellite cell (Miller et al., 2000; Rathbone et al., 2011; Serrano et al., 2008; Sheehan and Allen, 1999).
2. Regenerative phase (3-4wks) – characterized by the regeneration of the muscle fibers and concomitant production of connective scar tissue, as well as vascularization of the injured area. This phase initiates 2 days after injury with entry of the satellite cell into the cell cycle. Once activated, the stem cell is called a myoblast and undergoes rapid cellular proliferation and daughter cell

differentiation into fusion-competent myocytes, which generate new myofibers and repair damaged myofibers through the process of fusion. By 10 days post injury, this part of the repair phase is complete as newly formed fibers are similar in size to original fibers. However, in contrast to old fibers, these new myofibers contain centrally located myonuclei, suggesting that cell fusion is focal to the site of injury during regeneration (Blaveri et al., 1999). In addition, regenerated myofibers express the embryonic form of myosin heavy chain (eMyHC), which allows for molecular distinction from the uninjured fibers (Whalen et al., 1990).

3. Remodeling phase (up to 6 months) – regenerated myofibers mature by forming new myotendinous junctions (MTJs) and are re-innervated to allow for full restoration of the functional capacity of the muscle (Rantanen et al., 1995).

Many models of skeletal muscle injury have been developed to study the cellular and molecular underpinnings of regeneration. The most reproducible form of injury is cardiotoxin-induced damage, which leads to the degeneration of 80-90% of the fibers at the injection site without excessive loss of satellite cells (d'Albis et al., 1988). This allows for the examination of the role of this stem cell population in muscle regeneration.

Satellite cells

The first study on muscle regeneration, performed in 1960, demonstrated through thymidine pulse-chase analysis that only mononucleated cells, and not myonuclei, were synthesizing DNA during the regenerative process (Bintliff and Walker, 1960).

Furthermore, by utilizing a longer chase period, they were able to visualize thymidine incorporation in myotubes, suggesting single cells were capable of giving rise to new muscle. Alexander Mauro published the seminal work a year later, using electron microscopy to identify a novel cell population "wedged" in between the plasma and basement membrane (Mauro, 1961). Given its position he chose the name of the satellite cell.

Evidence accrued over the next half a century to suggest that the satellite cell was the stem cell population responsible for driving muscle regeneration. Pioneering single myofiber assays showed that presumed satellite cells proliferated and later fused to regenerate damaged fibers *in vitro* (Bischoff, 1975; Konigsberg et al., 1975). Transplantation assays were used to demonstrate that myoblasts as well as myofiber-associated cells were able to contribute to regeneration following transplantation into minced and radiation-ablated muscles respectively (Collins et al., 2005; Snow, 1977a). However, as satellite cells are defined by their location, and as this is compromised upon injury, conclusively determining the function of these cells was difficult. Indeed, it was possible that other resident cell types were actually being utilized for regeneration. Identification of the paired box transcription factor 7 (Pax7) as a molecular marker of the satellite cell allowed for isolation of this specific population (Seale et al., 2000). Further transplantation assays demonstrated that a single $Pax7^{+}$ satellite cell could give rise to muscle fibers as well as self-renewing mononuclei that could then be re-isolated for additional rounds of repair (Sacco et al., 2008).

While it was clear that satellite cells were muscle progenitors, controversy arose over if this cell type was the only stem cell source or if other populations could contribute. Evidence suggested that PWI^+ interstitial cells, mesangioblasts, and periocytes, among others, could also give rise to muscle (Dellavalle et al., 2007; Mitchell et al., 2010; Sampaolesi et al., 2003). Specifically ablating all satellite cells allowed researchers to conclusively determine whether there was any contribution to muscle regeneration from other cells after injury (Lepper et al., 2011; Sambasivan et al., 2011). Inserting the Cre recombinase gene downstream of the Pax7 promoter, and coupling this transgene with a floxed diphtheria toxin allele allowed for temporally and spatially controlled satellite cell death. Animals lacking $Pax7^+$ cells were unable to form new muscle fibers following injury, demonstrating the absolute requirement for the satellite cell in regeneration.

Molecular regulation of myogenesis

Skeletal muscle in the limb and trunk of vertebrate embryos is derived from somites, bilaterally paired blocks of pariaxial mesoderm (Tajbakhsh and Buckingham, 2000). During the process of somite maturation, myogenic progenitors are confined to the epithelium of the dermomyotome until they delaminate, which signals the start of myogenesis. These cells rapidly migrate under the dermoyotome and differentiate into skeletal muscle (Buckingham, 2006). Both embryonic progenitors and adult muscle satellite cells drive skeletal muscle growth through proliferation and differentiation through a conserved myogenic profile. The molecular regulation of myogenic differentiation that occurs during myogenesis as well as during muscle regeneration

depends on a highly conserved group of basic helix-loop-helix transcription factors called myogenic regulatory factors (MRFs).

The MRFs, *Myf-5*, *MyoD*, *Mrf-4*, and *myogenin*, are expressed in a specific sequence. Myf-5 protein is detected first and Myo-D next in the medial and lateral domain of the somites, respectively. These primary MRFs are responsible for initial determination of skeletal myoblasts (Kablar et al., 1997). The secondary MRFs, Mrf-4 and myogenin act as differentiation factors, transforming myoblasts into differentiated myocytes. Gene knockout experiments have demonstrated the functional redundancy of this regulatory network (Patapoutian et al., 1995; Wang and Jaenisch, 1997; Weintraub, 1993). Typical of bHLH protein, these transcription factors bind to specific DNA motifs known as E-boxes (Berkes and Tapscott, 2005). Activation leads to robust expression of transcription factors, cell cycle regulators, and muscle structural genes, like *M-cadherin*, *desmin*, and *myosin heavy chain*, which allow for myocyte fusion into muscle fibers.

Muscle progenitors of myogenesis and satellite cells share a common origin in the dermomyotome (Gros et al., 2005). A $Pax3^{+}Pax7^{+}$ population drives the secondary wave of myogenesis and is responsible for the tremendous growth in musculature that occurs during fetal and post-natal development. A subset of these cells persist into adulthood and are maintained as satellite cells (Relaix et al., 2005). Satellite cells are present in all skeletal muscles, although the relative number varies with muscle type and age (Allbrook et al., 1971). At birth, 30% of the sublaminar muscle nuclei in mice are satellite cells; this number drops to 5% in a 2 month-old adult (Hellmuth and Allbrook, 1971). This number

continues to decrease after sexual maturity and drops significantly in aged mice, a phenomenon that is believed to contribute to aging muscle dysfunction (Snow, 1977b; Thompson, 2009).

Molecular regulation of the satellite cell

The satellite cell is maintained between the muscle fiber and the basal lamina in a quiescent state. The quiescent satellite cell is heterogeneous; utilizing a transgenic mouse, researchers determined that there were at least two subpopulations, those that express high ($Pax7^{HI}$) or low levels ($Pax7^{LO}$) of Pax7 (Rocheteau et al., 2012b). Single cell mass cytometry (CyTOF) of the satellite cell population suggests additional heterogeneity with at least four groups of Pax7 expression that further correlates with variations in Myf5 expression. Satellite cells are poised in G_0 of the cell cycle, a stage characterized by low metabolism and resistance to DNA damage, and heterogeneity in the population dictates the variation in response to activation (Cheung and Rando, 2013).

Quiescence is maintained by numerous factors that together repress cell cycle genes and induce expression of cell cycle inhibitors (Fukada et al., 2007). Additionally factors that buffer activating signaling pathways, like fibroblast growth factor (FGF) signaling, are also expressed. Notably, *Cdkn1c* (cyclin-dependent kinase inhibitor 1), *Gas1* (growth arrest specific 1), *p57*, and *Spry1* (sprouty homolog 1) are all highly upregulated in quiescent satellite cells. Expression of *Spry1*, a negative regulator of FGF signaling, becomes increasingly heterogeneous upon aging, with the population that maintains SPRY1 sustaining dormancy and niche occupancy, and the subset that loses SPRY1

being lost from the niche due to FGF activation of the ERK signaling cascade (Chakkalakal et al., 2012). Additional factors important for regulating quiescence are the Notch signaling pathway, and various microRNAs that target the mRNA of cell cycle genes for degradation (miR-489), and others (miR-31) that target the 3'UTR of *Myf5* mRNA for storage in RNP granules, facilitating rapid translation upon activation (Bjornson et al., 2012; Cheung et al., 2012; Crist et al., 2012).

Cells enter the cell cycle and initiate myogenesis through expression of MyoD; however $Pax7^{HI}$ cells divide asymmetrically, preferentially segregating DNA to self-renew, while $Pax7^{LO}$ cells segregate DNA randomly and commit faster to differentiation (Rocheteau et al., 2012). Pax7 and MyoD expression can distinguish between the various subpopulations – $Pax7^{+}MyoD^{-}$ cells are self-renewing, $Pax7^{+}MyoD^{+}$ myoblasts are proliferative, and $Pax7^{-}MyoD^{+}$ cells are committed to differentiation (Zammit et al., 2004). Through asymmetric division, a fraction of $Pax7^{+}MyoD^{-}$ cells are preserved throughout regeneration, which revert back to quiescence and are therefore primed for further injuries.

Although direct molecular triggers of asymmetry have yet to be identified it is clear that the distinct components that make up the apical and basal sides of the satellite cell provide polarity cues (Kuang et al., 2007). Establishment of the mitotic spindle along this axis and concomitant activation of the PAR polarity complex segregates phosphorylated cell cycle determinants of the p38 MAPK pathway (Troy et al., 2012). The daughter cell that retains phosphorylated p38 (phospho-p38 or pp38) commits to differentiation. This

asymmetry is further maintained by a feedback loop, with the committed cell expressing the ligand Delta-like protein 1 (DLL1) to activate Notch signaling in the mother stem cell and maintain its fate (Kuang et al., 2007). Inhibiting this pathway by the γ-secretase inhibitor leads to loss of the stem cell.

Satellite cells can also divide symmetrically to maintain the stem cell pool. Basally-located ECM components, like collagen VI and fibronectin have been linked to symmetric self-renewal (Bentzinger et al., 2013; Urciuolo et al., 2013). Fibronectin stimulates Wnt7a signaling through the Syndecan-4/Frizzled-7 co-receptor complex to induce symmetric expansion via the planar cell polarity effector Vangl2 (Bentzinger et al., 2013; Le Grand et al., 2009). Knockdown of fibronectin or Wnt7a results in the loss of symmetric division and an inability of the satellite cell to repopulate its niche. Additionally, overexpression of fibronectin or Wnt7a *in vivo* improved muscle regeneration and led to an increase in satellite cell numbers throughout regeneration. Overall, both extrinsic and intrinsic factors contribute to regulate satellite cell quiescence and activation.

Integrins in the satellite cell niche

Integrins are heterodimers comprised of an α and a β chain that function to link the extra cellular matrix (ECM) to the actin cytoskeleton (Hynes, 1992). Each subunit contains a single transmembrane domain, a large ectodmain, and a short cytoplasmic tail. Mammals express 18 α and 8 β chains, which can combine to form at least 28 functional isoforms

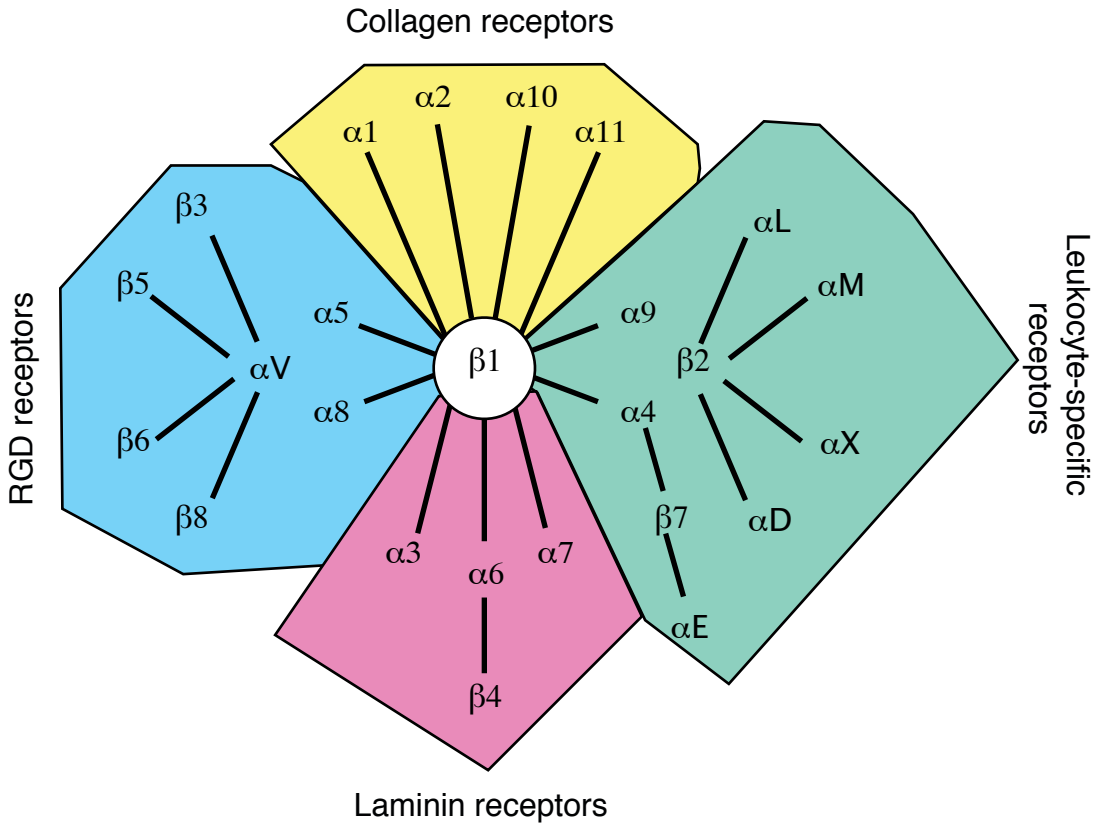

Figure 1.1. Representation of the integrin family. Binding partners indicated by lines. Ligand receptor-specificity depicted with colored blocks.

that possess binding specificity for individual ECM ligands such as collagen, fibronectin, and laminin (Hynes, 2002) (Figure 1.1). Integrins exist in three major conformational states: 'inactive' (low affinity), 'primed' or 'active' (high affinity), and ligand occupied. The crystal structure show that that these states correspond to conformations that are bent, extended, and extended with an open headpiece (Xiong et al., 2002). Intracellular and extracellular cues combine to control integrin cycling between these conformations.

There are two directions of integrin signaling with distinct biological functions. Outside-in signaling is the 'traditional' mode of signaling receptors where binding to the ligand drives intracellular gene expression changes (Shattil et al., 2010). As many ligands are multivalent, binding induces integrin clustering that drives intracellular signaling to affect cell polarity, survival, and proliferation. During inside-out signaling, an intracellular activator binds to the β-integrin tail, transforming the protein from its 'inactive' to its 'active' state thereby increasing its affinity for ligands. This mode of signaling controls cell adhesion, strength, migration, and ECM remodeling. Although these two processes are conceptually distinct, they are inherently linked – inside-out signaling can prime the heterodimer for binding to its ligand counterpart to drive outside-in signaling, and conversely ligand binding can generate signals that lead to inside-out signaling.

The largest subgroup of integrin heterodimers consists of the β1-integrin subunit, which contains 12 members that bind to various ligands (Brakebusch and Fässler, 2005). Mice lacking β1-integrin die shortly after implantation due to inner cell mass failure (Fässler and Meyer, 1995; Stephens et al., 1995). Inactivation of *β1-integrin* (*Itgb1*) in the

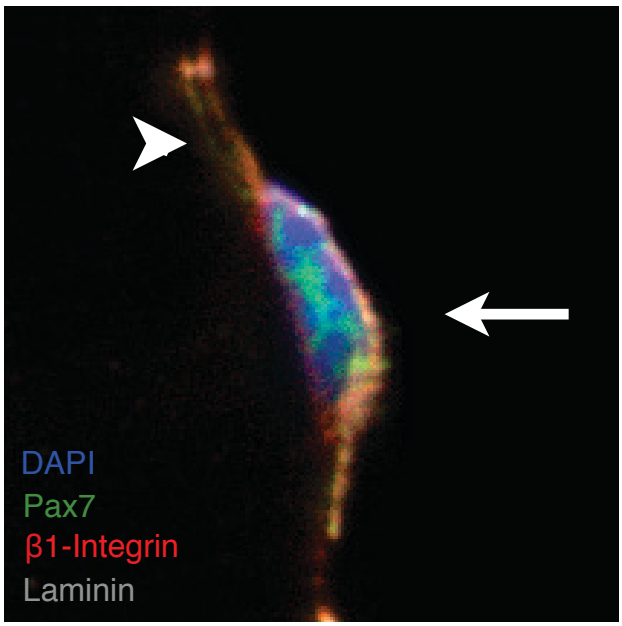

Figure 1.2. β1-integrin expression in satellite cells. Anti-β1-integrin immunofluorescence (red) is detected in a polarized fashion on the basal side of the $Pax7^{+}$ (green) satellite cell, indicated by the arrow. The muscle fiber also expresses β1-integrin, indicated by the arrowhead.

myogenic lineage reveals that it is essential for muscle cell fusion yet is dispensable for progenitor proliferation during embryogenesis (Schwander et al., 2003). Although β1-integrin is conspicuously expressed by adult quiescent $Pax7^{+}$ satellite cells (Figure 1.2), which implies a potential role in the 'stem-ness', its role in this stem cell population has not been examined.

CHAPTER 2

Characterization of the satellite cell specific knockout of *β1-integrin*

INTRODUCTION

In skeletal muscle, two major groups of protein complexes function at the plasma membrane to link the extracellular matrix to the cytoskeleton: the dystrophin-glycoprotein complex and the integrin family of receptors. Both complexes are essential, as mutations in constituent factors result in muscular dystrophy in mouse models and human patients (Chen et al., 2000; Rooney et al., 2006). Many conclusions regarding the function of integrins in vertebrate skeletal muscle have resulted from *in vitro* approaches combining human, rate, mouse, chicken, and quail models. Expression data cobbled together from the various species demonstrates the changes in family member presentation through development: in migrating myoblasts, α4–α7, αv, and β1A are expressed, during secondary myogenesis the β1A isoform is replaced by the β1D isoform, and α4–α7, αv are also expressed (Mayer, 2003). In the adult, only α7β1D is present at the sarcolemma and myotendinous junctions (MTJ). α3 and αv subunits are additionally localized to the neuromuscular junction (NTJ). Primary satellite cell-derived myoblasts express all known α and β isoforms (Siegel et al., 2009).

Studies performed in chick hosts indicated that β1-integrins are involved in mediating myogenic cell migration and terminal differentiation of myoblasts into myotubes. Utilizing a β1-integrin-specific antibody, CSAT, that blocks integrin function, perturbed migration and disrupted body muscle wall development (Jaffredo et al., 1988). Additionally adding CSAT to chick myoblasts perturbed differentiation and prevented myotube formation; removal of the antibody was sufficient to restore normal myogenic progression (Menko and Boettiger, 1987).

These studies, and others, contributed a wealth of important information, but can be difficult to interpret as some integrins are expressed in one species but not in another. In addition, many *in vitro* assays identified phenotypes that were not confirmable by *in vivo* genetic studies. For example, *in vitro* studies using functional blocking antibodies indicated that α4 integrins provided the major cell-cell contract for myoblast alignment and support for myotube formation (Rosen et al., 1992). However, chimeric mice with a high percentage of α4-deficient ES cells developed skeletal muscle normally, and muscles that lacked any detectable $\alpha4^+$ cells did not display gross morphological abnormalities (Yang et al., 1996). Additionally, various results implicated α7β1 as a crucial determinant of myoblast migration (Crawley et al., 1997; Echtermeyer et al., 1996; Yao et al., 1996). Yet, as with other α-integrin knockout animals, skeletal muscle develops normally in the absence of α7β1 (Mayer et al., 1997). These mice do develop progressive muscular dystrophy after birth however, demonstrating that integrins represent an indispensable linkage between the muscle fiber and ECM, independent of the dystrophin-glycoprotein complex. Overall, these results indicate that it is likely that integrins, especially α-integrins, are redundant and can substitute for one another, thereby potentially accounting for knockout studies that mask possible importance.

Targeting β-integrins instead of their α-integrin counterparts would potentially provide more functional information, but have been historically been more difficult due to lethality (Fässler and Meyer, 1995). β1-integrin is the subunit in the largest subgroup of integrin heterodimers and is ubiquitously expressed. Four isoforms of this protein have been described: β1A and β1D, which are the major forms, and β1B and β1C, which only exist in humans. β1A is expressed universally, except in skeletal and cardiac muscle,

where it is replaced by the β1D variant, which associates solely with the α7 chain. Replacing the β1A variant with the β1D subunit, demonstrated that the former functions in primary myogenesis while the latter is important to promote migration and inhibit proliferation (Cachaço et al., 2003). Muscles in these animals develop with few defects, however, complicating the analysis.

Availability of the β1-integrin conditional allele allowed for more conclusive examination of the functions of integrin during myogenesis. To inactivate *Itgb1* in skeletal muscle, mice carrying the β1-integrin floxed allele, constructed with two loxP sites flanking the first exon, were crossed with a transgenic mouse line expressing Cre under the control of the human skeletal-actin (HSA) promoter (Brennan and Hardeman, 1993; Graus-Porta et al., 2001; Schwander et al., 2003). Using a Rosa26R^{LacZ} allele to mark Cre expression, demonstrated that the line induced recombination in somites at E 9.5. Further characterization of these animals show that integrins regulate myoblast fusion but are dispensable for proliferation. These mice die at birth, failing to inflate their lungs, so analyses of integrin function in adult muscle was not possible.

To examine the function of β1-integrin in adult skeletal muscle, we utilized an inducible Cre recombinase to spatially and temporally control inactivation of integrin. We used a publically available Itgb1^{flox} allele (referred to as Itgb1^{KO}) generated to contain loxP sequences flanking the third exon, which, upon removal, produces a frame shift leading to termination of translation and loss of protein (Raghavan et al., 2000). The Pax7 CreER^{T2} (Pax7^{CE}) transgenic mouse restricts CreER^{T2} expression specifically to *Pax7* expressing satellite cells (Lepper et al., 2009). This fusion protein consists of the Cre protein, a P1 bacteriophage enzyme that catalyzes site-specific recombination between

loxP sites, and a mutated ligand-binding domain of the estrogen receptor (ER) (Feil et al., 1996; Metzger et al., 1995). The mutation ensures that the receptor does not recognize endogenous estrogen, but instead specifically binds to the estrogen agonist tamoxifen, which can be injected into the animal. Prior to injection, the $CreER^{T2}$ protein, which displays higher affinity for tamoxifen, is bound by heat shock protein Hsp90 and is sequestered in the cytoplasm (Feil et al., 1997). Upon binding to tamoxifen, $CreER^{T2}$ dissociates from Hsp90 to translocate into the nucleus where it induces site-specific recombination.

The R26R Cre reporter mouse allows for testing of the efficiency of the $Pax7^{CE}$ allele, as well as generation of a stable lineage label. The ROSA26 gene locus is ubiquitously expressed in all tissues of the mouse, although the function of the gene is unknown (Casola, 2010). In the R26R Cre reporter mice ($R26R^{LacZ}$ and $R26R^{YFP}$), *lacZ* or *YFP* expression is prevented by a floxed neomycin gene cassette preceding the reporter gene cassette (Soriano, 1999; Srinivas et al., 2001). Only upon Cre expression, and concomitant excision of the stop codon, is the reporter transcribed. Use of the $R26R^{LacZ}$ allele demonstrated the efficacy and specificity of tamoxifen-induced satellite cell labeling by the $Pax7^{CE}$ line, with 99.8% co-localization of Pax7 and β-gal (Lepper et al., 2009).

Here I report the characterization of the $Pax7^{CE}$; $Itgb1^{KO}$; R26R mouse line, which allowed for efficient inactivation of *Itgb1* specifically in the satellite cell. Through lineage-labeling of *Itgb1*-KO SCs, I demonstrate that these mutant stem cells are unable to maintain quiescence and cannot contribute to muscle regeneration following injury. I confirm that, as previously suggested, β1-integrin is required for myoblast migration and

myocyte fusion. However, in contrast to embryonic studies, I demonstrate that β1-integrin is required for proliferation and stemness of the satellite cell (SC). RNA sequencing of fluorescent activated cell sorted (FACS) SCs demonstrated that *Itgb1*-KO cells commit to differentiation by turning on myogenic regulatory factors and muscle-specific genes faster than their control counterparts. Furthermore, *Itgb1*-KO SCs were unable to replenish the stem cell pool, instead differentiating at the expense of self-renewal. Together, these data suggest that β1-integrin is a crucial component of the satellite cell niche.

MATERIALS AND METHODS

Animal studies

Animal experiments in this study were performed in accordance with protocols approved by the Institutional Animal Care and Use Committee (IACUC) of the Carnegie Institution for Science (Permit number A3861-01). The Pax7^{CE} allele (B6;129-*Pax7*$^{tm2.1(cre/ERT2)}$*Fan*/J) has been described (Lepper et al., 2009). The *Itgb1*^{FLOX} allele (B6;129-Itgb1tm1Efu/J) and the *R26R*^{lacz} (B6.129S4-*Gt*(*ROSA*)*26Sortm1Sor*/J) and *R26R*^{YFP} (B6.129X1-*Gt*(*ROSA*)*26Sor*$^{tm1(EYFP)}$*Cos*/J) reporter mice were obtained from the Jackson Laboratory (Raghavan et al., 2000; Soriano, 1999; Srinivas et al., 2001).

Mice were given Tamoxifen (Tmx)(Sigma; diluted to 20 mg/ml in corn oil (Sigma)), 3 mg per 40 g body weight per intraperitoneal injection, once a day consecutively for 5 days. Tmx was prepared by dissolving a freshly opened bottle of 5 g of tmx in corn oil in 50 ml conical tubes at the final concentration of 20 mg/ml. The tubes were then incubated at 37°C with periodic vortexes until tmx was fully dissolved. The tmx was aliquoted, frozen in dry ice chilled 95% Ethanol and stored at -80°C wrapped in aluminum foil until needed. All experiments except where noted were conducted 3-10 days after the final injection. Mice were anesthetized using 2,2,2-Tribromoethanol (Sigma), which was dissolved in 2-methyl-2-butanol (Sigma) as 100% (w/v) stock solution. For *Itgb1*-KO versus control injury, 50 µl of 10 µM cardiotoxin (CTX)(Sigma) was injected with an insulin syringe (BD) into TA muscles. Cardiotoxin from *Naja mossambica mossambica* was prepared by dissolving in PBS at 10 µM. The concentration and volume of injection was described in previously published work (Iezzi et al., 2004; Meeson et al., 2004; Melcon et al., 2006). Animals were then harvested at

either 5d or 10d post injury. For the *in vivo* proliferation assay, EdU (Invitrogen) was given by intraperitoneal injection at 0.1 mg per 20 g bodyweight per injection, at 2, 3, 4, or 5 d after injury. Animals were harvested 24h after injection. For activation analysis, BrdU (0.8 mg/mL; Sigma) was given in drinking water for 1 mo post tmx regimen.

Mice were sacrificed by cervical dislocation and TA muscles were harvested by (1) removing the epimysium, (2) carefully cutting the tendons above the ankle, (3) peeling back the TA muscle, and (4) severing the muscle below the knee, to remove whole muscle intact. Muscles were fixed for 8 min in cold 4% paraformaldehyde (EMS) in phosphate buffered saline (PBS; Gibco), and incubated sequentially overnight in 10% and then 20% sucrose in PBS. Muscles were then mounted on a slice of cork in Tragacanth (3 mg / mL H_20; Sigma, G1128) and flash frozen in liquid nitrogen cooled 2-Methylbutane (Sigma) for 30 seconds. This study was carried out in strict accordance with the recommendations in the Guide for the Care and Use of Laboratory Animals of the National Institutes of Health.

Muscle histology

10 μM frozen muscle cross sections (Leica CM3000 Cyrostat) were collected on Superfrost plus slides (VWR) and air-dried. Slides were either stored at -20°C or used immediately.

For histology, Haematoxylin and Eosin were utilized. Sections were fixed in 4% paraformaldehyde on ice for 10min. This step was skipped if sections were prefixed. Then sections were washed two times with PBS for 3min, stained with Gills #2 haematoxylin for 40 seconds, washed in warm tap water for 5 minutes, dipped in Scott's

tap water for 10 seconds, washed in warm tap water for 2 minutes, stained in Eosin solution twice, destained in 95% Ethanol, followed by 100% Ethanol, xylene, then mounted in Permount. All reagents were purchased from Surgipath.

For X-galactosidase reactions, sections were fixed with 0.2% glutaraldehyde / 0.1M phosphate buffer (pH 7.2) with 5mM EGTA, 1mM $MgCl_2$, for 8min on ice. Then washed and stained according to previously published protocols (Behringer et al., 2014). Once desired staining intensity is achieved (8-24 h), slides are washed in H_20, and then post-fixed with PFA on ice for 10-15 min. Nuclear Fast Red (Lab Vision, TA-125-NF) is used for counterstaining for 5 min. Sections are then dehydrated through a graded Ethanol series (75%, 95%, 95%, 100%), then dipped in xylene before mounting in Permount media (Fisher).

Cell isolation and culture

For myoblast preparation, muscles were dissected and incubated in 0.2% Collagenase Type I (Sigma) in DMEM at 37°C with gentle shaking for 1.5 h. Muscle was then triturated in 10% FBS in DMEM, washed with PBS, and incubated in 0.2% dispase (Gibco) in DMEM at 37°C with gentle shaking for 30 minutes. Cells were filtered through a 70μm cell strainer, and plated on Matrigel (BD Biosciences) coated tissue culture plates in proliferation medium (20% Fetal Bovine Serum, 5% Horse Serum, 1% Pen/Strep, 1% Glutamax). Cells were cultured for 3d before being removed from plates by .25% Trypsin/EDTA (Life Technologies) for 5 min, and purifying either through FACS or through differential plating. Differential plating is achieved by placing floating

myoblasts on uncoated dishes for 1 h to remove non-myogenic cells, which will adhere to the dish, and then returned to Matrigel-coated plates.

Myofibers with associated SCs were isolated from extensor digitorum longus (EDL) muscles by 1.5 h digestion in 0.2% Collagenase Type I in DMEM at 37°C. The digested muscle was then transferred to tissue culture dishes containing DMEM, 1%P/S, and 1% Glutamax. Live myofibers were isolated with a fire polished glass pipette. Isolation of individual myofibers by pipette was repeated to remove dead myofibers and cellular debris. Myofibers were either fixed immediately after isolation to preserve the SC in its niche, or placed in floating culture in either growth medium (DMEM + 10% Horse Serum + 1% Penn/Strep (Invitrogen) + 1% Glutamax (Invtrogen)) or proliferation media (DMEM + 25% Fetal Bovine Serum + 10% Horse Serum + 1% Chick Embryo Extract + 1% Penn/Strep + 1% Glutamax) and incubated (37°C, 5% CO_2) with daily medium and reagent changes.

Western blot

YFP labeled myoblasts were isolated by FACS. Using a BD FACS ARIA III and FACS Diva software, cells were sorting using the 488 channel and gating first for cell size using forward and side scatter, and then gating for YFP+ cells. Cells were lysed in T-Per Tissue Protein Extraction Reagent (Thermo), 1mM PMSF, 1x Halt Phosphatase Inhibitor Cocktail (Thermo), Complete Protease Inhibitor Tablet (Roche). Total protein extract was resolved by SDS-PAGE on precast gels (Bio-Rad) and then transferred to Immuno-blot PVDF Membranes (Bio-Rad) using a Bio-Rad mini-Protein II Transfer system. Membranes were blocked for 1h at RT in 5% low-fat milk, TBS-0.1% Tween (Sigma)

buffer. Primary antibodies against β1-integrin: 1:1000; Cyclin A: 1:200; Cyclin B1: 1:200; Cyclin D1: 1:200; Cyclin D2: 1:200; Cyclin D3: 1:200; Cyclin E: 1:200; GAPDH: 1:5000 were diluted in 5% low-fat milk, TBS- 0.1% Tween (Sigma) buffer. Membranes were incubated in primary antibody overnight at 4 degrees. Horseradish peroxidase-conjugated antibodies were diluted 1:10,000 in 5% low-fat milk, TBS- 0.1% Tween (Sigma) buffer and incubated for 1 h at RT. Blots were developed with the ECL reaction using Femto Chemiluminescent Substrate (Thermo) and exposed to X-ray film.

Immunofluorescence

Cells or muscle sections were fixed for 10 min in 4% paraformaldehyde, permeabilized with 0.1% Triton-X-100 (Sigma) for 15 min and incubated with primary antibody diluted in staining buffer (10% Normal Goat Serum; Genetex, 1% Blocking powder; Perkin Elmer, 0.05% Triton-X 100) overnight at 4°C. Primary antibodies were diluted as follows: α7-integrin: 1:50; activated β1-integrin: 1:200; β1-integrin: 1:200; BrdU: 1:200; Cleaved Caspase-3: 1:400; eMyHC: 1:200; GFP (used to detect YFP): 1:500 (rabbit) or 1:200 (chick); ILK: 1:50; Laminin: 1:2000; M-cadherin: 1:250; MLC: 1:20; MyoD: 1:50; Parvin: 1:400; Pax7: 1:20; Paxillin: 1:250; pp38: 1:50; Vinculin: 1:400. Cells or muscle sections were washed with staining buffer and incubated with an Alexa-Fluor-conjugated secondary antibody (1:1,000, Invitrogen) in staining buffer for 1 h at room temperature. After 5 min incubation with DAPI (1μg/ml), slides were then mounted with Fluoromount-G (SouthernBiotech). For BrdU detection, slides treated were with antigen unmasking solution (Vector) by boiling for 10 minutes prior to staining with the primary

antibody. For EdU detection, the Click-iT reaction kit (Invitrogen) was used prior to incubation in DAPI.

Chemicals and antibodies

Antibodies against β1-integrin and Cleaved Caspase-3 were purchased from Cell Signaling (4706 and 5A1E respectively). GAPDH antibody was purchased from Chemicon (MAB374). α7-integrin antibody was purchased from MBL International Corporation (clone 3C12, K0046-3). β1-integrin antibody was purchased from Millipore (MAB1997). BrdU antibody was purchased from Exalpha (A250P). GFP antibodies were purchased from Invitrogen (G10362, rabbit) and Aves (GFP-1020, chick). Antibodies against eMyHC, MLC, and Pax7 were purchased from Developmental Studies Hybridoma Bank (F1.652, MF20, and PAX7, respectively). Antibody against Laminin was purchased from Sigma Chemical (L9393). Antibodies against Cyclin A, Cyclin B1, Cyclin D1, Cyclin D2, Cyclin D3, Cyclin E, M-cadherin, and MyoD were purchased from Santa Cruz (sc-596, sc-245, sc-717, sc-593, sc-182, sc-198, sc-81471, and sc-304, respectively).

Microscopy and image processing

Images of haematoxylin and eosin stained muscle sections were captured from a Nikon 800 microscope equipped with a 10x/.45 Plan Apo objective and Canon EOS T3 camera using EOS Utility image acquisition software. Fluorescent images of muscle sections were captured using Leica SP5 confocal equipped with 40x/1.25 Plan Apo oil objectives using Leica image acquisition software. Images of cells on single fibers were captured

using the Leica SP5 setup or a Zeiss Axioscope equipped with a 40x/0.5 Plan Apo oil objective and Axiocam camera using Zeiss image acquisition software. Identical exposure times were used and images were processed and scored with blinding using ImageJ64. If necessary, brightness and contrast were adjusted for an entire experimental image set.

Live cell imaging was done with a Nikon TE2000 10x ELWD using Hoffman Modulation Contrast (HMC) and a Photometrics Coolsnap HQ camera using Metamorph software. All images were processed using Imaris software. Myoblasts were plated on matrigel in a 6-well dish, 20,000 cells per well, and cultured for 24h in PM. Prior to imaging, GM was substituted into the wells. Images were captured every 6minutes from 2 fields in each well for 96h. The GFP filter was used to locate YFP^+ SCs, subsequent images were taking using DIC. For migration analysis, individual cell velocities were measured using Metamorph software. Migratory traces were based on Metamorph generated cell position data (x and y coordinates) and assembled using Microsoft Excel.

Flow cytometry and analysis

For RNA-seq analysis, SCs were isolated and cultured in growth medium on Matrigel (BD Biosciences) coated plates for 72 h. Cells were then harvested for sorting. FACS isolation was performed as described above. Purified cells were used immediately after sorting for RNA isolation. RNA was isolated using the Arcturus PicoPure RNA isolation kit (Applied Biosystems). The Ovation RNA-Seq System (NuGEN) was used to prepare amplified cDNA. Libraries for single-end sequencing were prepared using Illumina's TruSeqDNA sample prep kit LT. Sequencing was carried out on an Illumina HiSeq2000

to generate single-end 100bp reads, which were aligned to the mouse genome (mm9) using TopHat (v2.0.7). Cufflinks (v2.1.1) was used for differential expression analysis.

For FACS analysis of DNA content, cells were collected at staggered time points post activation (24, 48, 72 h). Cells were centrifuged (2500 x g, 4°C, 10min) and washed twice in cold PBS. Cell pellets were resuspended in solution of 70% cold ethanol and fixed overnight at 4°C. After washing twice with cold PBS, the cells were resuspended in 1 mL of a 1:1 PI solution (0.1 mg/mL propidium iodide in 0.6% Triton-X in PBS (Sigma; P4170)) : RNase solution (2 mg/mL in milli-Q H_20 (Sigma; R5125)) and stained in the dark for 45 min. Cells were passed through meshed capped falcon tubes prior to running on FACS machine to avoid clumping. FACS analysis was carried out with a BD FACS ARIA III machine and FACS Diva software, gating first for cell size and using forward and side scatter and then gating for YFP+ cells using the 488 channel. ModFit LT V2.2.11 was used to analyze percentages of each phase of the cell cycle, $G_{1,}$ S, and G_2/M. All data were determined to have "good" RCS, measurement of fit.

The CellTrace Violet Cell Proliferation dye (Invitrogen) was used to determined generation time of myoblasts cultured for various time points post activation (24, 48, 72 h). This fluorescent compound covalently binds to intracellular amines, and is successively diluted with each generation. Myoblasts were harvested and pelleted by centrifugation (2500 x g, 4°C, 10min). Pellets were resuspended in 10 μM Cell Trace Violet / DMSO in PBS prewarmed to 37°C. Cells were then incubated for 20 min at 37°C. Unbound dye was quenched by adding 5x the original volume of GM and incubating for 5 minutes. Cells were then repelleted and resupended in fresh GM. One set was incubated for 10min and then fixed at T=0 for baseline comparison. The rest were

plated for 24, 48, or 72 h, before harvesting and running on the FACS ARIA III. ModFit LT Proliferation Wizard Model was used to determine the generation of cells.

RESULTS

Temporal and spatial control allows for specific depletion of the α7β1 heterodimer

Pax7 is specifically expressed in the satellite cell (Seale et al., 2000). To deplete β1-integrin exclusively in this stem cell population, the $Pax7^{CE}$;R26R mouse line was crossed with the $Itgb1^{KO}$ mice purchased from Jackson Lab. An additional cross was performed to recover two copies of the floxed allele and two copies of the reporter allele under the control of one copy of Cre knocked-in to the Pax7 endogenous locus. As this knock-in replaces exon1 of Pax7 it is a null allele. Therefore, only one copy of $Pax7^{CE}$ was used. Animals heterozygous for *Pax7* develop muscle normally and regenerate comparably to wild-type controls (Lepper and Fan, 2010). The experimental mice used in this study were therefore, $Pax7^{CE/+}$; $Itgb1^{flox/flox}$; $R26R^{LacZ/LacZ}$ or $Pax7^{CE/+}$; $Itgb1^{flox/flox}$; $R26R^{YFP/YFP}$, referred to as *Itgb1*-KO. Reporter alleles were chosen based on the assay; YFP is preferable for immunofluorescence and necessary for live-imaging and FACS sorting, while LacZ is useful for histology analyses. Controls used were $Pax7^{CE/+}$; $R26R^{LacZ/LacZ}$ or $Pax7^{CE/+}$; $R26R^{YFP/YFP}$. Heterozygous $Itgb1^{flox/+}$ animals and isolated myoblasts were grossly normal, however upon injury, muscles displayed a mild regeneration phenotype at significant prevalence (~25%) (not shown). Therefore, they were not used for analysis.

Several tamoxifen regimens were tested previously for efficacy of *loxP* recombination at R26R, including 3 mg per 40 g body weight per intraperitoneal injection on 1, 3, 5, and 8 consecutive days. Of these trials, 5- and 8-days of tamoxifen injections were found to induce the most recombination as assessed by number of β-gal+ cells (Lepper and Fan, 2010). This tamoxifen regimen was therefore selected for induction for all subsequent studies (Figure 2.1a). Tibialis anterior muscle was harvested at staggered

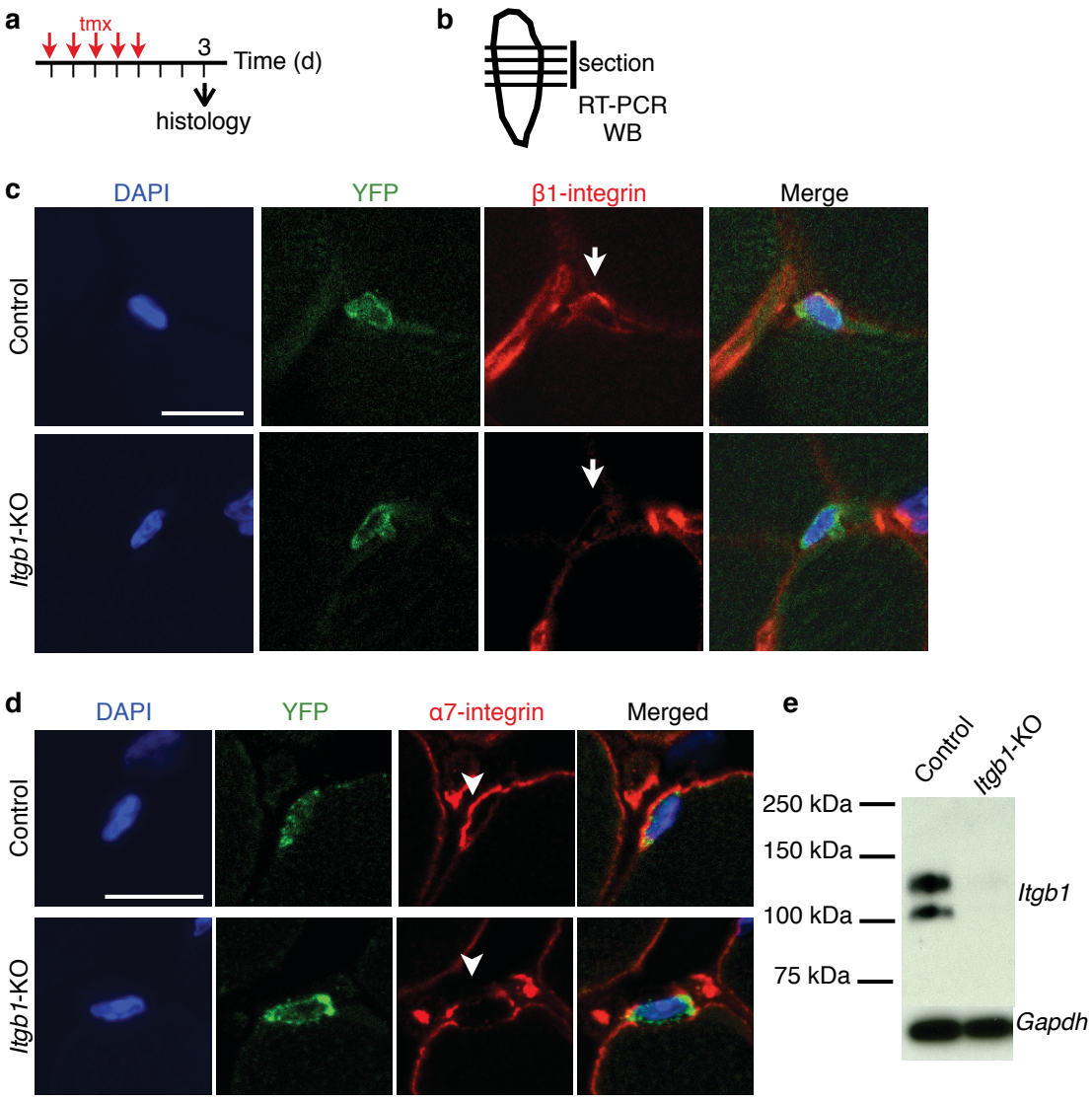

Figure 2.1. Temporal and spatial control allows for specific depletion of the α7β1 heterodimer. a, Tamoxifen (tmx) regimen and tibialis anterior (TA) harvest scheme, vertical lines indicate daily intervals. **b,** Tibialis anterior musce diagram. Horizontal lines indicate cross-sections. **c-d,** SCs of Tibialis Anterior (TA) muscle from control ($Pax7^{CE/+}$; $R26R^{YFP/YFP}$) and *Itgb1*-KO ($Pax7^{CE/+}$; $Itgb1^{f/f}$; $R26R^{YFP/YFP}$) animals harvested 3 d after the 5 d tamoxifen (tmx) regimen and stained for YFP and β1-integrin (**c**) or α7-integrin (**d**); arrowhead, laminar side of the SC; scale bar = 10μm. **e,** Western blot performed on total protein from FACS-isolated YFP^{+} myoblasts. Western analysis of β1-integrin protein shows presence in control cells, while *Itgb1*-KO lack the presence of the protein.

time points post completion of the tamoxifen injections (3, 7, and 10 days after the final tamoxifen dose) to assess the minimum time necessary to remove β1-integrin from the SC. Muscles were sectioned (Figure 2.1b) and immunofluorescence analysis was performed against β1-integrin and the reporter allele (YFP), to mark SCs with active Cre recombinase (Figure 2.1c). Control SCs maintain β1-integrin expression along the plasma membrane regardless of the chase time, with preferential distribution of the protein towards the basal lamina. In contrast, after 3 days post tamoxifen regimen, *Itgb1*-KO SCs lose β1-integrin expression specifically in the satellite cell. Muscle fibers maintain expression. Given the high turnover of integrins via endocytosis, it was perhaps unsurprising that 3 days was sufficient to deplete the *Itgb1*-KO SC of β1-integrin (Arjonen et al., 2012) (Figure 2.1c).

To confirm the depletion of β1-integrin protein, Western Blots were performed on protein extracts from YFP^{+} SCs, sorted from whole hindlimbs, based on fluorescence intensity via FACS. As previously reported, two bands are typically observed in blots of β1-integrin; a 115 kD partially glycosylated precursor and a 130 kD fully glycosylated mature form (Argraves et al., 1987). Both bands are detected by Western Blot in protein extract from $Pax7^{CE}$;$R26R^{YFP/YFP}$ mice (Figure 2.1e). Neither can be detected in protein extract from *Itgb1*-KO mice at 3 days post tamoxifen regimen, confirming that β1-integrin is efficiently inactivated by tamoxifen in all hindlimb muscle SCs.

Although satellite cells express the majority of the α-integrin partners of β1-integrin (α1- α11), the relevant subunits are α5, α6, and α7 integrin, the former is the fibronectin receptor and the latter two are exclusive laminin receptors (Siegel et al., 2009). Although, the function of these α-integrins have not been examined in the adult,

α5β1 and α6β1are expressed in developing myoblasts and downregulated upon fusion, where α7β1 is upregulated upon myotube formation (Blaschuk and Holland, 1994; Bronner-Fraser et al., 1992; Song et al., 1993). Additionally the expression of α7-integrin is restricted to skeletal and cardiac muscle, suggesting a unique function, and indeed this marker is commonly used for purification of primary myoblasts (Blanco-Bose et al., 2001). We examined the localization of α7-integrin in *Itgb1*-KO SCs by immunofluorescence analysis using the reporter allele (YFP) to mark the recombined SCs (Figure 2.1d). Expression of α7-integrin is robust in control SCs, and the protein displays the same polarized localization as its heterodimer partner, β1-integrin, preferentially associating with the basal laminar side of the SC. In *Itgb1*-KO SCs, α7-integrin is visible, although relative expression compared to control is difficult to ascertain given these methods. Regardless, localization of α7-integrin to the basal lamina is disrupted in these mutant SCs, with protein now present in a non-polarized distribution. The loss of β1-integrin disrupts α7-integrin localization as β1-integrin is the only β-integrin that α7-integrin can associate with.

β1-integrin senses proper SC-niche interaction to maintain quiescence

β1-integrin has been shown to maintain the integrity of stem cell niches in neural stem cells and germline stem cells in both fly and mouse to maintain stem-cell properties (Kanatsu-Shinohara et al., 2008; Loulier et al., 2009; Tanentzapf et al., 2007). To determine if β1-integrin plays a similar role in the SC niche, we first examined the morphology of *Itgb1*-KO SCs 21 days after completion of the tamoxifen regimen (Figure 2.2a,b). The SC can be identified in its niche: it is maintained near a myonucleus,

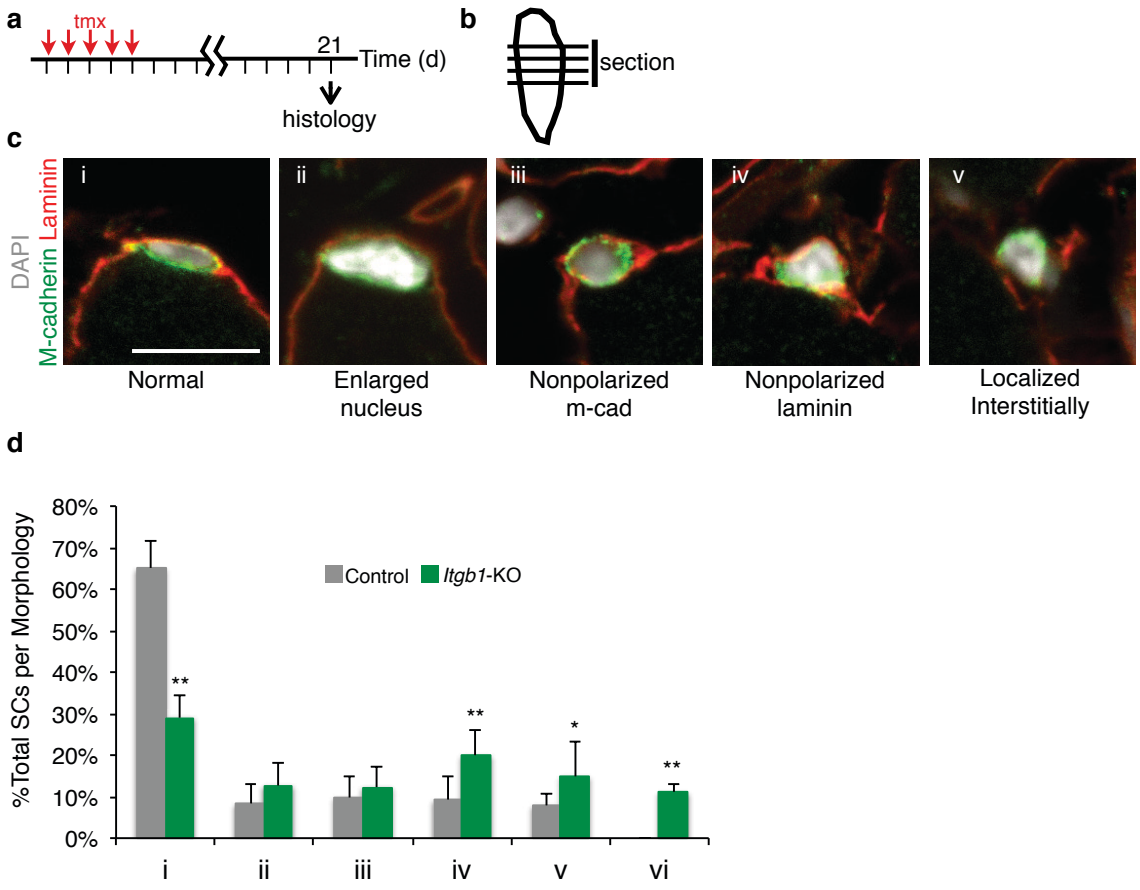

Figure 2.2. *Itgb1*-KO SCs display abnormal niche morphology. a, Tamoxifen (tmx) regimen and tibialis anterior (TA) harvest scheme. Vertical lines, daily intervals. **b,** Tibialis anterior muscle diagram. Horizontal lines, cross sections. **c,**YFP^{+} SCs from control and *Itgb1*-KO muscle (1 mo after tmx regimen) stained with anti-laminin (for basal lamina, which is oriented towards the top) and anti-M-cadherin (for contact with the myofiber); scale bar =10μm. We scored 6 categories of SC morphology (**i-vi**): (**i**) normal, (**ii**) enlarged nucleus, (**iii**) non-polarized M-cadherin, (**iv**) non-polarized laminin, (**v**) interstitially localized, (**vi**) belonging to more than one category from (**ii-v**). **d,** Percentages of cells belonging to each category in control and *Itgb1*-KO samples; data are expressed as mean ± s.e.m, n = 4 experiments, and subjected to two-way ANOVA; * = p<0.05, ** = p <0.01.

underneath the basal lamina, and expresses M-cadherin along the apical side for connection to the muscle fiber (Luisa Boldrin, 2012; Zammit et al., 2006) (Figure 2.2c, panel i). Additionally, it is mitotically quiescent and therefore possesses a small nucleus with virtually no cytoplasm. The majority of control SCs displayed these characteristics and therefore were morphologically normal (Figure 2.2d). In contrast, *Itgb1*-KO SCs displayed abnormal characteristics as assessed by nuclear size (ii), non-polarized M-cadherin (iii), non-polarized laminin (iv), and residence outside of the niche entirely (v) (Figure 2.2c,d). *Itgb1*-KO SCs typically displayed more than one of these abnormal morphologies and in these instances were scored in multiple categories: 20% belonged to all groups (Figure 2.2d, vi). These characteristics are typical of SCs that have lost quiescence, as upon activation SCs expand their nuclear content to enter mitosis, exit from beneath the basal lamina and display non-polarized M-cadherin.

Other requirements for maintaining the quiescent SC include activated Notch signaling. After the depletion of Rbpj protein, the downstream effector of the pathway, the number of $Pax7^{+}$ SCs declined over time, with a 75% reduction after 40 days (Bjornson et al., 2012; Mourikis et al., 2012). Using our $R26R^{LacZ/LacZ}$ genetic model to conditionally abrogate β1-integrin and stably lineage label SCs, we assessed for satellite cell number at staggered time points after tamoxifen injection via X-galactosidase reaction (Figure 2.3a-c). While the number of control SCs remained stable up to 6 months after tamoxifen, a sharp decline in satellite cell numbers in the *Itgb1*-KO tissue was observed (50% reduction after 21 days; and 80% reduction by 180 days) (Figure 2.3e). Interestingly, although β1-integrin protein is depleted after 3 days (Figure 2.1e), the loss of SCs was gradual under homeostatic conditions, suggesting a stochastic or

Figure 2.3. *Itgb1*-KO SCs are lost from the niche over time. a, Tamoxifen (tmx) regimen and tibialis anterior (TA) harvest scheme. Vertical lines, daily intervals. **b,** Tibialis anterior muscle diagram. Horizontal lines, cross sections. **c,** Representative X-gal stained muscle cross section images from 7 and 90 d post tmx; arrowheads, SCs; scale bar = 50 μm. **d,** Ratios of blue fibers over total fibers; data are expressed as mean ± s.e.m.; $n = 4$ animals per group, 10 sections per animal; Student's *t*-test; * = $p<0.05$. Blue fibers with diffuse X-gal signals at later time points were observed in rare clusters with uneven intensity (asterisks), and did not have SCs associated with them. These fibers also did not possess centrally located nuclei, suggesting that the mutant SC nuclei fused into existing fibers rather than creating new fibers *de novo*. Some control and mutant myofibers had blue punctas in later time points, likely representing low levels of homeostatic incorporation of SCs into myofibers over time that diluted LacZ enzyme to result in punctated X-gal signals. **e,** Ratios of SCs per fiber at 7, 21, 90, and 180 d post tmx of control (black boxes) and *Itgb1*-KO (white boxes) TA muscles; n = 3 per group; * = $p<0.05$, ** = $p<0.01$.

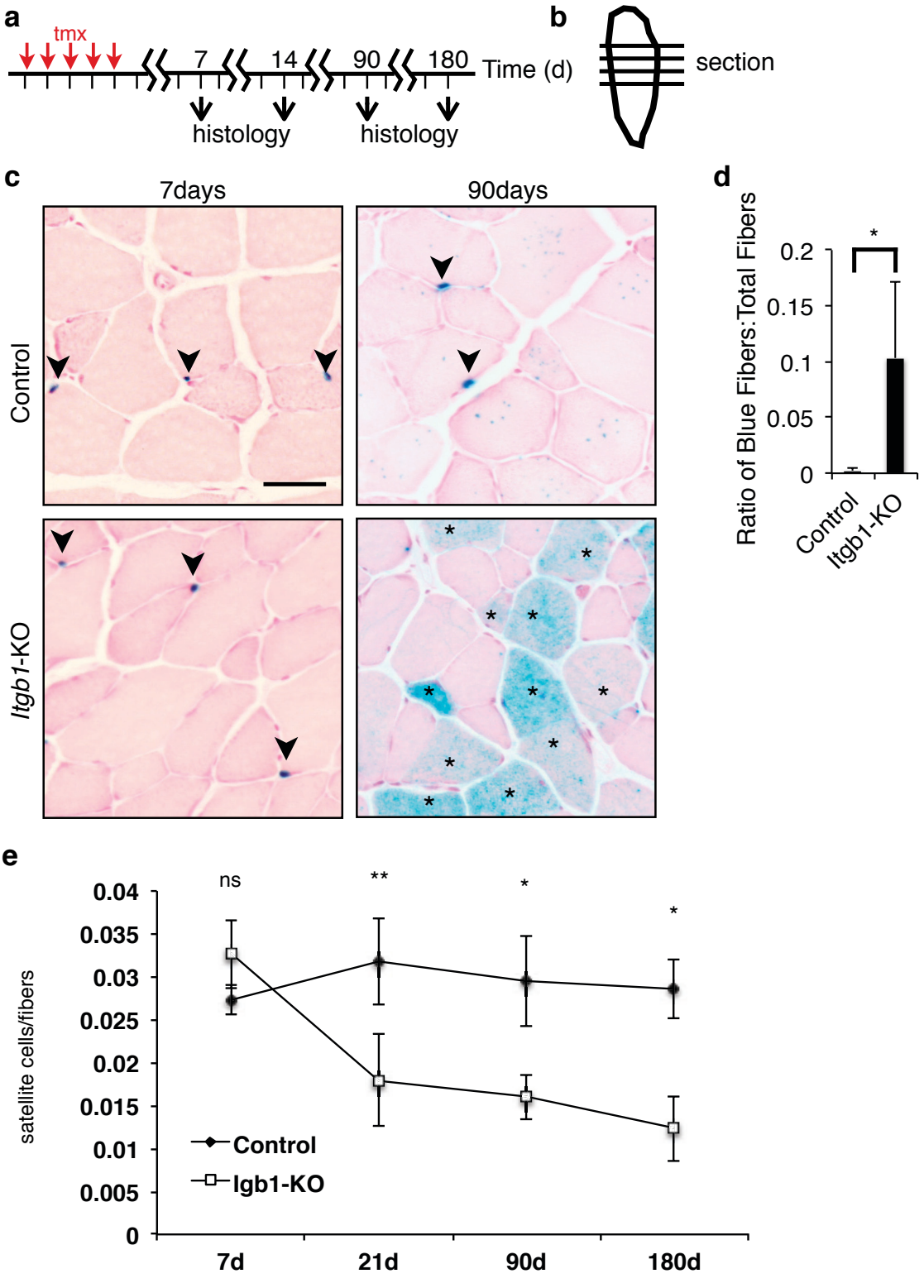
a
tmx
7
14
90
180
Time (d)
histology
histology
b
section
c
7days
90days
Control
Itgb1-KO
d
Ratio of Blue Fibers:Total Fibers
0.2
0.15
0.1
0.05
0
Control
Itgb1-KO
e
satellite cells/fibers
0.04
0.035
0.03
0.025
0.02
0.015
0.01
0.005
0
ns
**
*
*
Control
Igb1-KO
7d
21d
90d
180d

combinatorial effect. We examined the possibility that β1-integrin provided a physical attachment to the niche, which could be abrogated quicker by increased muscle tension or force. However, we did not observe an increased rate of SC loss after 5 consecutive days of exercise (swimming; data not shown), although it is possible alternative forms of muscle stimulation not yet tested would provide the necessary force to stimulate SC loss.

The sharp decline in the satellite cell numbers in *Itgb1*-KO animals suggest their elimination either by apoptosis, shifting cell fate, or fusing with myofibers. The presence of the lineage label allows for examination of *Itgb1*-KO SCs throughout their lifetime to assess these possibilities. Staining for cleaved caspase-3 to mark apoptotic cells did not show any cell death at any stage examined post-tamoxifen induction (data not shown). To further test the proclivity of *Itgb1*-KO SCs to undergo cell death we isolated myoblasts from mutant and control animals and again probed for cleaved caspase-3 (Figure 2.4). Without pretreatment with staurosporine, which induces cell death, no labeling with the apoptotic marker was visualized (Belmokhtar et al., 2001). Additionally, treatment with staurosporine yielded comparable numbers of apoptotic cells between mutant and control myoblasts. Although *Itgb1*-KO SCs were found in the interstitum (Figure 2.3c), no expression of nonmuscle markers was detected to suggest a change in cell fate. Therefore, this suggests the progressive reduction of the satellite cell pool was accompanied by fusion of β-gal-positive lineage-labeled derivatives of the SCs into myofibers. Accordingly, a significant number of labeled, β-gal-positive, myofibers were observed at 21 days post tamoxifen regimen (Figure 2.3d). No centrally located nuclei were observed, indicating that the process of myocyte fusion into existing myofibers is

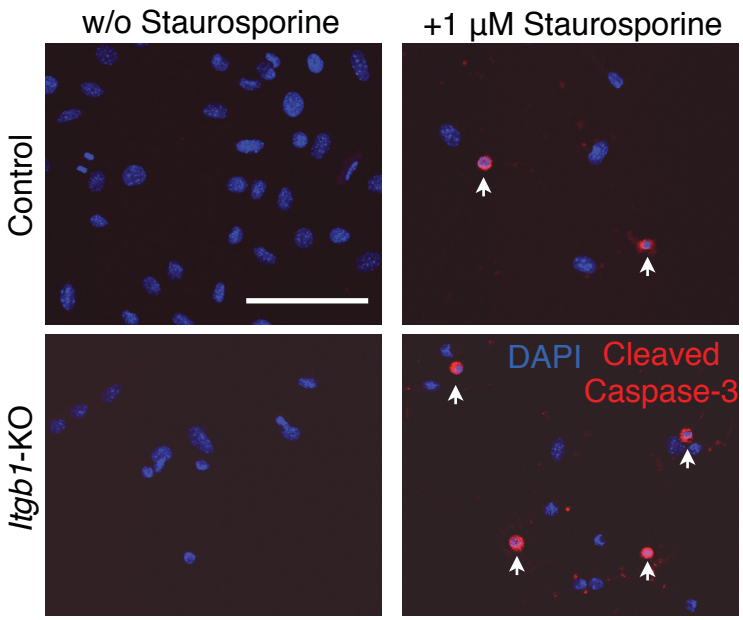

Figure 2.4. *Itgb1*-KO and control myoblasts do not undergo programmed cell death. Neither control nor *Itgb1*-KO myoblasts grown in growth media for 3d post isolation incorporate cleaved caspase-3 unless they are pretreated with 1μM staurosporine (Cell Signaling, 9953) 3h before fixation (scale bar, 50μm).

distinct from regeneration of new myofibers, which yields centrally located nuclei in mouse models (Chargé and Rudnicki, 2004). These findings indicate that β1-integrin is required to maintain quiescence and in its absence, satellite cells undergo differentiation into myofibers.

Evidence suggests that, while a portion of SCs lacking Notch signaling ($RBPK^{KO}$) undergo at least one round of mitosis before fusing into adjacent myofibers, a significant percentage may undergo differentiation and fusion without entering the cell cycle (Bjornson et al., 2012; Mourikis et al., 2012). To monitor the potential of *Itgb1*-KO SCs to enter the cell cycle, we dissolved the thymidine analog BrdU in drinking water and administered to animals for 30 days post tamoxifen before harvesting tibialis anterior muscles and sectioning for analyses (Figure 2.5a,b). Lineage-labeled (YFP^+) cells were scored for the incorporation of BrdU, indicating entry into S-phase of the cell cycle during the time course we observed SC reduction (Figure 2.5c,e). We observed significantly higher $BrdU^+$ SCs in *Itgb1*-KO sections compared to controls, indicative of the loss of quiescence in mutant satellite cells (Figure 2.5e). However, we did not observe any $BrdU^+$ myonuclei present in cross-sections of *Itgb1*-KO muscles suggesting that the cells fusing to myofibers do so without entering the cell cycle, consistent with previous results. Additionally, the numbers of differentiation-competent *Itgb1*-KO SCs solely at isolation, as assessed by MyoD expression, is 10% higher than BrdU labeling during the entire 30-day chase period (Figure 2.5d,f). Unless the BrdU labeling protocol does not account for all cells entering the cell cycle, these data suggest that *Itgb1*-KO SCs may undergo terminal differentiation and fusion without proliferating. This observation of cycling and non-cycling *Itgb1*-KO SCs, along with the time differences in SC loss,

Figure 2.5. *Itgb1*-KO SCs are prematurely activated. a, Tamoxifen (tmx) regimen and tibialis anterior (TA) harvest scheme. For long-term proliferation assay, BrdU was administered in drinking water (0.8 mg/ml) for 1 mo post tmx regimen. Vertical lines, daily intervals. **b,** Tibialis anterior muscle diagram. Horizontal lines, cross sections. **c,e,** SCs from control and *Itgb1*-KO animals fed with BrdU; $n = 4$ per group. **c,** Immunostained for YFP and BrdU; scale bar = 25μm. **e,** Percentages of $BrdU^+$/total YFP^+ cells of control and *Itgb1*-KO animals. **d,f,** The same animals in (**c**) immunostained for MyoD (**d**) and quantified (**f**). Arrowheads indicate $YFP^+marker^-$ cells. Arrows indicate $YFP^+marker^+$ cells. All numerical data are presented as mean ± s.e.m, and subjected to Student's *t*-test: * = $p < 0.05$; ** = $p < 0.01$.

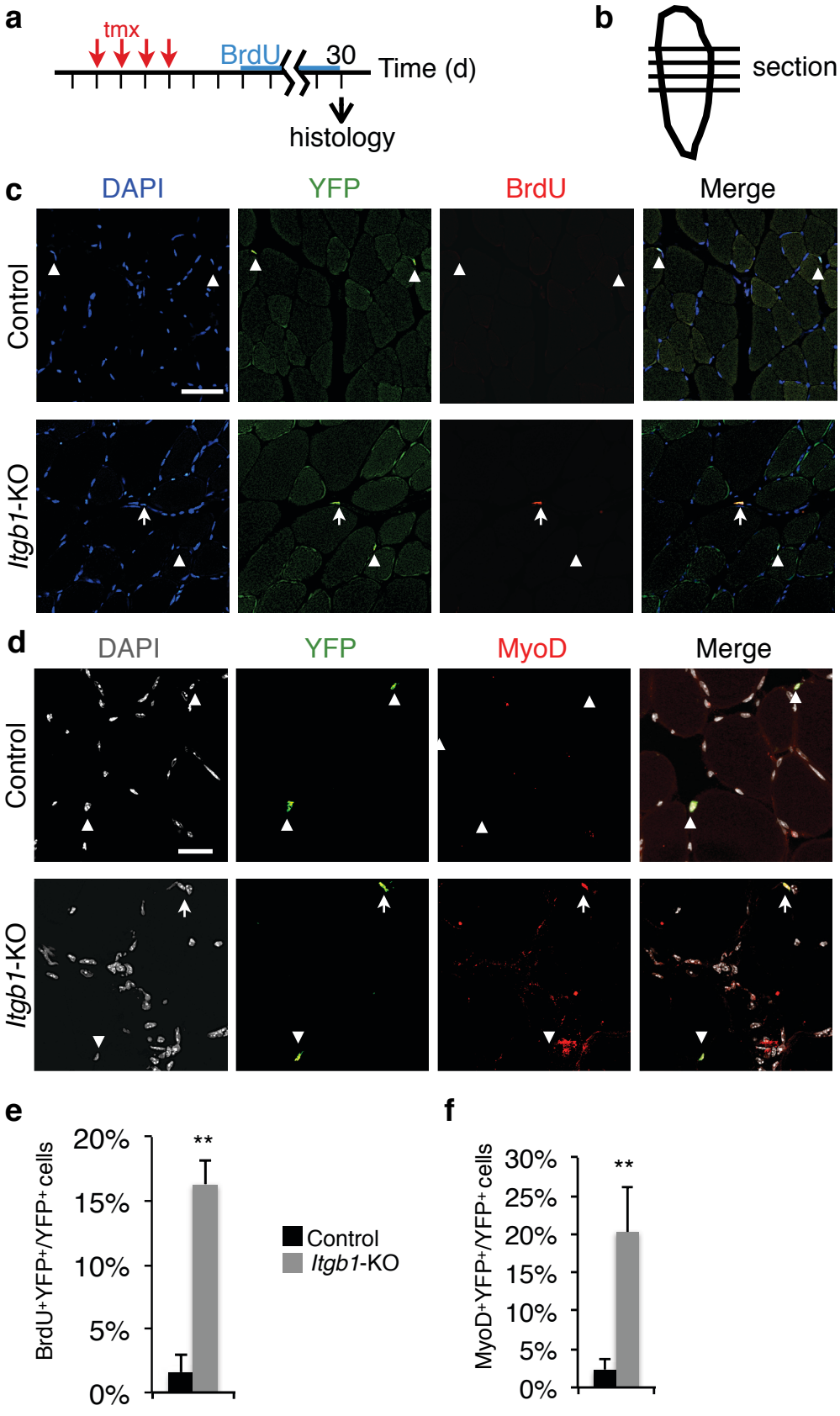
a
tmx
BrdU
30
Time (d)
histology
b
section
c
DAPI
YFP
BrdU
Merge
Control
Itgb1-KO
d
DAPI
YFP
MyoD
Merge
Control
Itgb1-KO
e
BrdU+YFP+/YFP+ cells
20%
15%
10%
5%
0%
**
Control
Itgb1-KO
f
MyoD+YFP+/YFP+ cells
30%
25%
20%
15%
10%
5%
0%
**

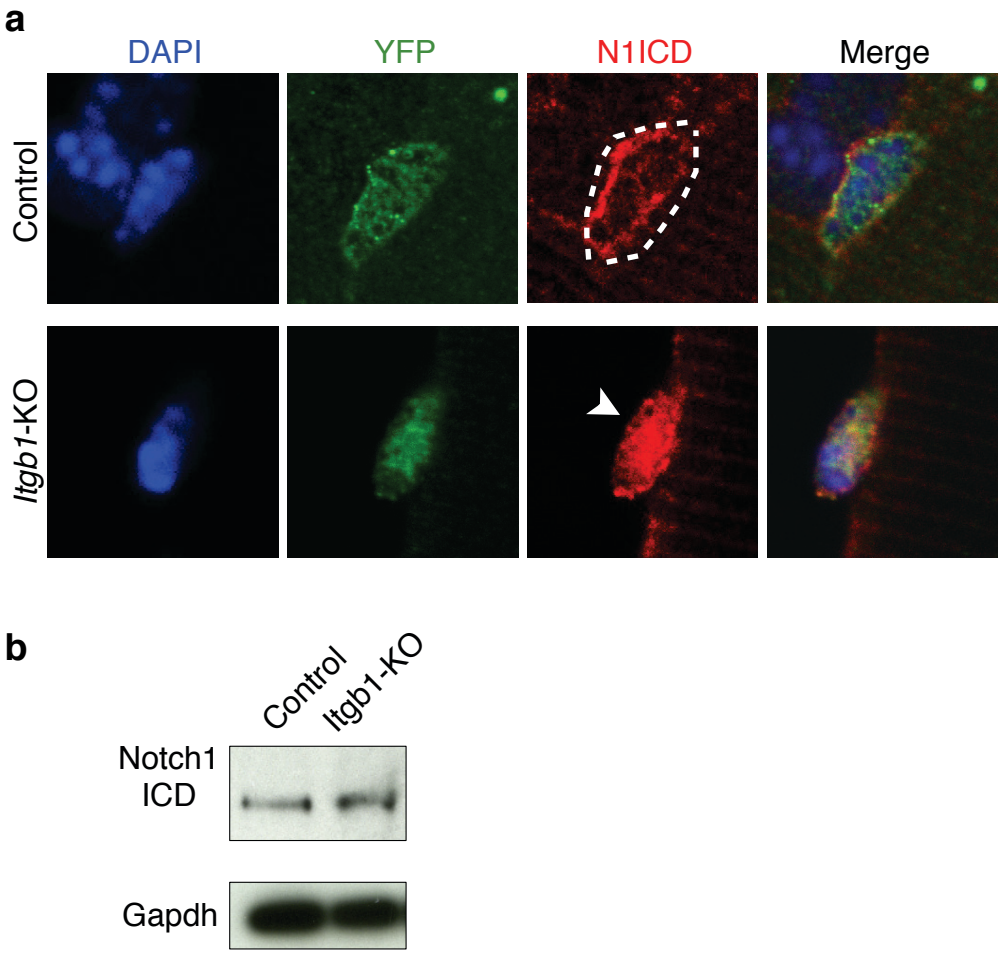

Figure 2.6. *Itgb1*-KO SCs are abnormally activated but possess normal levels of Notch1 signaling upon activation. a, Myofiber-associated YFP^{+} SCs of control and *Itgb1*-KO mice were fixed immediately after harvesting to preserve the quiescent SC in its niche and stained for the intracellular domain of Notch1 (N1ICD), which is cleaved to translocate into the nucleus upon Notch pathway activation. Dotted lines indicate N1ICD present in its pre-cleaved, membrane-bond form. Arrowhead indicates nuclear localization of N1ICD. **b,** Western blot of myoblasts from control and *Itgb1*-KO mice probed for N1ICD indicate that *Itgb1*-KO SCs display comparable levels of Notch1 signaling upon activation. Myoblasts were harvested and cultured in growth media (GM) (20%FBS, 10%HS, 1%CEE) for 48h before administration of 0.4 μM 4-OH tamoxifen. Cells were then cultured for an additional 72 h in GM before lysis buffer was added for collection of protein. Differential plating was utilized to obtain a pure myoblast population.

points to heterogeneity in the SC pool and differential requirements for β1-integrin in the niche.

Given the similarities between satellite cells depleted of RBP-J and β1-integrin, we next assessed whether the Notch signaling pathway could be functioning downstream of integrin. We examined Notch activity by probing for the Notch1 intracellular domain (N1ICD). Binding of Notch receptors to ligands triggers proteolytic cleavage of the intracellular domain, which translocates to the nucleus to activate transcription of target genes (Andersson et al., 2011). Therefore, not only the amount, but also the localization of the ICD correlates with Notch activity; the membrane-bound form indicates inactivity, while nuclear localization signifies active signaling. A significant proportion of N1ICD is nuclear in *Itgb1*-KO SCs in contrast to control YFP^+ SCs that have the majority of N1ICD present on the membrane with only a subset in the nucleus (Figure 2.6a). However, the relative amount of N1ICD does not differ between protein lyses from control and *Itgb1*-KO myoblasts 3 days after activation, suggesting that the aberrant Notch activity is merely a reflection of the quiescent *Itgb1*-KO phenotype and does not indicate a link between the two pathways. Together, these data suggest that β1-integrin senses proper SC-niche interaction to prevent spurious activation and differentiation.

β1-integrin is required for muscle regeneration

To determine if *Itgb1*-KO conditional mutant SCs can support muscle regeneration, cardiotoxin was used to injure the tibialis anterior muscle of tamoxifen-treated animals (Figure 2.7a). The lineage label allows for tracking the fate of mutant cells in

Figure 2.7. β1-integrin is required for muscle regeneration. a, Tamoxifen (tmx) regimen cardiotoxin (CTX) regimen and regeneration assay scheme. Animals harvested either at 5d or 10d post injury. Images unless otherwise noted are from muscles harvested at 5d post injury. Vertical lines, daily intervals. Tibialis anterior muscle diagram with injury in grey. Horizontal lines, cross sections. **b,** Whole TA muscle from control and *Itgb1*-KO animals harvested 5d post CTX. **c,** X-galactosidase stained muscle sections (scale bars, 150μm). Black boxes indicate the area that is magnified in the subsequent image. **d**, Average number of fibers per field at 5 d and 10 d post injury; n = 3-4 animals, 20 sections scored per animal. Only fibers with centrally localized nuclei were quantified. **e,** Mean diameter at 5 d and 10 d post injury; n = 3-4 animals, 20 sections scored per group. Numerical data are presented as mean ± s.e.m, and subjected to Student's t-test: * = $p < 0.05$; ** = $p < 0.01$.

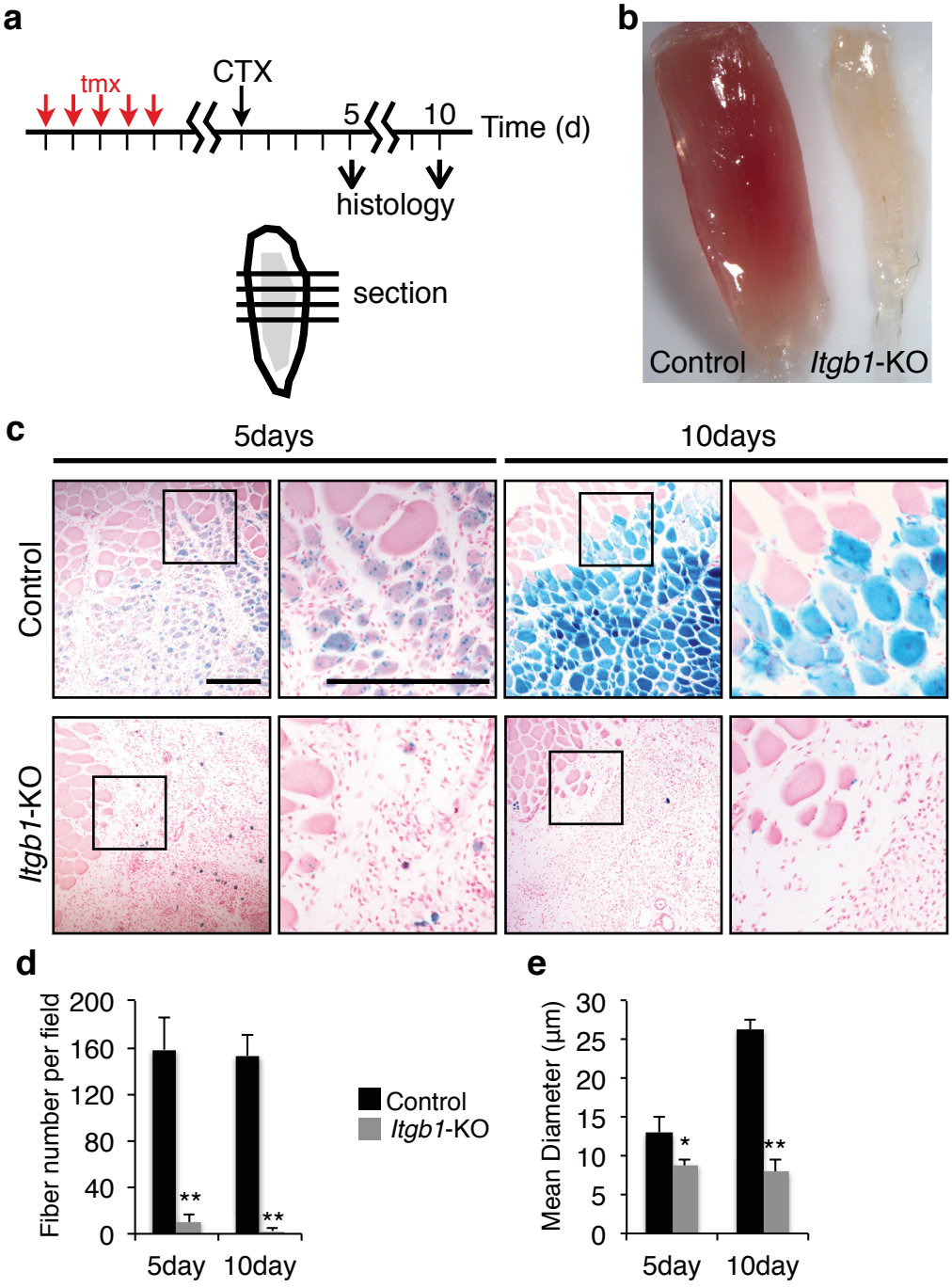
a
tmx
CTX
5
10
Time (d)
histology
section
b
Control
Itgb1-KO
c
5days
10days
Control
Itgb1-KO
d
Fiber number per field
200
160
120
80
40
0
**
**
5day
10day
Control
Itgb1-KO
e
Mean Diameter (μm)
30
25
20
15
10
5
0
*
**
5day
10day

regenerative myogenesis, as assessed by X-galactosidase reactions at both 5-day and 10-day time points after injury. The contrast between control and mutant muscles was grossly apparent in whole muscle immediately upon isolation of the tibialis anterior (Figure 2.7b). *Itgb1*-KO muscles were significantly smaller and devoid of any red color, which is indicative of the higher innervation of muscle tissue, suggesting a substantial regenerative defect. Indeed, regenerative myogenesis was almost completely absent in *Itgb1*-KO animals (Figure 2.7c). Uninjured muscle fibers are β-gal$^-$; all newly regenerated myofibers are positive for β-gal signifying their succession from labeled SCs. While thousands of labeled myofibers are present in control muscles 5-days after injury, and continue to grow in diameter until 10-days after injury, there are almost no myofibers at 5-day and 10-days post injury (Figure 2.7d,e). Indeed, significant reduction was found between the numbers of new muscle fibers generated from *Itgb1*-KO and control SCs at 5- and 10-day post injury (Figure 2.7d,e). Labeled myofibers are virtually absent at 10-days post injury. The loss of β-gal$^+$ myofibers from 5- to 10-days post injury in *Itgb1*-KO animals is likely due to muscle fiber instability and degeneration, as β1-integrin is required to maintain muscle integrity and prevent dystrophy (Mayer et al., 1997). Further, significant differences in fiber size were detected by measuring mean diameter (Figure 2.7e). This almost complete absence of muscle repair is reminiscent of that observed in the Pax7$^{-/-}$ mice, which was described as "the most striking regeneration deficit reported in any mouse model" (Kuang et al., 2006). The severity of the phenotype, which corresponds to that reported in *Pax7* deficient mice, suggests a role for β1-integrin in stem cell function.

Figure 2.8. *Itgb1*-KO SCs can differentiate but cannot self-renew. a, Tamoxifen (tmx) regimen cardiotoxin (CTX) regimen and regeneration assay scheme. Animals harvested either at 5d or 10d post injury. Images unless otherwise noted are from muscles harvested at 5d post injury. Vertical lines, daily intervals. **b,** Tibialis anterior muscle diagram with injury in grey. Horizontal lines, cross sections. **c-d,** Regeneration capacity was assessed by embryonic myosin heavy chain (eMyHC) to assess newly regenerating fibers (**c**), MRF myogenin to mark terminally differentiated cells (**d**). All markers are in red, YFP in green, and DAPI in blue. Arrows indicate YFP^+;$marker^+$ cells. Arrowheads, YFP^+/$marker^-$ cells. Scale bars, 25μm. Quantification for each marker analysis is shown below the representative images. YFP^+ cells or fibers were evaluated for marker expression from random fields of TA muscle sections from 3 independent samples for each condition. The percentages were calculated as YFP^+;$marker^+$/$marker^+$ cells averaged from 3 samples. All numerical data are presented as mean ± s.e.m, and subjected to Student's *t*-test: ** = $p < 0.01$.

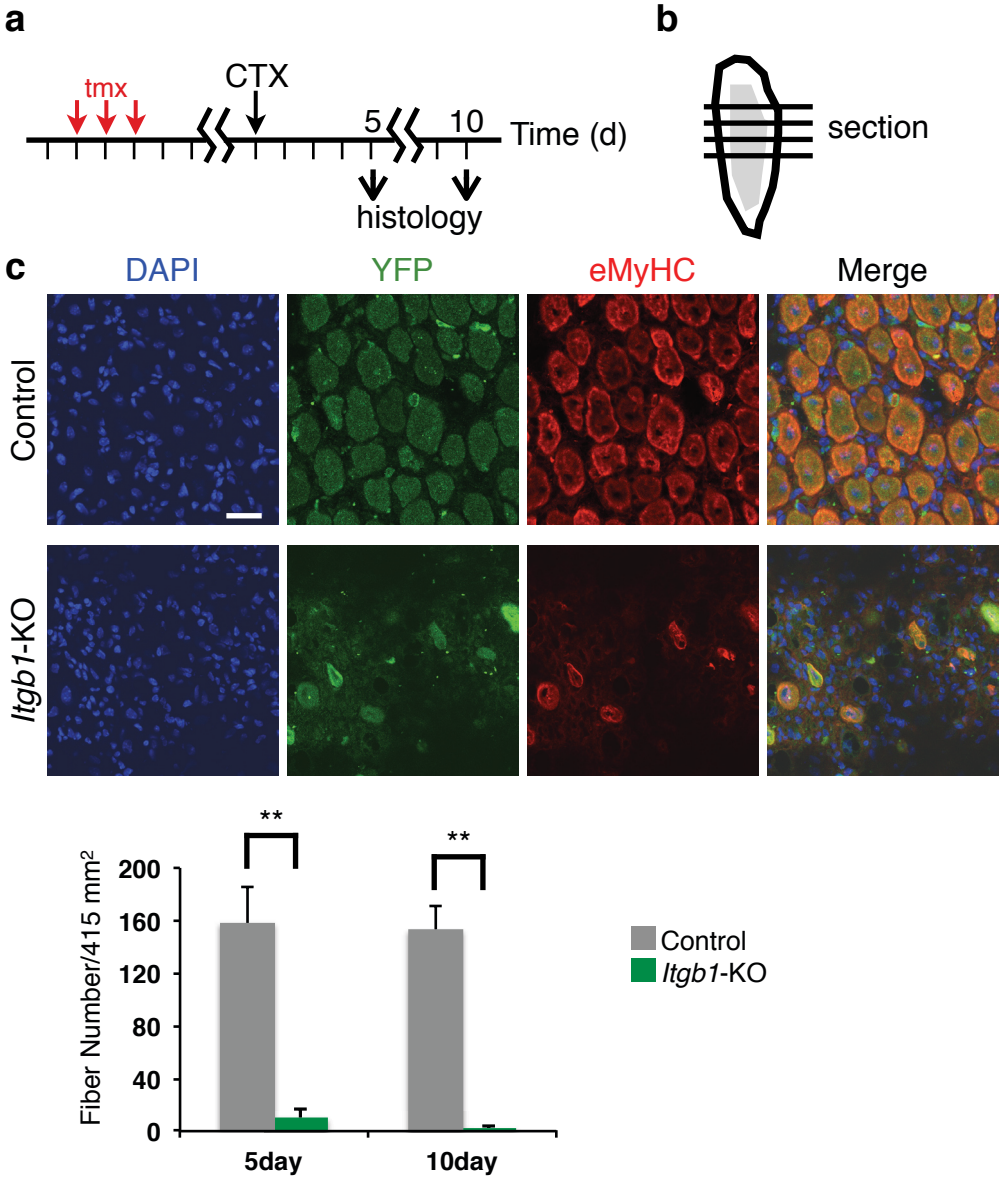
a
tmx
CTX
5
10
Time (d)
histology
b
section
c
DAPI
YFP
eMyHC
Merge
Control
Itgb1-KO
Fiber Number/415 mm2
200
160
120
80
40
0
**
**
5day
10day
Control
Itgb1-KO

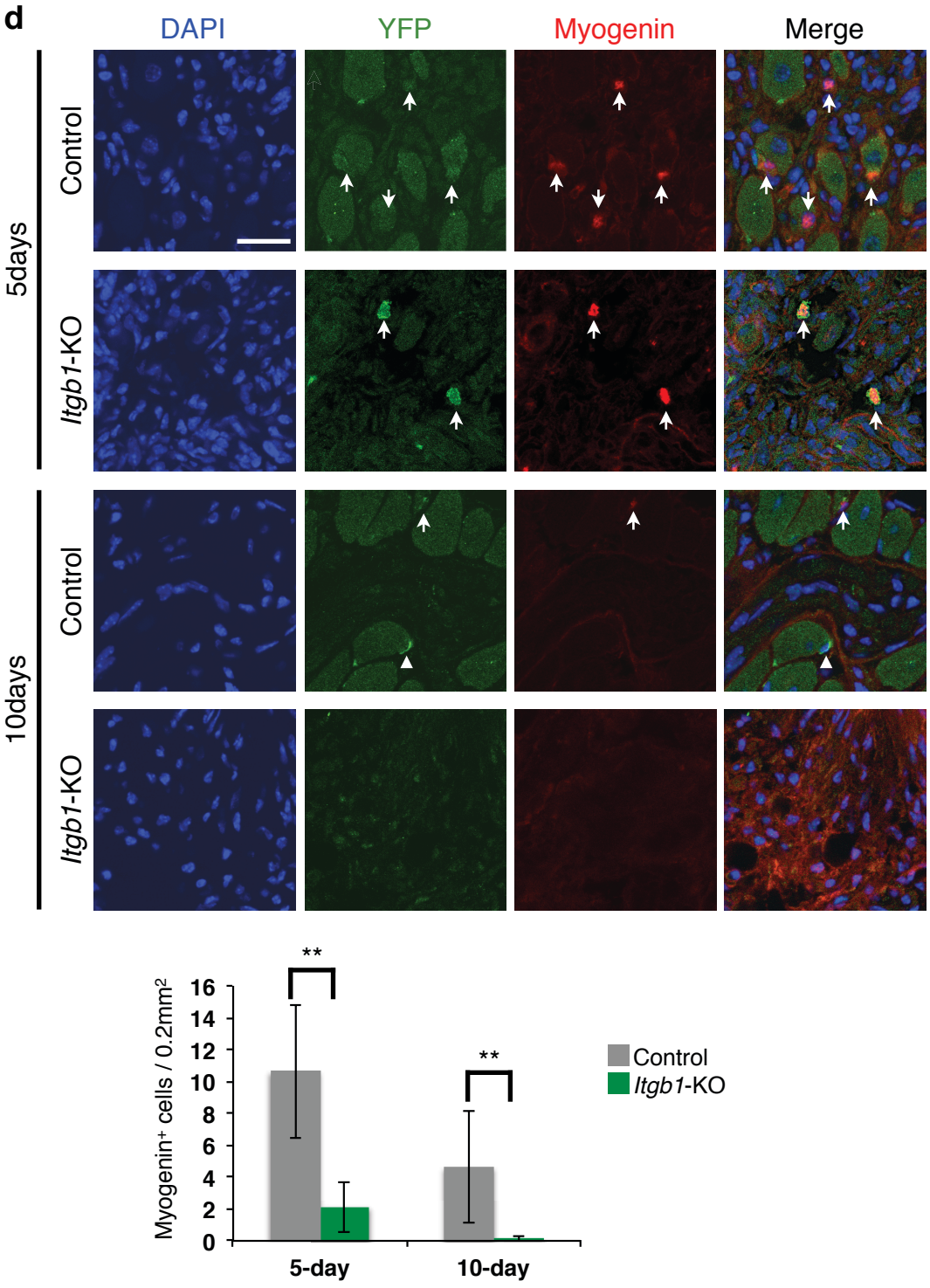
d
DAPI
YFP
Myogenin
Merge
5days
Control
Itgb1-KO
10days
Control
Itgb1-KO
Myogenin+ cells / 0.2mm2
16
14
12
10
8
6
4
2
0
**
**
5-day
10-day
Control
Itgb1-KO

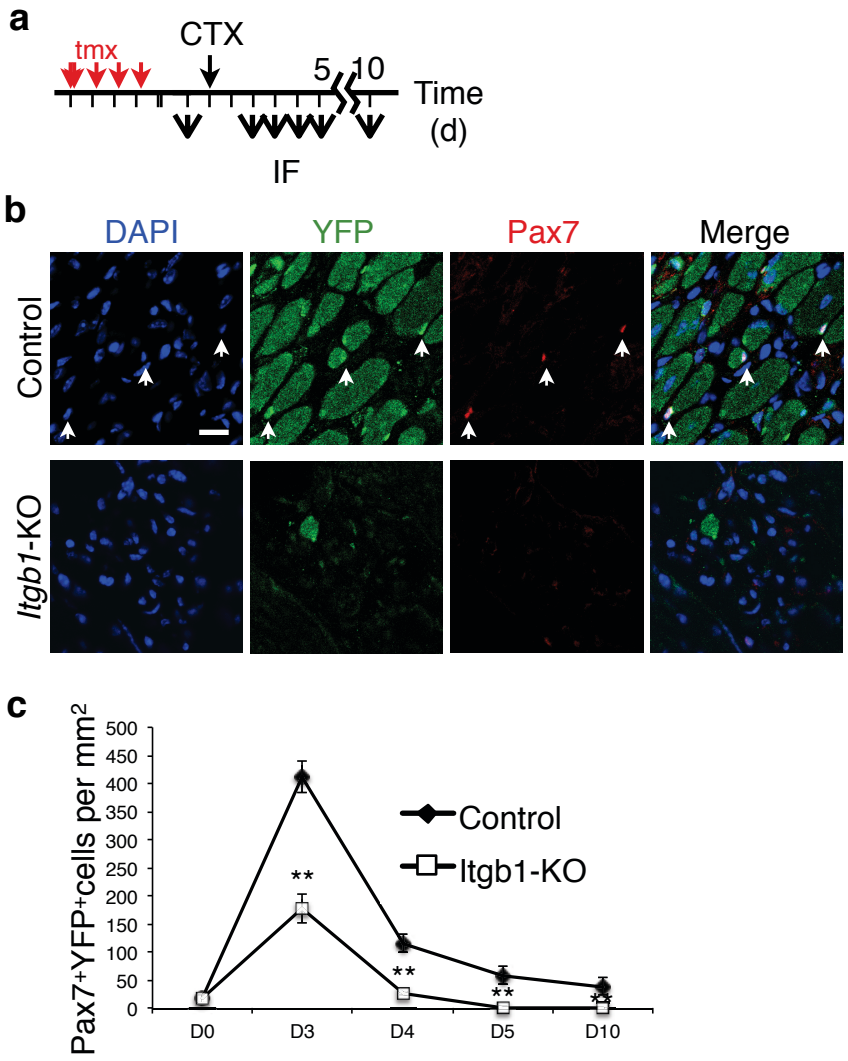

Figure 2.9. *Itgb1*-KO SCs cannot maintain Pax7 expression. a, Schematic of tmx and CTX regimen and regeneration assay to assess self-renewal capacity of *Itgb1*-KO SCs. **b,** Image of control and *Itgb1*-KO TA sections 10 d after injury. Arrows indicate $Pax7^+$ SCs; scale bar = 25 μm. **c,** Average number of $Pax7^+/YFP^+$ cells per mm^2 through the course of the regenerative process. Data are expressed as mean ± s.e.m, and subjected to Student's *t*-test: * = $p < 0.05$; ** = $p < 0.01$; $n = 3$ animals per timepoint, 10 sections scored per animal.

Itgb1-KO SCs can differentiate but cannot self-renew

β1-integrin is absolutely required for injury-induced myogenesis. To investigate the defects in *Itgb1*-KO SCs, we assessed whether mutant cells were capable of following the myogenic developmental program. The presence of small numbers of myofibers with centrally located nuclei in *Itgb1*-KO muscle at 5 days after injury suggests a limited capacity for muscle differentiation. As in wildtype animals, the centrally nucleated fibers expressed embryonic MyHC, which confirms their newly regenerated state (Figure 2.8c). Furthermore, incorporation of the myogenic marker myogenin was also seen 5-days after injury (Figure 2.8d). Although the number of lineage-labeled myogenin$^+$ cells is significantly decreased in *Itgb1*-KO animals compared to controls, the myogenic potential of *Itgb1*-KO SCs is maintained, as cells are still capable of differentiating. In contrast, the ability for self-renewal is compromised in *Itgb1*-KO SCs (Figure 2.9). YFP$^+$/Pax7$^+$ SCs are essentially absent even at 5-days after injury, demonstrating the inability of *Itgb1*-KO SCs to maintain the stem cell pool.

Consistent with previous studies, we also found adult *Itgb1*-KO myoblasts migrated and fused poorly *in vitro* (Schwander et al., 2003; Siegel et al., 2009) (Figure 2.10). Lineage-labeled myoblasts derived from *Itgb1*-KO SCs were plated in growth media to induce activation and then serum-starved to induce differentiation into myotubes. Myoblasts from control animals fused robustly into multi-nucleate fibers, while *Itgb1*-KO myoblasts were rarely able to form myofibers, instead predominating in single cells or doublets (Figure 2.10a,b). However, it is unlikely that these defects

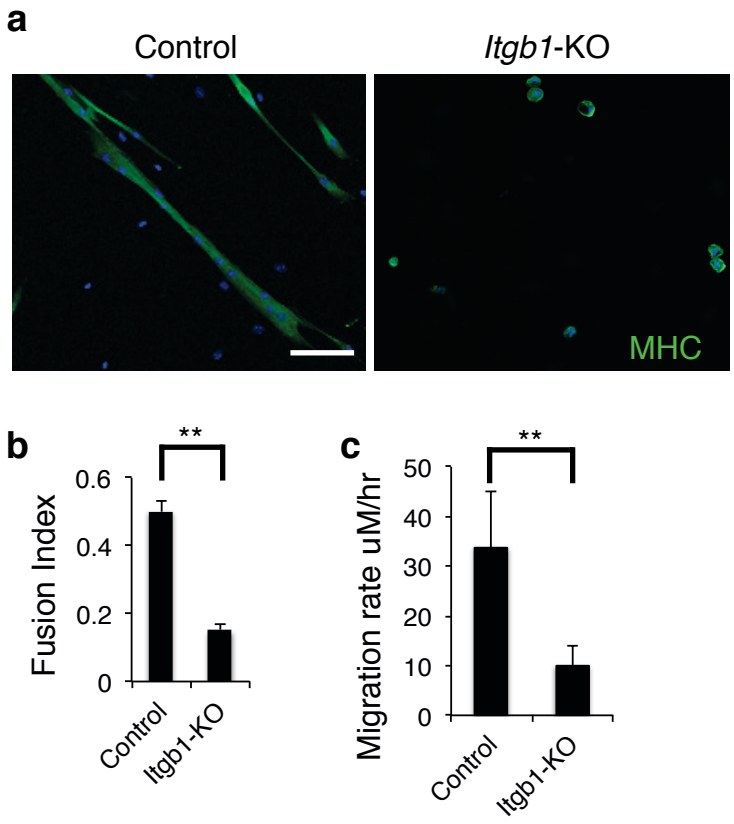

Figure 2.10. *Itgb1*-KO myoblasts are defective in fusion and migration. a, Control and *Itgb1*-KO myoblasts isolated from bulk culture were plated on matrigel-coated 8-well chamber slides at high-density (49,000 cells/cm2). Differentiation media (10%HS) was added to wells and cells were cultured for 3d before fixation and staining with myosin heavy chain (MHC). Scale bar, 50μm (**a**) to assay for fusion index (**b**). Fusion index was determined by the ratio of MHC+YFP+ cells with more than one nuclei per total nuclei in MHC+YFP+ cells. (c) To measure cell velocities, brightfield images were captured every 6 minutes from 1 field per well of control and *Itgb1*-KO myoblasts plated at 10,000 cells per well in a 12-well dish. A series of images using the GFP filter was taken prior to migration analysis for identification of YFP^+ cells. Individual cell velocities were measured using Metamorph software. Numerical Data are expressed as mean ± s.e.m., n = 3 experiments; Student's t-test;** = $p<0.01$.

account for the severe regeneration defects observed in *Itgb1*-KO muscles post-injury. Previous studies disrupted focal adhesion kinase (FAK) and PKCθ signaling, both factors required for upregulating the expression of the 1D isoform of β1-integrin during differentiation (Madaro et al., 2011; Quach et al., 2009). While impairment of muscle regeneration was reported in both studies, defects were mild compared to the *Itgb1*-KO phenotype (50% reduction in myofiber number compared to the 90% reduction reported here). Analysis revealed a delay instead of a block in regeneration characterized by smaller regenerating myofibers and heterogeneity of myofiber sizes at day 5-post injury that is resolved by 1-month post injury (Quach et al., 2009). The requirement of β1D-integrin for fusion most likely explains the reduced diameter of regenerated fibers observed at 5-days post injury in *Itgb1*-KO animals (Figure 2.7e), however the severity of the detected defect suggests a deficiency earlier in the regenerative process.

β1-integrin is required to sustain SC proliferation

Integrins function to coordinate growth factor signals in many cell types, together constituting a checkpoint that monitors cell progression from G1 to S phase controlling advancement through the cell cycle (Moreno-Layseca and Streuli, 2014). To test if β1-integrin is required for proliferation, we injected animals with thymidine analog EdU at daily intervals post cardiotoxin injection, and then harvested whole muscle on each subsequent day to label the proliferative cells each day after injury (Figure 2.11a,b). Comparable levels of EdU^+ nuclei in YFP^+ fibers were detected in both control and *Itgb1*-KO regenerates at 2 days after injury (Figure 2.11d). However, the number of cycling

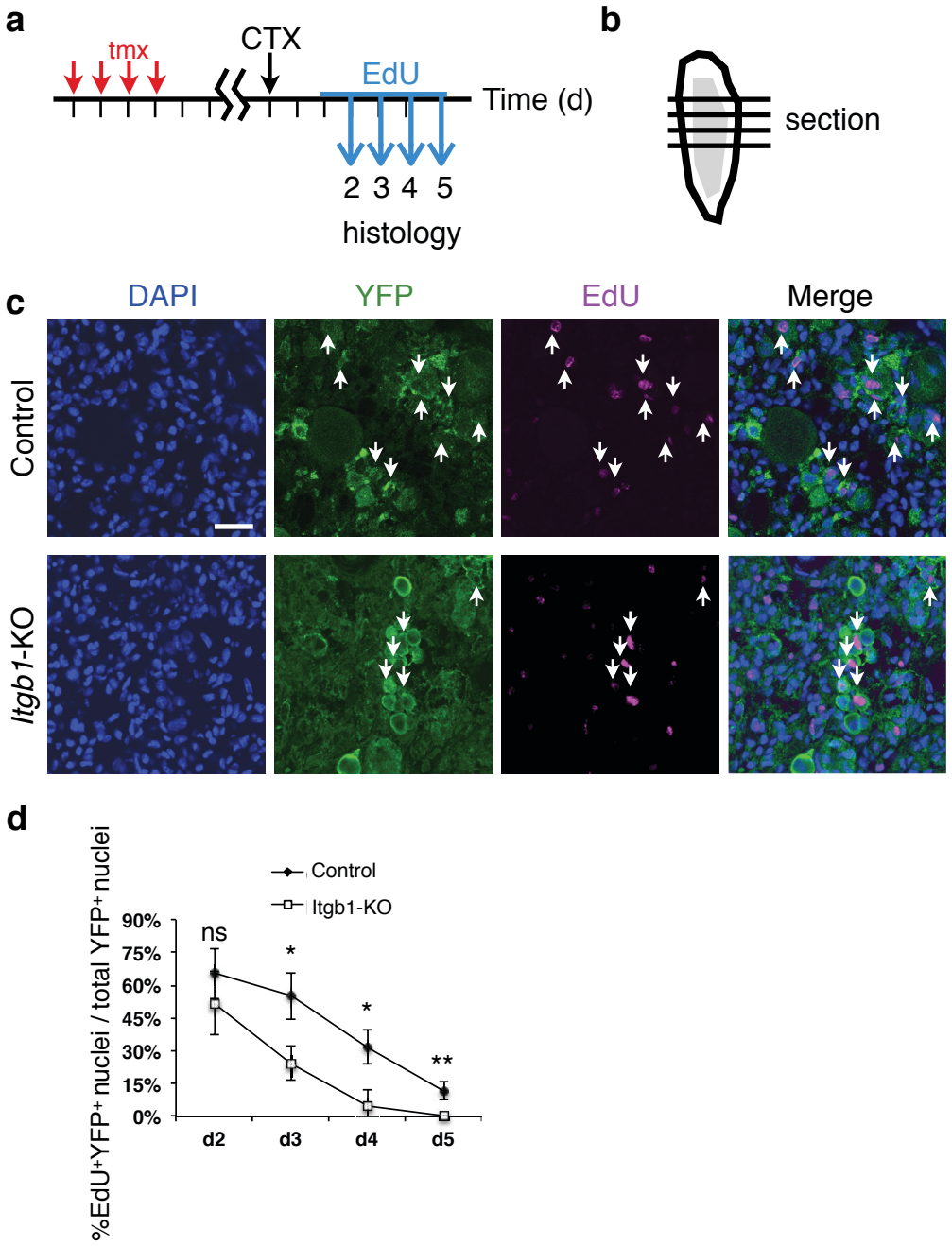

Figure 2.11. β1-integrin is required to sustain SC proliferation. a, Tamoxifen (tmx) regimen cardiotoxin (CTX) regimen and regeneration assay scheme. Vertical lines, daily intervals. **b,** Tibialis anterior muscle diagram with injury in grey. Horizontal lines, cross sections. **c,d,** Animals were injected with EdU (0.1 mg per 20 g bodyweight) 12 h prior to harvesting to label cells proliferating on each day post injury (d2-d5), and stained with YFP and EdU (scale bar, 50μm) (**c**) and plotted as percent EdU^+ nuclei over total YFP^+ nuclei (**d**) Data are expressed as mean ± s.e.m., n = 3 experiments per condition; Student's t-test; * = p <0.05; ** = p <0.01; ns = non-significant.

cells was significantly reduced by 3 days after injury with a 50% reduction in EdU^+ labeled cells in mutant sections compared to controls (Figure 2.11c,d). EdU incorporation continued to decline at 4 and 5 days post injury, with *Itgb1*-KO cells halting proliferation earlier than control cells.

To analyze proliferative capacity at a single-cell resolution, we utilized time-lapse microscopy to follow labeled SCs and their subsequent daughters through cell divisions (Figure 2.12a). Cells were harvested and plated in growth media for 24 hours to induce activation before being transferred to differentiation media for imaging for a subsequent 72 hours, which captured not only the first round, but all subsequent rounds, of the cell cycle (Siegel et al., 2011). During the course of this assay, SCs carried out an *in vitro* approximation of myogenesis: proliferating, differentiating, and fusing into myotubes. We scored the number of divisions that a single SC was capable of sustaining by following a single labeled cell and each of its daughters through the course of the imaging protocol. The number of divisions per cell was scored as the maximal numbers of daughters produced. The majority of *Itgb1*-KO SCs did not divide at all (60%), and those that did proliferate were able to complete two rounds of the cell cycle at most, compared to as many as four in control cells (Figure 2.12c). Consistent with these observations at a single-cell level, global FACS analysis utilizing a protein cell tracking dye that permits the determination of the number of generations through which cells progressed, showed control cells contributing to more generations than *Itgb1*-KO over 72 hours (Tario et al., 2012)(Figure 2.13e). For those cells that did divide, the time prior to the first division was not significantly different between control and mutant myoblasts: both divided at around 50 hours post isolation (Figure 2.12d). However, the majority of

Figure 2.12. Live imaging of *Itgb1*-KO myoblasts reveal defects in cytokinesis. a, Tamoxifen (tmx) regimen and myoblast harvest scheme. Myoblasts were plated on matrigel in a 6-well dish, 20,000 cells per well, and cultured for 24 h in PM. Prior to imaging, GM was substituted into the wells. Images were captured every 6minutes from 2 fields in each well for 72 h. The GFP filter was used to locate YFP^+ SCs, subsequent images were taking using DIC. **b,** Sequence of Hoffman modulation contrast (HMC) images showing live *Itgb1*-KO myoblast undergoing division. The cell is unable to complete cytokinesis (iv) and eventually fuses (v). Scale bar, 10μm. **c-e,** Followed a single cell over the course of the 72 h imaging period; counted the number of divisions (**c**) it sustained, the time to first division (**d**), and the duration of division (**e**). Did not count cells that migrated out of frame. Student's *t*-test; * = $p < 0.05$. **d-e,** Plotted as box plot with vertical lines depicting the median of the set. Max outliers shown as red x's. **d,** Added 24 h to raw number, the time from isolation to first image. **e**, Duration from doublet (iii) to cells separating, *Itgb1*-KO cells that did not separate during imaging (v), were scored as maximum time. n=3, between 50-100 cells/animal.

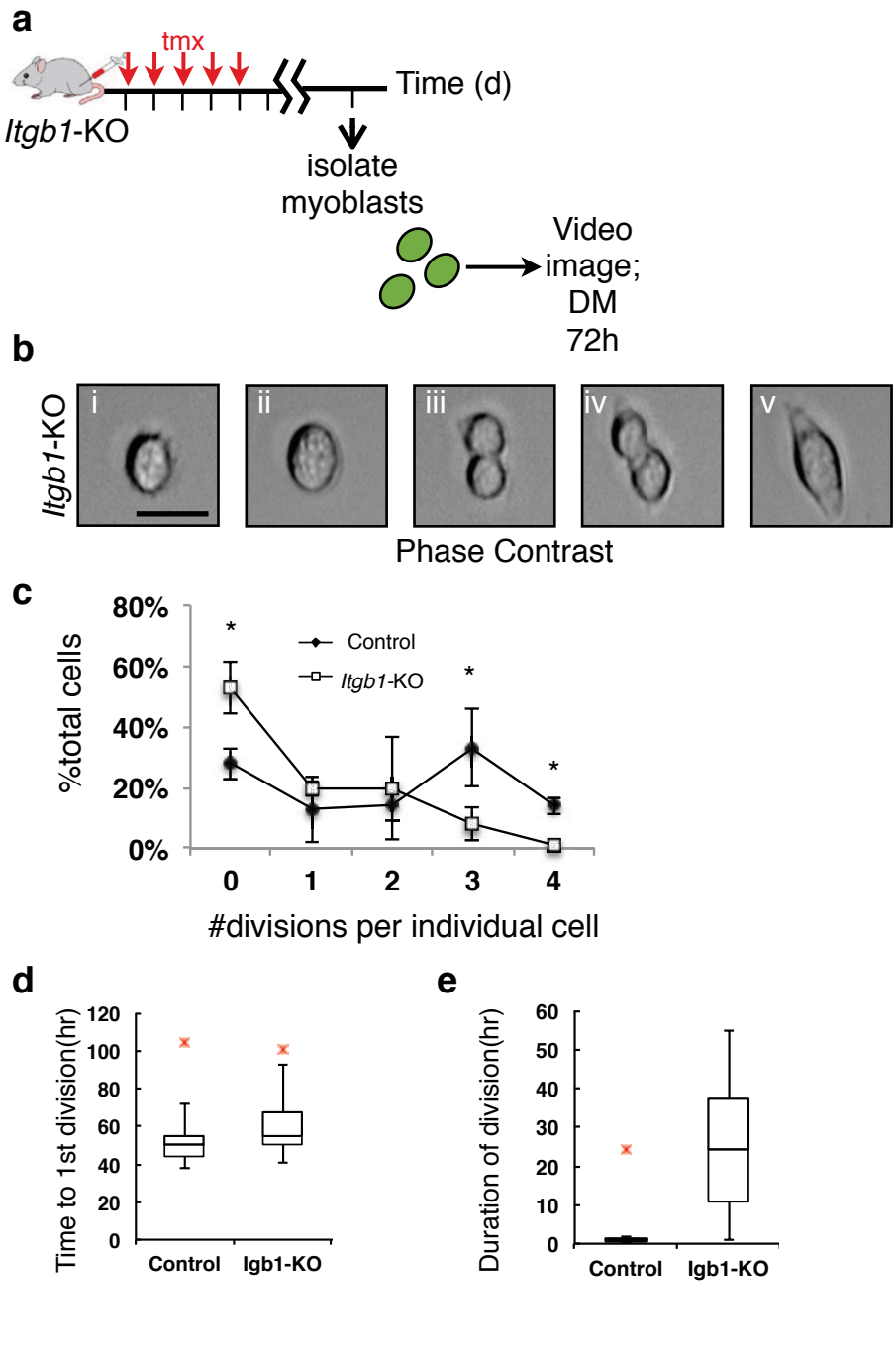
a
tmx
Time (d)
Itgb1-KO
isolate
myoblasts
Video
image;
DM
72h
b
Itgb1-KO
i
ii
iii
iv
v
Phase Contrast
c
%total cells
80%
60%
40%
20%
0%
Control
Itgb1-KO
*
*
*
0
1
2
3
4
#divisions per individual cell
d
Time to 1st division(hr)
120
100
80
60
40
20
0
Control
Igb1-KO
e
Duration of division(hr)
60
50
40
30
20
10
0
Control
Igb1-KO

Itgb1-KO cells remain associated for many hours, while control cells quickly complete cytokinesis and regain migration (Figure 2.12e). Mutant cells appear to stall, elongate into a shape characteristic of differentiated myocytes, and then fuse to create binucleate cells (Figure 2.12b).

To determine whether proliferative defects were associated with misregulation of the cell cycle, DNA content of control and mutant cells labeled with propidium iodide were determined by FACS analysis at 24 hour intervals following isolation (Figure 2.13a). We gated YFP^+ cells and then plotted them in the histogram of PI staining (Figure 2.13b). Cell cycle analysis showed a clear transition of populations through the various stages of the cell cycle: at 24 hours post-activation, prior to completion of the first division, the majority of control and *Itgb1*-KO cells were present in G1 (91.4 and 89.7% respectively), by 48 hours many had transitioned through the first round of the cell cycle, accumulating in G2/M (29% and 35%, respectively), and by 72 hours control cells were in the middle of their second round of the cell cycle (44% in S phase) (Figure 2.13c). While *Itgb1*-KO cells are indistinguishable from their control counterparts in cell cycle progression through 48 hours, by 72 hours they arrested in G1 and G2/M (Figure 2.13d).

To further support the observation that loss of β1-integrin induced cell cycle arrest, we used Western blotting to probe the level of cell cycle regulatory proteins (cyclins D1, D2, D3, E, A, and B). We examined total protein lysate harvested from control and *Itgb1*-KO cells at 72 hours post activation when the arrest phenotype was observed (Figure 2.14). There was no observed difference in levels of cyclin E, which regulates the checkpoint from G1 to S, cyclin A, which regulates transition from S to G2/M, or cyclin D3 between control and *Itgb1*-KO cells.

Figure 2.13. *Itgb1*-KO myoblasts stall in G1 and G2/M of the cell cycle. a, Tamoxifen (tmx) regimen and myoblast harvest scheme. Myoblasts were plated on matrigel in a 12-well dish, 10,000 cells per well, and cultured in GM. **b-d,** Cells were fixed sequentially at 24, 48, and 72 h after isolation and stained with propidium iodide (PI) overnight. Cells were run on a BD FACS ARIA III and FACS Diva software, gating first for cell size and using forward and side scatter and then gating for YFP+ cells using the 488 channel. **b,** Representative FACS plot from control and *Itgb1*-KO cells 72 h after isolation. **c,** Percentage of cells in G1(black), S(light grey), and G2/M(dark grey) at the three timepoints, as determined by running FACS plots through ModFit LT V2.2.11. All data were determined to have "good" RCS, measurement of fit. Percent at bottom of pie char is the % in G1. n=3; 10,000 cells per animal. **d,** Percent differences from *Itgb1*-KO to control cells over time. No differences observed until 72 h post activation. Student's *t*-test; ** = $p < 0.006$. **e,** Cells isolated and plated in GM with CellTrace Violet Cell Proliferation dye, which is diluted with each successive generation. One set was fixed at T=0 for comparison. ModFit LT Proliferation Wizard Model was used to determine the generation of cells at 24, 48, and 72 h. n=3, 10,000 cells per animal. Student's *t*-test; * = $p < 0.05$, ** = $p < 0.03$.

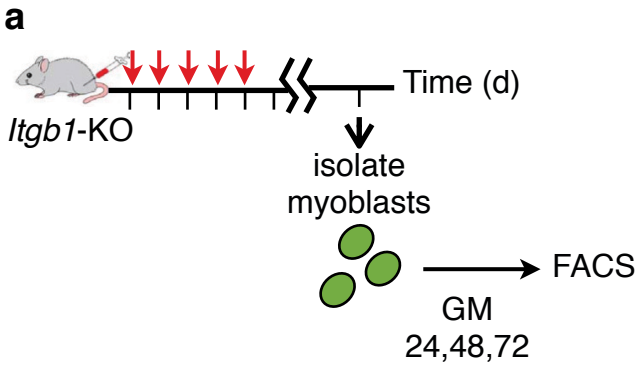
a
Time (d)
Itgb1-KO
isolate
myoblasts
FACS
GM
24,48,72

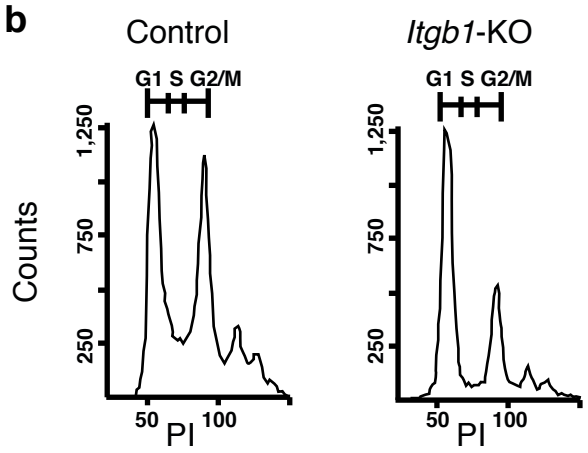
b
Control
Itgb1-KO
G1 S G2/M
G1 S G2/M
Counts
1,250
750
250
1,250
750
250
50
100
PI
50
100
PI

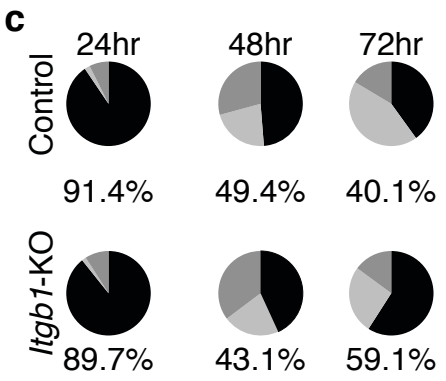
c
24hr
48hr
72hr
Control
91.4%
49.4%
40.1%
Itgb1-KO
89.7%
43.1%
59.1%

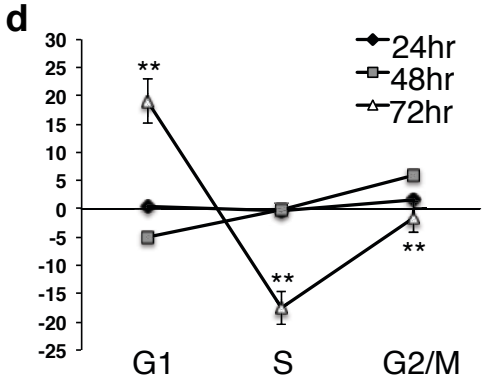
d
30
25
20
15
10
5
0
-5
-10
-15
-20
-25
**
**
**
24hr
48hr
72hr
G1
S
G2/M

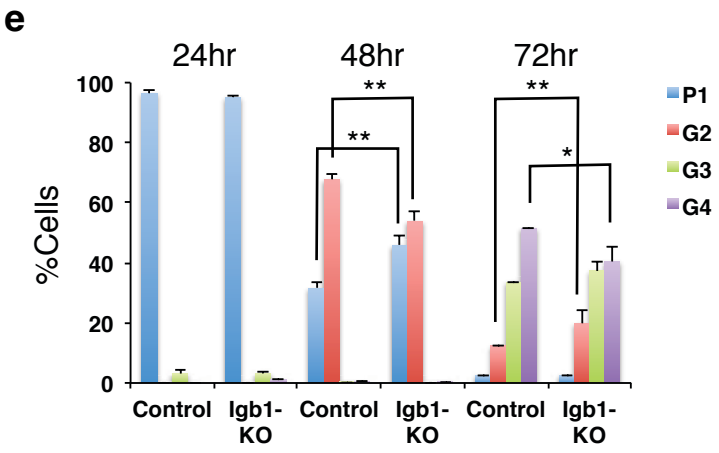
e
24hr
48hr
72hr
%Cells
100
80
60
40
20
0
**
**
**
*
P1
G2
G3
G4
Control
Igb1-KO
Control
Igb1-KO
Control
Igb1-KO

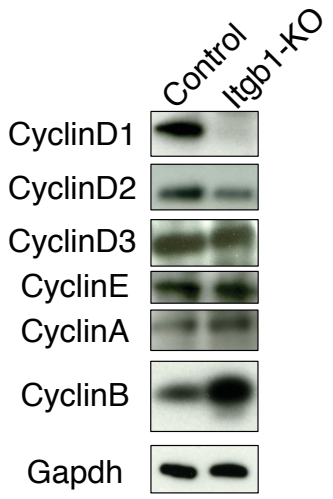

Figure 2.14. Cell cycle defects in *Itgb1*-KO cells are correlated with cyclin expression disregulation. Western blot of total protein lysates prepped from control *Itgb1*-KO myoblasts 72 h after activation.

However, consistent with the FACS analysis, no cyclin D1 protein, which regulates progression through G1, could be detected by Western Blot of protein lysate from *Itgb1*-KO cells harvested 72 hours after activation. Additionally, levels of cyclin D2 were reduced compared to controls. The role of integrin-mediated adhesion in regulating progression through G1 of cell cycle has been examined previously, and has been found to induce ERK activity to regulate levels of cyclin D1 (J. L. Walker and Assoian, 2005).

An increase in cyclin B was also observed (Figure 2.14), consistent with the FACS data demonstrating *Itgb1*-KO cells stalling in G2/M. Degradation of this cyclin is required for inactivation of its partner protein kinase and exit from mitosis (Hershko, 1999). Previous studies using cell lines demonstrated the requirement of integrin trafficking to the cleavage furrow of dividing cells to properly form a spindle in order to complete cytokinesis (Pellinen et al., 2008; Reverte et al., 2006). Further analysis will be required to assess if β1-integrin is functioning similarly in the satellite cell.

To ascertain the molecular changes in *Itgb1*-KO SCs underlying the severe regenerative phenotype, we examined their gene expression profiles (Figure 2.15). High-throughput sequencing was performed on RNA prepared from FACS-sorted satellite cells harvested at 24, 48, 72, and 96 hours after activation. While there were no differentially expressed genes at 24 hours between cultured mutant and control myoblasts, they became progressively different at 48 and 72 hours, with 252 and 627 genes differently expressed, respectively (Figure 2.15a). Although the numbers increase significantly from 48 to 72 hours, the functional categories of genes as assessed by PANTHER did not change (Figure 2.15b). Notably, at 72 hours, many genes associated with muscle differentiation were up-regulated in mutant cells, suggesting a commitment to differentiation at the

Figure 2.15. *Itgb1*-KO SCs differentiate at the expense of self-renewal. Animals injected with tmx *in vivo*, cells isolated and plated in GM for 24, 48, 72, and 96 h before FACS sorting. Isolation was done based on YFP fluorescence, using the 488 channel and gating first for cell size and then for YFP+ cells. FACS purified cells were used immediately after sorting for RNA isolation using the Arcturus PicoPure RNA isolation kit (Applied Biosystems). Sequencing was then peformed on an Illumina HiSeq2000 to generate single-end 100bp reads. **a,** Global view of sequencing data at 24, 48, 72 h post activation. Differentially expressed genes were determined by Cuffdiff to have significant q-values. **b,** Schematic representation of (**a**). Functional categories provided by PANTHER. Similar gene categories represented between 48 and 72 h, although in different numbers. **c,** Fold changes of normalized expression of muscle differentiation genes that are up-regulated in *Itgb1*-KO myoblasts compared to control myoblasts 72 h after culture. **d,** *Itgb1*-KO myoblast are more similar to 96 h control cells than 72 h.

a

Category	Number of differentially expressed genes	Number of up-regulated genes >2-fold	Percentage	Number of down-regulated genes >2-fold	Percentage
24hr	0	——	——	——	——
48hr	252	15	5.95%	28	11.11%
72hr	627	304	48.48%	61	9.73%

b

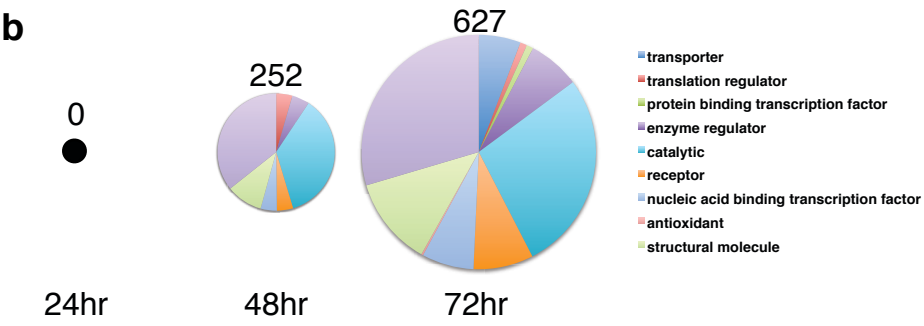

c

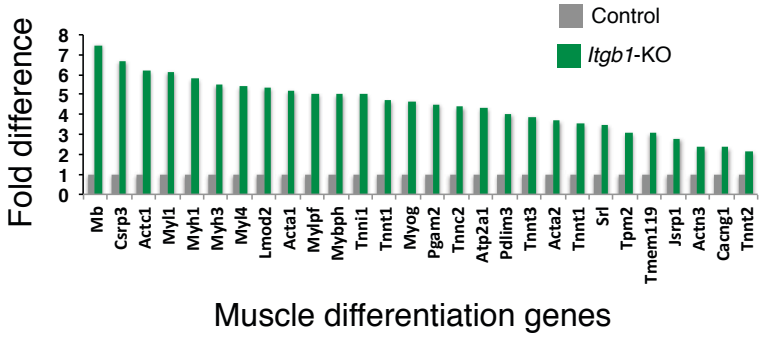

d

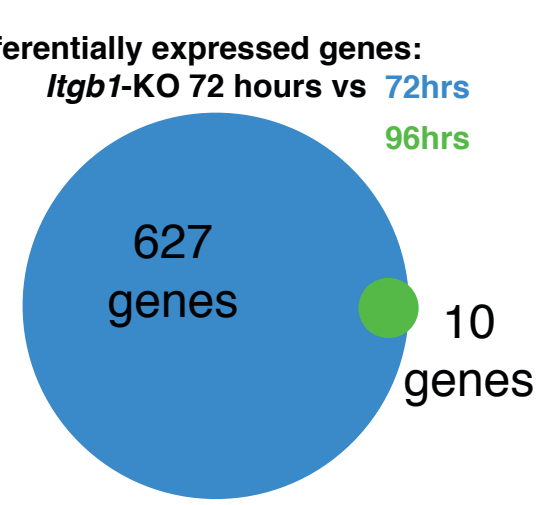

expense of proliferation (Figure 2.15c). Indeed, gene profiles of *Itgb1* KO cells at 72 hours are more similar to control cells 96 hours after activation (Figure 2.15d). The role of β1-integrin in SC proliferation has not previously been noted.

DISCUSSION

Integrins form an indispensible linkage between the muscle fiber and ECM, independent of the dystrophin-glycoprotein complex. There are 18 α and 8 β chains, which can form at least 28 isoforms. Of particular relevance to skeletal muscles are α7 and α5 integrins and laminin α2 for their mutations cause muscular dystrophies. Inactivation of *Itgb1* (encoding β1-integrin) in the myogenic lineage reveals that it is essential for muscle cell fusion yet dispensable for progenitor proliferation during embryogenesis. However, the role of β1-integrin in the satellite cell had previously had not been examined.

Here I report the characterization of the $Pax7^{CE}$; $Itgb1^{KO}$; R26R mouse line, which allowed for efficient inactivation of *Itgb1* specifically in the satellite cell (SC). I found that β1-integrin has dual functions in the SC: 1) it functions to maintain SC quiescence, and 2) upon injury-induced activation it primarily functions to regulate proliferative capacity and self-renewal. As cells progress further down myogenesis, β1-integrin is required for efficient myoblast fusion, although this is secondary to its earlier role.

My findings demonstrated that β1-integrin is required to maintain SC quiescence. By lineage-labeling of *Itgb1*-KO SCs, I demonstrate that mutant SCs leave the niche, differentiate, and fuse into existing myofibers. I report a significant reduction of *Itgb1*-KO SCs compared to control SCs at 21 d, with a declining trend over 180 d. Additionally a significant portion of *Itgb1*-KO SCs were present outside the basal lamina and incorporated BrdU during this period revealing loss of quiescence and aberrant activation and entry into the cell cycle. These SCs were prone to differentiation and fusion into existing myofibers, as shown by incorporation of the lineage label. Together, these data

suggest that β1-integrin senses proper SC-niche interaction to prevent spurious activation and differentiation.

We examined the possibility that β1-integrin provided a physical attachment to the niche by increasing the load on muscle fibers via exercise, however we were unable to find a condition that induced an increased rate of SC loss. This was not an exhaustive study, and additional protocols could be utilized to test this more thoroughly (Konhilas et al., 2005; Warren et al., 1994). As there are no genetic differences between quiescent control and *Itgb1*-KO SCs 1 month after tamoxifen regimen (data not shown), this suggests that integrin is providing a structural role and is not signaling to affect gene transcription in order to maintain quiescence. However, it is possible that sequencing did not reveal any differences due to the heterogeneity in the SC pool (Rocheteau et al., 2012). Perhaps the SCs that were stimulated to leave the niche are the ones with differential gene expression, however as these cells would have fused into fibers at the time of RNA isolation, they would not have been sorted via FACS and these differences would not be revealed in the sequencing data.

We additionally assessed whether the Notch signaling pathway could be functioning downstream of integrin. Although a significant proportion of N1ICD is nuclear in *Itgb1*-KO SCs, in contrast to control YFP^+ SCs that have the majority of N1ICD present on the membrane, the relative amount of N1ICD protein does not differ 3 days after activation. Interpreting this phenotype is complicated given recent experimental evidence that has revised the concept of the role of Notch signaling during activation. Previously, it was believed that Notch signaling drives proliferation of activated satellite cells, consistent with the pro-mitotic function of Notch in other systems

(Fre et al., 2005). However, expression data demonstrated that Notch signaling is dramatically reduced upon activation; indeed its constitutive expression blocks proliferation (Liu et al., 2013; Wen et al., 2012). Further investigation into a link between the two pathways will be necessary, however the data suggests that aberrant Notch activity in *Itgb1*-KO SCs is merely a reflection of the quiescent phenotype.

β1-integrin has a secondary function upon injury-induced activation to regulate proliferative capacity and self-renewal, in contrast to embryonic studies that reported it was indispensible for muscle progenitor proliferation (Schwander et al., 2003). *Itgb1*-KO SCs are unable to drive efficient muscle regeneration; in contrast, the observed defect is comparable to that seen in animals lacking satellite cells, supporting the function of β1-integrin in maintaining stemness. Furthermore, *Itgb1*-KO SCs were unable to replenish the stem cell pool, instead differentiating at the expense of self-renewal. Together, these data suggest that β1-integrin is a crucial component of the satellite cell niche.

CHAPTER 3

β1-integrin dysfunction underlies the age-related decline in satellite cell function

INTRODUCTION

Sarcopenia, the slow but progressive loss of muscle mass concomitant with advancing age, affects all elderly people. This age-related muscle wasting is characterized by loss of muscle quantity and quality (Ryall et al., 2008). Muscle fiber size, number, and strength decreases with age, reducing the 'quantity' of muscle mass (Brooks and Faulkner, 1994; Einsiedel and Luff, 1992). Additionally, a reduction of muscle 'quality' occurs due to increased fat depositions, infiltration of connective tissue, as well as changes in metabolism (Conley et al., 1995; Cree et al., 2004; Kragstrup et al., 2011). This metabolic dysregulation includes reduction in insulin sensitivity, impaired defense mechanisms against oxidative stress, and decreased mitochondrial function (Giresi et al., 2005). Overall, the deterioration of muscle upon aging leads to the gradual impairment of movement and decline in strength, greatly impacting quality of life.

Although satellite cell numbers decline during aging in mice and humans, the poor regenerative capacities of aged muscle are not solely due to the loss of stem cells themselves (Chakkalakal et al., 2012). Instead, the impaired regeneration has been attributed to aged-related changes in the systemic and local environments (Brack et al., 2007; Conboy, 2003). Exposure of aged SCs to a young environment by heterochronic parabiosis improved SC function and regeneration (Conboy et al., 2005). Furthermore, transplantation of young myofiber-associated SCs, which maintain the young microenvironment, prevented age-associated loss of muscle mass and strength, hallmarks of sarcopenia (Hall et al., 2010).

However, recent studies demonstrated that both intracellular and extracellular defects account for aged SC impairment, and both must be corrected for rejuvenation to

support regeneration and improve muscle function (B. D. Cosgrove et al., 2014). Cosgrove et al. demonstrated that the reduced function of SCs from aged mice can be improved by intracellularly reducing the levels of p38α/β mitogen-activated protein kinase (MAPK), through use of a small-molecule inhibitor, and extracellularly matching the soft elasticity of young muscle tissue by culturing SCs on a porous hydrogel substitute. These rejuvenated SCs demonstrated restored regenerative potential and were able to contribute to greater yields of engraftment upon transplantation.

However, this restoration of function requires isolating aged SCs, culturing *ex vivo*, and transplanting the rejuvenated cells back into muscle, which is a complicated protocol to imagine applying in human patients. Future work should focus on examining the relationships among the different pathways that are deregulated in aged SCs to attempt to identify additional molecules that may be targeted in a simpler manner in order to restore function.

Young SCs are maintained in a quiescent state in their niche on top of the myofiber, which expresses FGF-2 (Chakkalakal et al., 2012). These cells experience high Notch signaling, low TGF-β/pSmad3, and high Sprouty1 that functions to repress FGF signaling and keep levels of phospho-p38α/β MAPK low in order to maintain quiescence (Carlson et al., 2008; Mourikis et al., 2012). Upon activation, SCs segregate phosphorylated p38α/β MAPK asymmetrically (Troy et al., 2012). The daughter cell that does not receive phospho-p38α/β MAPK retains Pax7 expression and self-renews. The daughter cell that receives phospho-p38α/β MAPK induces MyoD expression and differentiates.

Aged SCs reside on myofibers that express elevated levels of FGF-2, which

downregulates Sprouty1 removing the block on FGF signaling (Chakkalakal et al., 2012). This effect, coupled with low Notch signaling, and high TGF-β/pSmad3, results in loss of quiescence in a proportion of aged SCs, which undergo activation, and either apoptosis or differentiation (Carlson et al., 2008; Conboy, 2003; Shea et al., 2010). The aged SCs that remain are insensitive to external FGF stimulation, and develop elevated levels of phospho-p38α/β MAPK (Bernet et al., 2014). Upon injury-induced activation, the cell fails to segregate phospho-p38α/β MAPK asymmetrically; both daughters receive the kinase and differentiate at the expense of self-renewal. Antagonizing phospho-p38α/β MAPK by small molecule inhibitor, or surprisingly increasing FGFR signaling intracellularly, restores self-renewal (Bernet et al., 2014; B. D. Cosgrove et al., 2014). The authors conclude, "Attenuation of intracellular responses initiated by extracellular FGF-2 in aged SCs could arise from changes in FGFR1 interactions with other cell surface proteins".

Notably, integrins and growth factor receptors interact with each other at several levels (Mori and Takada, 2013). First, integrins control growth factor receptor activity by recruiting adaptor proteins to receptors. Second, integrins modulate growth factor receptor activity by localizing them to focal adhesions where signaling molecules are concentrated. Third, growth factor receptors can regulate binding affinity of integrins for ligands affecting adhesion and motility. Fourth, growth factor receptor pathways regulate integrin effector proteins, FAK, ERK, JNK, Akt, among others. Additionally, several growth factors have been reported to act as direct ligands for integrins; FGF1 directly binds to αvβ3 integrin to induce fibroblast proliferation and migration (Mori et al., 2013). Indeed, a dominant-negative FGF1 mutant that cannot bind to integrin is incapable of

inducing signals, and therefore, suppresses angiogenesis. Finally, in contrast to crosstalk that involves growth factors, fibronectin-mediated activation of FGFR1 in fibroblasts requires β1-integrin but not FGF (Zou et al., 2012). Therefore, it has been well established that integrins are involved in mediated FGF signaling in many other systems, although many specifics of the crosstalk between the pathways have not yet been elucidated.

Here I show that β1-integrin underlies the insensitivity of aged SCs to FGF, which results in reduced regeneration and self-renewal capacity. β1-integrin deficient young SCs lose their quiescence and their ability to self-renew, properties reminiscent of aged SCs. Aged SCs, on the other hand, display aberrant patterns of active β1-integrin and its effectors, revealing their dysregulation. By enhancing β1-integrin activation in aged SCs, we can restore SC self-renewal by rescuing their sensitivity to FGF *in vitro* and muscle regenerative capacity *in vivo*. Our results show β1-integrin senses the SC niche to maintain self-renewing responsiveness to FGF, and provide potential therapeutics for age-related muscle decline. β1-integrin is the sensor of the SC niche that declines in function upon aging.

MATERIALS AND METHODS

Animal studies

Animal experiments in this study were performed in accordance with protocols approved by the Institutional Animal Care and Use Committee (IACUC) of the Carnegie Institution for Science (Permit number A3861-01). The $Pax7^{CE}$ allele (B6;129-*Pax7*$^{tm2.1(cre/ERT2)}$*Fan*/J) has been described (Lepper et al., 2009). The *Itgb1*^{FLOX} allele (B6;129-Itgb1tm1Efu/J) and the *R26R*^{lacz} (B6.129S4-*Gt*(*ROSA*)*26Sortm1Sor*/J) and *R26R*^{YFP} (B6.129X1-*Gt*(*ROSA*)*26Sor*$^{tm1(EYFP)}$*Cos*/J) reporter mice were obtained from the Jackson Laboratory (Raghavan et al., 2000; Soriano, 1999; Srinivas et al., 2001). Young (2-6 months of age) mice were purchased from Jackson Laboratories. Aged C57BL/6 mice (18-24 months of age) were obtained from the National Institute of Aging. Also, the $Pax7^{CE}$;$R26^{YFP/YFP}$ colony was maintained in a C57BL/6 background and aged to 18-24 months for lineage labeling studies.

For young versus aged comparisons, mice were used at 3-6 months of age (young) or 18-24 months of age (aged). For labeling $Pax7^{+}$ cells, both aged and young $Pax7^{CE}$;$R26R^{YFP}$ animals were injected with tmx as described previously (Materials and Methods, Chapter 2) and harvested for analysis or single fiber culture the following week.

TA muscles were injured as described previously (Conboy, 2003). Briefly, 3 needle-track injuries were performed on both TA muscles in each animal. The needle is inserted at an angle of approximately 45° with respect to the longitudinal axis of the fibers. 2d post-injury the right "experimental" TA received 60µl anti-TLR2 [TS2/16] (10µg/ml) or RGD peptide (10µg/ml) while the left "control" TA received 60µl vehicle

(IgG) or scrambled peptide (10μg/ml) by intramuscular injections. Muscles were harvested 3d after these injections for analysis.

Mice were sacrificed by cervical dislocation and TA muscles were harvested as described (Materials and Methods, Chapter 2).

Muscle histology

Haematoxylin and Eosin were performed as described previously (Materials and Methods, Chapter 2).

Cell isolation and culture

For myoblast preparation and single myofiber isolation, harvest was performed as described previously (Materials and Methods, Chapter 2).

For self-renewal experiments, myofibers were cultured for 48 h or 72 h in growth media with or without 1ng/ml FGF-2 (R and D systems) before fixation. For phosphorylated p38 analysis, myofibers were cultured for 36 h with or without 1ng/ml FGF-2. Phosphatase Inhibitor Cocktail Set II (Calbiochem) was used as directed during fixation in phosphorylation experiments.

For aged assays, myofiber-associated cells were cultured in growth medium and treated with FGF-2 or Anti-TLR2 [TS2/16](10μg/ml) (Abcam) or both after 8 h. Media and reagents were changed at 24 h intervals afterwards until fixation at 72 h.

Immunofluorescence

Immunofluorescence staining were performed as described (Materials and Methods, Chapter 2).

Chemicals and antibodies

Anti-TLR2 used to activate integrin was purchased from Abcam (TS2/16). FGF-2 was purchased from R/D systems. RGD peptide was purchased from Santa Cruz (sc-201176); scrambled peptide was purchased from AnaSpec. Antibodies against β1-integrin, Parvin, and p38 MAPK were purchased from Cell Signaling (4706, 4026, and 9216, respectively). α7-integrin antibody was purchased from MBL International Corporation (clone 3C12, K0046-3). Antibodies against activated β1-integrin and Paxillin were purchased from BD Biosciences (9EG7 and 610619, respectively). β1-integrin antibody was purchased from Millipore (MAB1997). GFP antibodies were purchased from Invitrogen (G10362, rabbit) and Aves (GFP-1020, chick). Antibodies against eMyHC, MLC, and Pax7 were purchased from Developmental Studies Hybridoma Bank (F1.652, MF20, and PAX7, respectively). Antibodies against Laminin and Vinculin were purchased from Sigma Chemical (L9393 and V9131, respectively). Antibodies against ILK, M-cadherin, and MyoD were purchased from Santa Cruz (sc-20019, sc-81471, and sc-304, respectively).

Microscopy and image processing

Images of hematoxylin and eosin stained muscle sections were captured from a Nikon 800 microscope equipped with a 10x/.45 Plan Apo objective and Canon EOS T3 camera using EOS Utility image acquisition software. Fluorescent images of muscle sections

were captured using Leica SP5 confocal equipped with 40x/1.25 Plan Apo oil objectives using Leica image acquisition software. Images of cells on single fibers were captured using the Leica SP5 setup or a Zeiss Axioscope equipped with a 40x/0.5 Plan Apo oil objective and Axiocam camera using Zeiss image acquisition software. Identical exposure times were used and images were processed and scored with blinding using ImageJ64. If necessary, brightness and contrast were adjusted for an entire experimental image set.

RESULTS

β1-integrin activity declines in aged SCs

Aged SCs are insensitive to FGF and have a reduction in the subset of cells displaying pp38 asymmetry, which leads to premature differentiation (Bernet et al., 2014; Chakkalakal et al., 2012). Previous work has shown that ECM composition and stiffness is altered in aged SCs and this global environment in aged mice inhibits the SC, suggesting that proper sensing of extracellular signals is essential for SC function (Kragstrup et al., 2011; Wood et al., 2014). Additionally, aforementioned characteristics of *Itgb1*-KO SCs (Chapter 2) are reminiscent of aged SCs: both are gradually lost from the niche, cannot sustain proliferation, and are committed to differentiation (Chakkalakal et al., 2012; Conboy, 2003; B. D. Cosgrove et al., 2014). Therefore, we wondered whether β1-integrin signaling is altered in aged SCs, leading to the attenuation of intracellular responses to FGF.

To assess β1-integrin activity, we probed aged SCs with an antibody (9EG7) that specifically recognizes the "high-affinity" ligand-bound active β1-integrin and compared to pan-β1-integrin antibody staining (Takagi and Springer, 2002). Antibody 9EG7 recognizes an epitope on β1-integrin that is induced in response to treatment with manganese or soluble integrin ligands (Bazzoni et al., 1995). However, its expression does not always correlate with the high-affinity state prior to ligand binding. Yet it can reliably be used to detect ligand-bound, active, conformation of β1-integrins.

When probing with this antibody, the majority of young myofiber-associated SCs were found to display well-aligned basal membrane-bound β1-integrin in its active

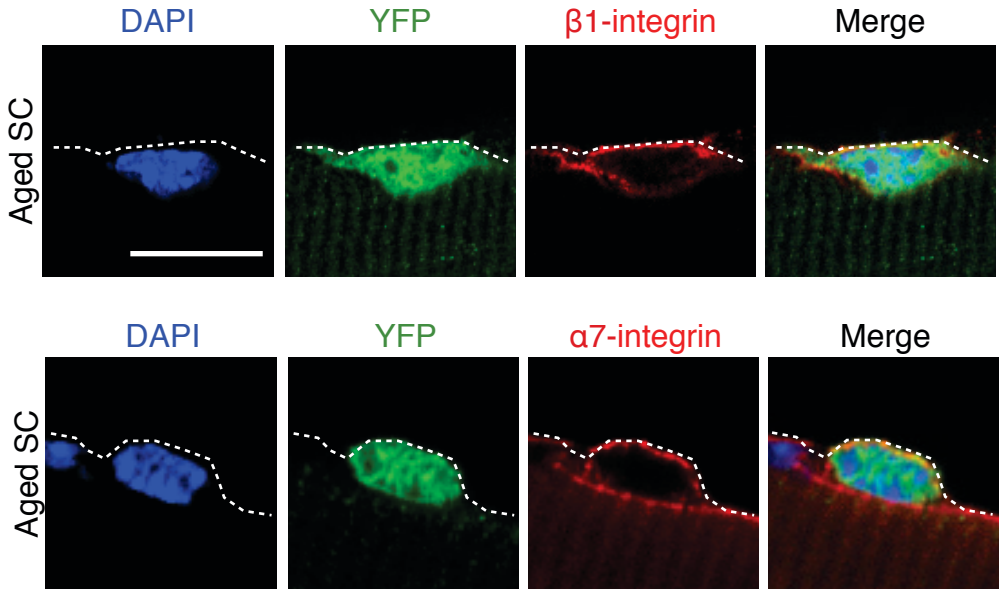

Figure 3.1. Aged SCs express laminar-localized pan β1-integrin and α7-integrin. YFP$^+$ myofiber-associated SCs from aged mice at 1 h after dissection stained for pan β1-integrin and α7-integrin. Expression mirrors young control SCs. Dashed lines outline the basal side of the myofiber. Scale bar, 10μm.

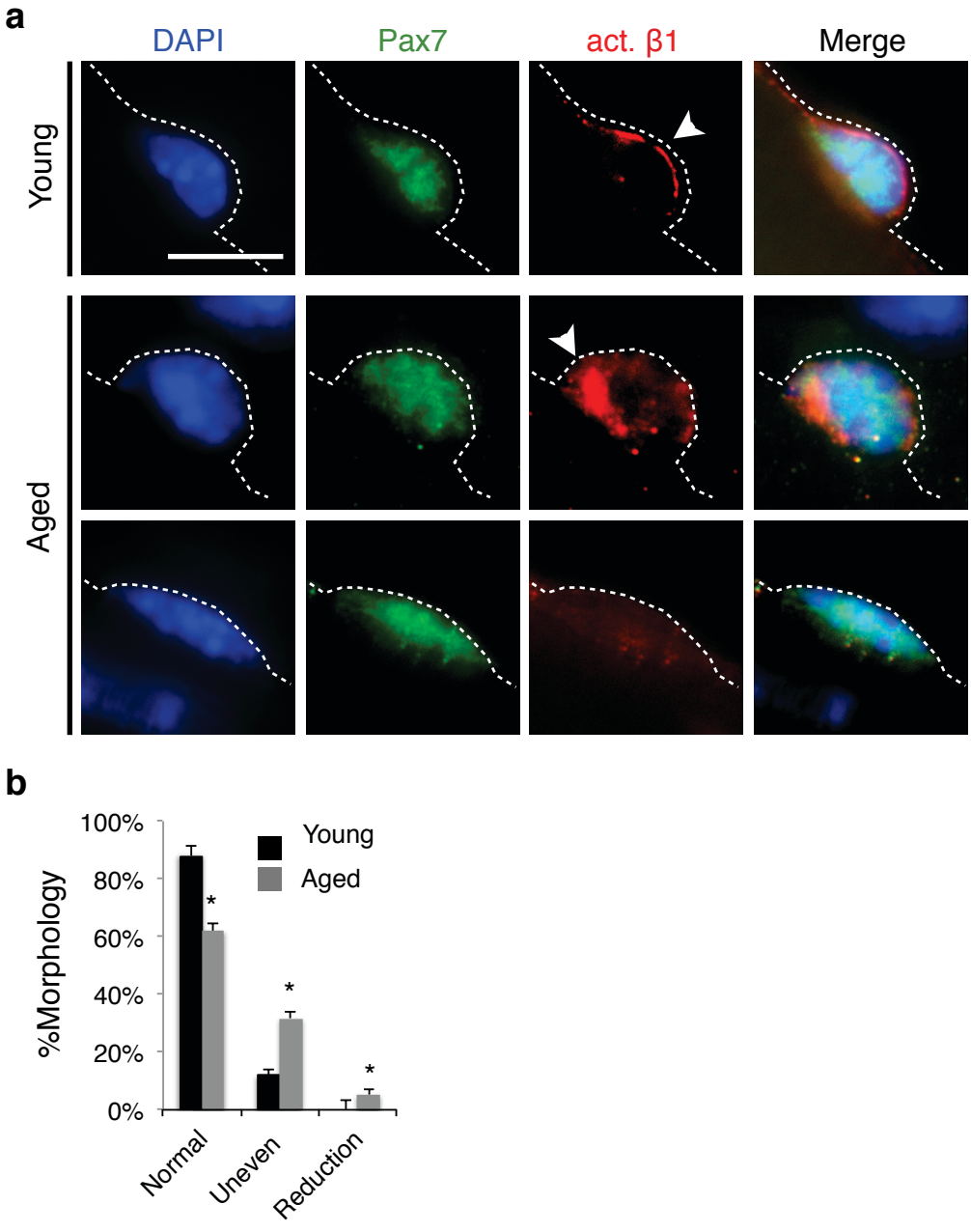

Figure 3.2. β1-integrin activity declines in aged SCs. a, Myofiber-associated Pax7^{+} SCs from young and aged mice stained for activated β1-integrin (act. β1) at 1 h after dissection. Act. β1 patterns were scored as normal, uneven, or reduced in level (reduction); dashed lines, basal surface; scale bar = 10μm. **b,** Percentages of Pax7^{+} SCs with different patterns of act. β1 from (**a**). β1; n = 3 experiments, ≥ 20 myofibers.

conformation 1 h after isolation, mirroring total β1-integrin (Figure 3.2a). Despite a normal pattern of total β1-integrin (Figure 3.1), significantly more aged SCs displayed active β1-integrin in abnormal patterns: in disorganized puncta or severely reduced (Figure 3.2a-b). Integrin trafficking plays a large role in their function, as they must undergo constant recycling to facilitate the dynamics of cell adhesion. Previous work has demonstrated that active integrins are more rapidly endocytosed, suggesting that increased ECM stiffness and composition is affecting integrin presentation in a subset of aged SCs leading to its misregulation (Arjonen et al., 2012). Additionally, a small fraction of aged SCs display almost no active β1-integrin, again supporting the misregulation of integrin activity.

We next asked whether there were associated changes in integrin effectors, suggesting misregulation of outside-in integrin signaling. Specifically we examined integrin-linked kinase (ILK), parvin, and paxillin (Figure 3.3), which make up the IPP complex (Legate et al., 2005). This complex serves as an important transducer of extracellular signals from integrin to control many aspects of cell morphology and behavior. When talin is recruited to the plasma membrane and activated, it binds to the cytoplasmic tail of β integrins. Paxillin recruits ILK and parvin to focal adhesions, which then stimulates recruitment of vinculin and FAK that then associate with actin, completing the link to the cytoskeletal machinery. In young control SCs, ILK, parvin and paxillin were localized to the laminar side (Figure 3.4), adopting the same position as β1- and α7-integrin (Figure 2.1c-d). In contrast, their expression was drastically reduced and localization non-polarized in *Itgb1*-KO SCs, reflecting the loss of binding partner β1-integrin.

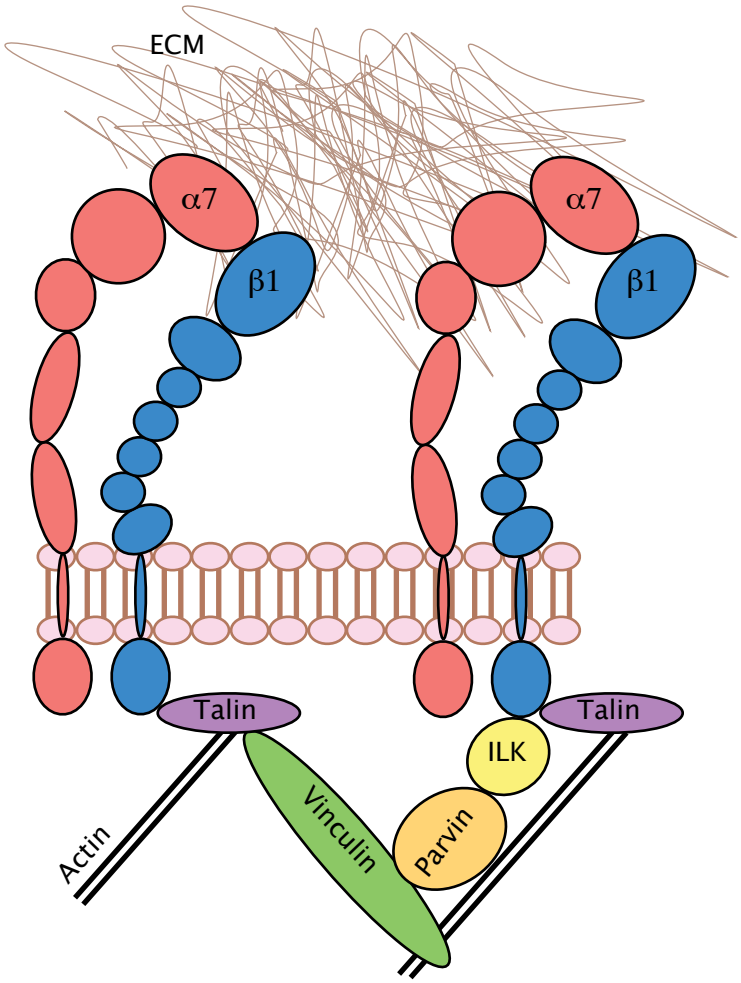

Figure 3.3. Schematic of integrin effectors.

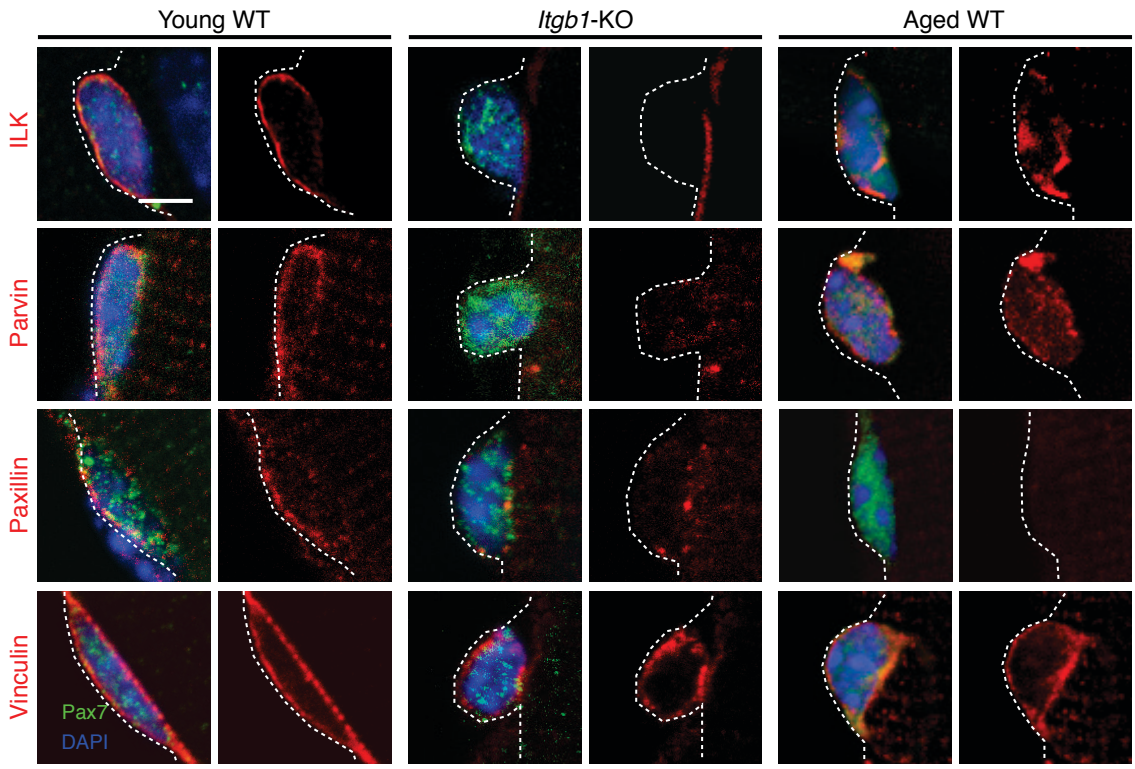

Figure 3.4. Mislocalization of integrin effectors suggest defects in downstream signaling. Myofiber-associated Pax7^{+} SCs from young, *Itgb1*-KO, and aged animals stained for ILK, Parvin, Paxillin, and Vinculin, 1 h after isolation; dashed lines, basal surface; scale bar = 5μm.

In contrast, aged SCs lost paxillin expression, similar to *Itgb1*-KO young SCs, but the expression of ILK and parvin appeared unchanged, simply distributed in a disorganized pattern (Figure 3.4). Vinculin encircled young SCs; this pattern was slightly disorganized in mutant young SCs, as well as in aged SCs. As this effector binds to actin but not directly to integrin, it suggests that the cytoskeleton is unperturbed by loss of β1-integrin (Calderwood et al., 2000). However, the abnormal localization and disparate changes among the other probed integrin effectors indicate a dysregulation instead of an absence of integrin signaling in aged SCs, likely reflecting a broader disturbance than β1-integrin alone.

Activating β1-integrin in aged SCs restores regeneration capacity of aged muscle

Skeletal muscle function and mass decline with age; associated with a decrease in muscle innervation, general increase in interstitial fibrotic connective tissue, and a reduction in the number of satellite cells and their capacity to self-renew (Day et al., 2010; Grounds, 1998). Efforts to rejuvenate aged SCs have demonstrated restoration of aged muscle function and regenerative capacity (Conboy, 2003; B. D. Cosgrove et al., 2014; Elabd et al., 2014). Given the defects in β1-integrin localization and activation in aged SCs, we theorized that we might be able to rejuvenate these cells by properly activating β1-integrin via specific monoclonal antibodies (Byron et al., 2009). We injected candidate antibodies (TS2/16, 9EG7, and LIBS) into injured aged TA muscles and then assessed for regeneration capacity based on the number of newly formed myofibers containing centrally located nuclei (Figure 3.5a-b). TS2/16, which recognizes an epitope expressed

Figure 3.5. Activating β1-integrin in aged SCs restores regeneration capacity of aged muscle. a, Schematic representation treatment and skeletal muscle injury in 3- and 24-month-old wildtype mice. TA muscle injury: 2 d post injury, 6 x 10 μl injections of into the injury site of either vehicle (IgG, 10 μg/ml per injection), β1-integrin activating antibody (TS2/16, 10 μg/ml per injection), or β1-integrin inhibitor (RGD peptide, 10 μg/ml per injection). **b,** Tibialis anterior muscle diagram with injuries in grey. Horizontal lines, cross sections. **c,** TA muscles were harvested for analyses 3 d later (5 d post injury). Cross-sections were stained for haematoxylin and eosin (H&E) or embryonic Myosin Heavy Chain (eMyHC); scale bar = 150μm. **d,** Muscle regeneration was quantified by scoring the number of newly formed fibers (eMyHC$^+$ fibers with centrally located nuclei) in the injured area; ** = p<0.01, ns = not significant, one-way ANOVA. Data represent mean ± s.e.m.; n=3 for young-inhibitor (YI), n = 3 for young-vehicle (YV), n = 4 young-activator (YA), n = 3 aged-vehicle (AV), n = 4 aged-activator (AA).

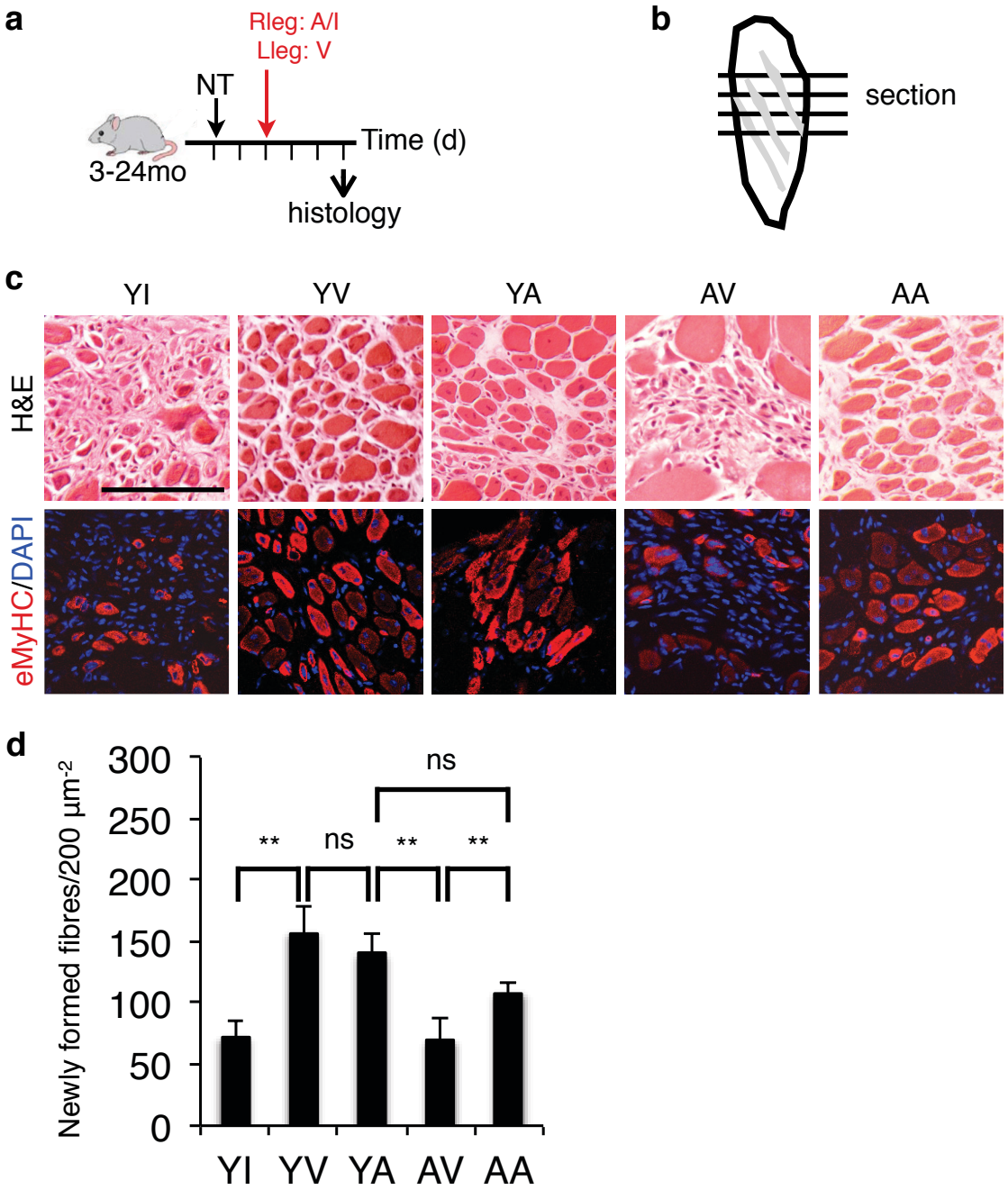
a
Rleg: A/I
Lleg: V
NT
Time (d)
3-24mo
histology
b
section
c
YI
YV
YA
AV
AA
H&E
eMyHC/DAPI
d
Newly formed fibres/200 µm-2
300
250
200
150
100
50
0
ns
**
ns
**
**
YI
YV
YA
AV
AA

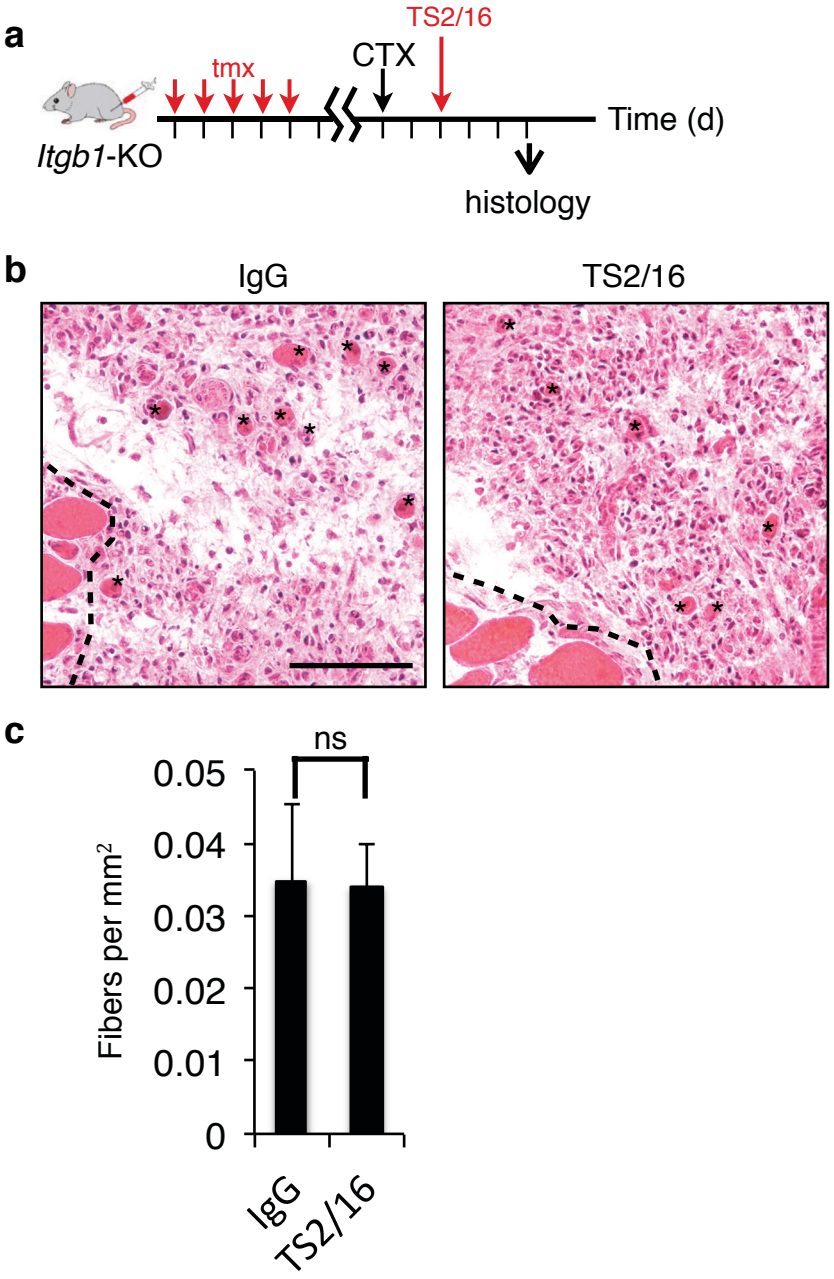

Figure 3.6: TS2/16 does not rescue the regeneration deficiency of *Itgb1*-KO muscle. **a,** Tmx regimen, CTX injury, and TS2/16 injection scheme. TA muscle injury: 2-4 d post injury, 6 x 10 µl injections into the injury site of either vehicle (IgG, 10 µg/ml per injection), or β1-integrin activating antibody TS2/16 (10 µg/ml per injection). TA muscles were harvested for analyses 3 d later (5 d post injury). **b,** Cross-sections were stained for haematoxylin and eosin (H&E); scale bar = 150 µm. **c,** Muscle regeneration was quantified by scoring the number of newly formed fibers (centrally located nuclei) in the injured area; ns = not significant, one-way ANOVA. Data represent mean ± s.e.m.; *n* = 3 animals per condition; 10 sections per animal.

on all β1-integrins, showed the best response in initial screens and was further characterized (Tsuchida et al., 1997).

Robust muscle regeneration was observed in control young mice injected with vehicle (YV) (Figure 3.5c-d). Inhibition of integrin-ECM interactions by the RGD peptide repressed muscle regeneration in young mice (YI) to a level comparable to the aged mice injected with vehicle, either mouse IgG or scrambled peptide in PBS (AV). While TS2/16 did not significantly enhance the already robust regeneration in young animals (YA), it improved muscle regeneration in aged mice (AA) to a level comparable to the young. As a control, we showed that TS2/16 did not rescue the regeneration deficiency of *Itgb1*-KO muscle (Figure 3.6). Interestingly, TS2/16 enhances the force generated between β1-integrin and its ECM ligand, while RGD peptide disrupts integrin-ECM interactions (Humphries et al., 2006; Li et al., 2003). These opposite effects on muscle regeneration argue that mechanical sensing of the SC to its niche via β1-integrin is critical.

Integrin signaling coordinates with FGF to drive aged SC self-renewal

A greater proportion of freshly isolated SCs from aged mice exhibit persistently elevated p38α/β MAPK activity, along with expression of cell cycle inhibitors $p16^{Ink4a}$ and $p21^{Cip1}$ when compared to SCs isolated from young mice (Bernet et al., 2014; B. D. Cosgrove et al., 2014). p38α/β MAPK signaling inhibits self-renewal by promoting myoblast differentiation and restricting stem cell gene expression (Brien et al., 2013; Jones et al., 2005; Lluís et al., 2006). Along with higher p38α/β MAPK signaling in aged SCs, is an attenuation of FGFR1 response to stimulation by FGF ligands (Bernet et al., 2014).

Figure 3.7. FGF rescues self-renewal of Itgb1-KO SCs. a, Schematic of tamoxifen (tmx) regimen and myofiber harvest. **b,** Myofiber-associated YFP^+ SCs of control and *Itgb1*-KO mice were cultured for 48 h with or without FGF-2 and immunostained for Pax7 and MyoD. SCs are either quiescent ($Pax7^+$; arrow), proliferating ($Pax7^+MyoD^+$; asterisk), or differentiating ($Pax7^-MyoD^+$; open arrowhead); scale bar = 10μm. **c,** Pie charts are used to summarize data in (a); $n = 3$ animals; ≥ 20 myofibers per condition; two-way ANOVA was used for paired comparison: control vs. control+FGF-2 for $Pax7^-MyoD^+$, $p < 0.05$; control vs. *Itgb1*-KO for $Pax7^-MyoD^+$, $p<0.05$; *Itgb1*-KO vs. *Itgb1*-KO+FGF-2 for $Pax7^-MyoD^+$, $p< 0.01$.

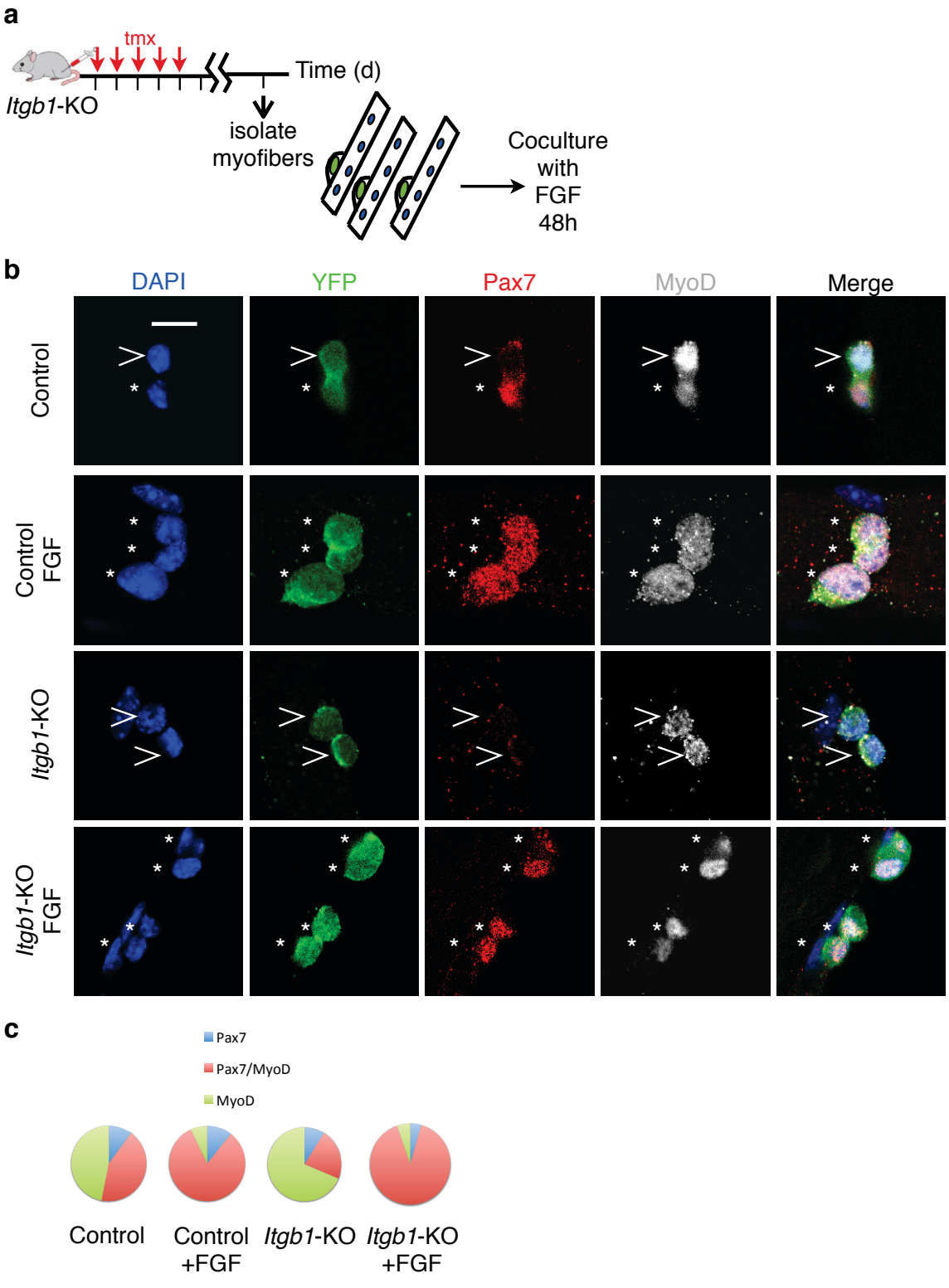
a
tmx
Time (d)
Itgb1-KO
isolate
myofibers
Coculture
with
FGF
48h
b
DAPI
YFP
Pax7
MyoD
Merge
Control
Control
FGF
Itgb1-KO
Itgb1-KO
FGF
c
Pax7
Pax7/MyoD
MyoD
Control
Control
+FGF
Itgb1-KO
Itgb1-KO
+FGF

Figure 3.8. FGF rescues asymmetric segregation of phospho-p38 (pp38) in *Itgb1*-KO SCs. a, Schematic of tamoxifen (tmx) regimen and myofiber harvest. **b,** Myofiber-associated YFP+ SCs were cultured for 36 h with or without FGF-2, and stained for pp38 (asymmetric; arrowhead, non-asymmetric; dashed line); scale bar = 10μm. **c,** Percentages of asymmetric pp38+YFP+ SCs with or without FGF-2: numerical data are expressed as mean ± s.e.m.; n = 3 experiments, ≥ 25 myofibers per condition. Data were compared by two-way ANOVA: $P < 0.05$ for both control vs. Itgb1-KO with 0 ng/ml FGF-2, as well as Itgb1-KO with 0 vs. 1 ng/ml FGF-2.

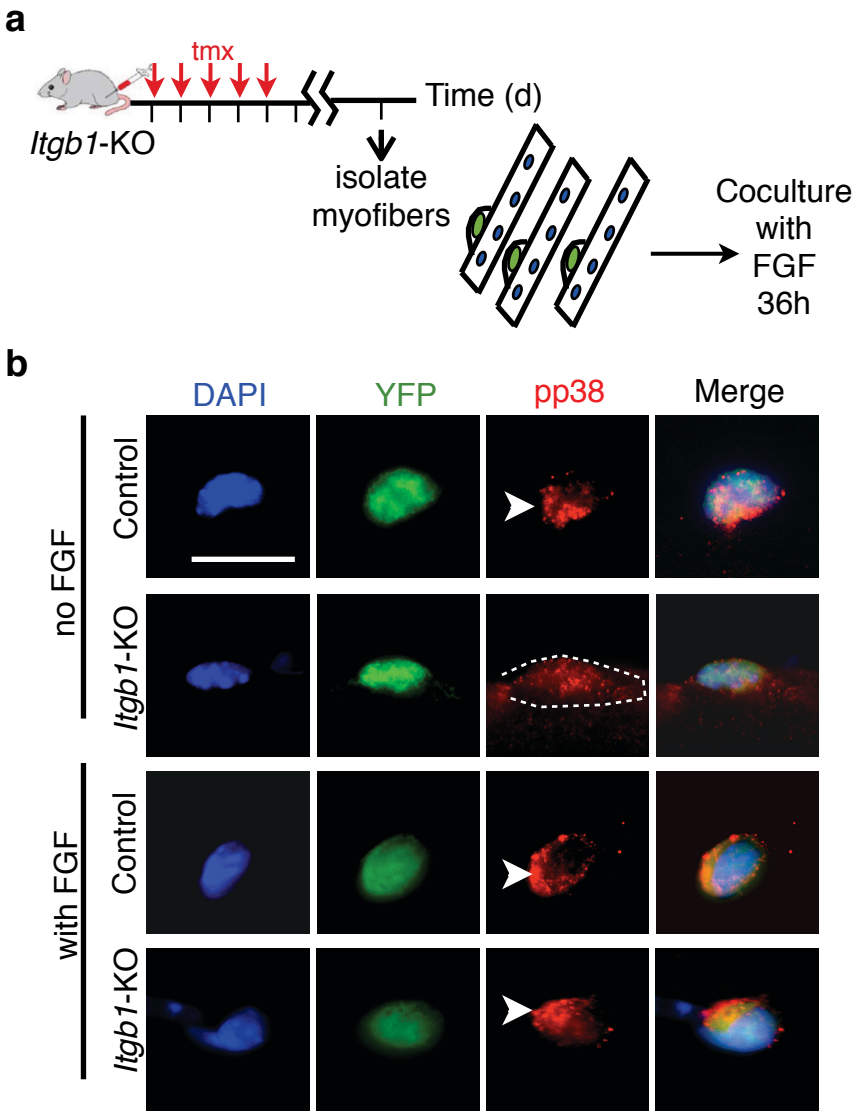
a
tmx
Itgb1-KO
Time (d)
isolate
myofibers
Coculture
with
FGF
36h
b
DAPI
YFP
pp38
Merge
no FGF
with FGF
Control
Itgb1-KO
Control
Itgb1-KO
c
Control
Itgb1-KO
%polarized pp38
75%
50%
25%
0%
*
*
ns
-FGF
+FGF

Although FGF-2 ligand activates p38α/β MAPK signaling, ligand-independent activation of FGFR1 in aged SCs puzzlingly reduces p38α/β MAPK activation to restore self-renewal. While the mechanism behind this association is unclear, the relevance of these factors to SC fate and function has been determined. Given the regulatory role that integrins seem to have in the activation of growth factor receptors, we examined the interplay between these pathways in the young and aged SCs (Yamada and Even-Ram, 2002).

The single myofiber assay allows for assessment of self-renewal capacity. Myofibers with lineage-labeled SCs were isolated and cultured for 48 h before fixing and immunostaining with Pax7 and MyoD (Figure 3.7a). Three populations of SCs can be viewed: quiescent ($Pax7^+$ $MyoD^-$), proliferating ($Pax7^+MyoD^+$), and differentiating ($Pax7^-$ $MyoD^+$). Employing this paradigm, we found that the majority of *Itgb1*-KO SCs were differentiating ($MyoD^+Pax7^-$) at 48 h, while most control SCs maintained Pax7 expression in a proliferative ($Pax7^+MyoD^+$) state (Figure 3.7b-c). *Itgb1*-KO SCs lose the proliferative population that is present in control SCs, instead turning off Pax7 to enter differentiation. Proportions of quiescent ($Pax7^+MyoD^-$) cells do not differ between control and *Itgb1*-KO SCs suggesting β1-integrin regulates self-renewal during division, perhaps by delivering cues from the niche to the SC to drive asymmetry. Reserve cell or SC transplantation assays will be additionally necessary to examine the role of β1-integrin SCs regaining quiescence after activation.

SC self-renewal is driven by asymmetric, FGF-stimulated p38a/b MAPK phosphorylation (Bernet et al., 2014; Troy et al., 2012). Myofibers containing lineage-

labeled SCs were isolated and cultured for 36 h before fixing, to assess phosphorylated p38 (pp38) localization prior to the first division (Figure 3.8a). Quantitative analysis of myofiber-associated SCs showed a 50% reduction in the percentage of *Itgb1*-KO SCs possessing asymmetric phospho-p38 compared to the numbers of SCs from control mice with asymmetric phospho-p38 (Figure 3.8b-c). This decrease is comparable to what is seen in aged SCs, which also fail to segregate phospho-p38 (Bernet et al., 2014).

The FGF-dependent activation of p38a/b MAPK signaling prompted us to assess how addition of FGF-2 to cultured myofibers would affect self-renewal and phospho-p38 asymmetry. Myofibers containing lineage-labeled SCs were isolated and cultured as described previously (Figure 3.7a, Figure 3.8a), except for the added presence of a working dose of bFGF-2. As expected, these culture conditions increased the $Pax7^{+}MyoD^{+}$ fraction of control cells at the expense of the differentiating $Pax7^{-}MyoD^{+}$ population (Figure 3.7b-c), consistent with the mitogenic properties of FGF in SCs (Allen et al., 1984). Surprisingly, a shift in *Itgb1*-KO SCs towards $Pax7^{+}MyoD^{+}$ comparable to control SCs was also seen (Figure 3.7b-c), indicating that FGF can rescue the self-renewal defect in SCs lacking β1-integrin. In fact, between *Itgb1*-KO and control cells cultured with FGF-2, there was no observed difference in the percentages of cells belonging to the 3 subsets of SCs. The proportion of quiescent SCs is not altered by addition of FGF in both control and *Itgb1*-KO SCs. Myofiber-associated *Itgb1*-KO SCs cultured in the presence of FGF also displayed a 50% gain in the numbers of asymmetric phospho-p38 compared to numbers of *Itgb1*-KO SCs cultured without FGF (Figure 3.8b-c). FGF did not increase phospho-p38 asymmetry in control SCs, however, even while the proliferative population of these cells increases, indicating that the two metrics are not

Figure 3.9. RGD peptide-treated young SCs do not respond to FGF treatment. a, Schematic of tamoxifen (tmx) regimen and myofiber harvest. **b,** Myofiber-associated YFP^+ SCs of control young mice were cultured for 48 h with scrambled or RGD peptide and with or without FGF-2 and immunostained for Pax7 and MyoD. SCs are either quiescent ($Pax7^+$), proliferating ($Pax7^+MyoD^+$; asterisk), or differentiating ($Pax7^-MyoD^+$; open arrowhead); scale bar = 10μm. **c,** Pie charts are used to summarize data in (a); $n = \geq 25$ myofibers per condition; two-way ANOVA was used for paired comparison: scrambled vs. scrambled+FGF-2 for $Pax7^-MyoD^+$ and scrambled vs. RGD+FGF-2, $p < 0.05$; RGD vs. RGD+FGF-2 for $Pax7^-MyoD^+$, *n.s.*

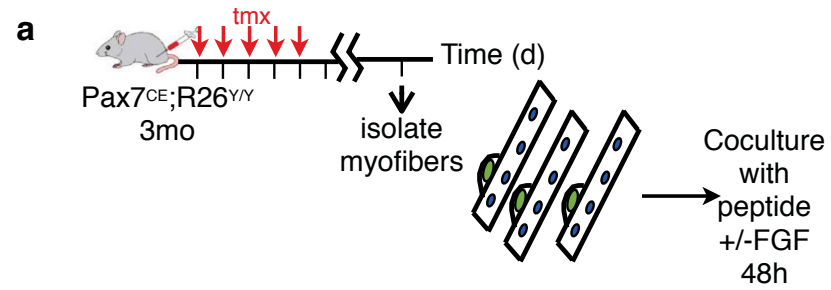
a
tmx
Time (d)
Pax7CE;R26Y/Y
3mo
isolate
myofibers
Coculture
with
peptide
+/-FGF
48h

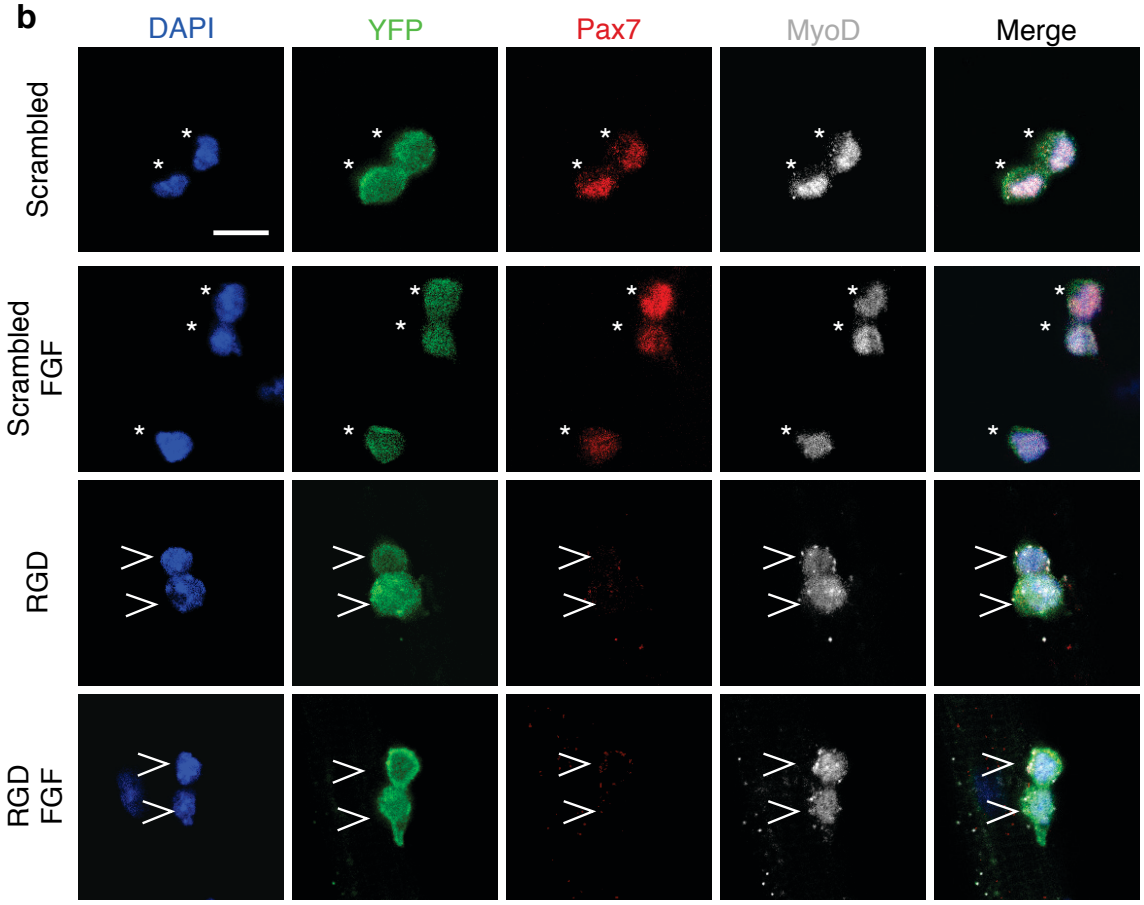
b
DAPI
YFP
Pax7
MyoD
Merge
Scrambled
Scrambled
FGF
RGD
RGD
FGF

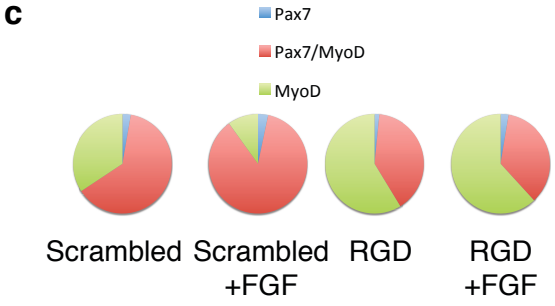
c
Pax7
Pax7/MyoD
MyoD
Scrambled
Scrambled
+FGF
RGD
RGD
+FGF

wholly coupled.

Integrins can activate growth factor receptors by creating an environment in which the receptors can properly interact with the downstream signaling molecules (Ivaska and Heino, 2010). The rescue of *Itgb1*-KO SCs by FGF could indicate that in this population, the pathways are parallel but distinct, or that other integrins can compensate for β1-integrin in KO SCs. To distinguish between these possibilities, we repeated the self-renewal assay with myofibers-associated control ($Pax7^{CE}$;$R26^{YFP/YFP}$) SCs cultured in the presence of the RGD peptide (Figure 3.9a). The peptide binds to a subset of integrins that recognize the RGD motif in fibronectin, vitronectin, and fibrinogen to interfere with their interaction to the ECM, namely α3β1, α5β1, αvβ1, αMβ2, αvβ3, and α5β5 (D'Souza et al., 1991). As previously shown, RGD peptide inhibits integrin-ECM interactions to impair muscle regeneration in young mice (Figure 3.5). Consistently, SCs treated with RGD peptide also had reduced $Pax7^{+}$ cells when compared to SCs treated with scrambled RGD peptide; instead cells populated the differentiating $Pax7^{-}MyoD^{+}$ proportion (Figure 3.9b-c). However, in contrast, to *Itgb1*-KO SCs, the proliferative fraction could not be rescued by FGF2 (Figure 3.9b-c). Control SCs cultured with the scrambled peptide, as well as FGF2, display the expected shift from the $Pax7^{-}MyoD^{+}$ population towards the $Pax7^{+}MyoD^{+}$ subset. This result suggests that other RGD-binding β-integrins can compensate for the loss of β1-integrin in *Itgb1*-KO SCs to respond to FGF and activate growth factor receptors. Blocking all RGD-binding β-integrins abolishes this cooperativity. RGD-binding integrins - including several β1-containing integrins, cooperate with FGF to drive SC self-renewal. Thus, loss

or dysregulation of β1-integrin activity has a direct implication on FGF sensitivity of SCs.

Activating β1-integrin in aged SCs restores responsiveness to FGF for self-renewal

If dysregulated integrin signaling underlies the inability of aged SCs to sense the niche for self-renewal, activating β1-integrin may be sufficient for rescue. To test this, we applied an integrin-activating antibody (TS2/16) to myofiber-associated aged SCs and assessed for their expansion and Pax7 expression (Figure 3.10a). Aged SCs treated with vehicle, are predominately $Pax7^{-}MyoD^{+}$, with only 20% of the cells expressing Pax7. TS2/16 treatment showed alone no rescue of Pax7 expression (Figure 3.10b-c). Consistent with previous studies, FGF treatment also did not rescue Pax7 expression due to insensitivity of SCs from aged mice to FGF-2 (Figure 3.10b-c). However, the combination of TS2/16 and FGF did significantly increase the fraction of $Pax7^{+}$ cells as well as fiber-associated myogenic cell numbers (Figure 3.10c,d). Interestingly, the proportion of proliferating aged SCs with TS2/16 and FGF is comparable to young SCs treated with FGF alone, demonstrating that restoring β1-integrin can rejuvenate aged SCs.

Next, we examined the localization of phospho-p38 in aged SCs treated with TS2/16 and FGF (Figure 3.11a). Consistent with restoration of self-renewal, culturing aged SCs with TS2/16 and FGF reestablishes phospho-p38 asymmetry (3.11b-c). Integrin signaling has been shown to regulate the levels of p38 phosphorylation both positively and negatively (D. Cosgrove et al., 2008; Smeeton et al., 2010). These data provide the first example of regulation of phospho-p38 polarization, which may be uniquely relevant

Figure 3.10. Activating β1-integrin in aged SCs restores responsiveness to FGF for self-renewal. a, Schematic of tamoxifen (tmx) regimen and myofiber harvest. Myofiber-associated YFP^+ SCs from control and aged mice cultured for 72 h with vehicle (mouse IgG, 10μg/ml), β1-integrin activating antibody TS2/16 (10μg/ml), FGF-2 (1ng/ml), or both. They were stained for Pax7 and MyoD. **b,** Representative images for vehicle (top panel) and TS2/16+FGF-2 (bottom panel) treated cultures: asterisk, proliferating $Pax7^+MyoD^+$ cells; open arrowhead, differentiating $Pax7^-MyoD^+$ cells; scale bar = 25μm. **c,** Percentages of $Pax7^+$ or $MyoD^+$ of total SCs in all four groups; n = 3 experiments, ≥ 30 myofibers each; for TS2/16+ FGF-2 vs. other conditions, $p<0.05$ by one-way ANOVA, while there is no significant differences between the other 3 groups.

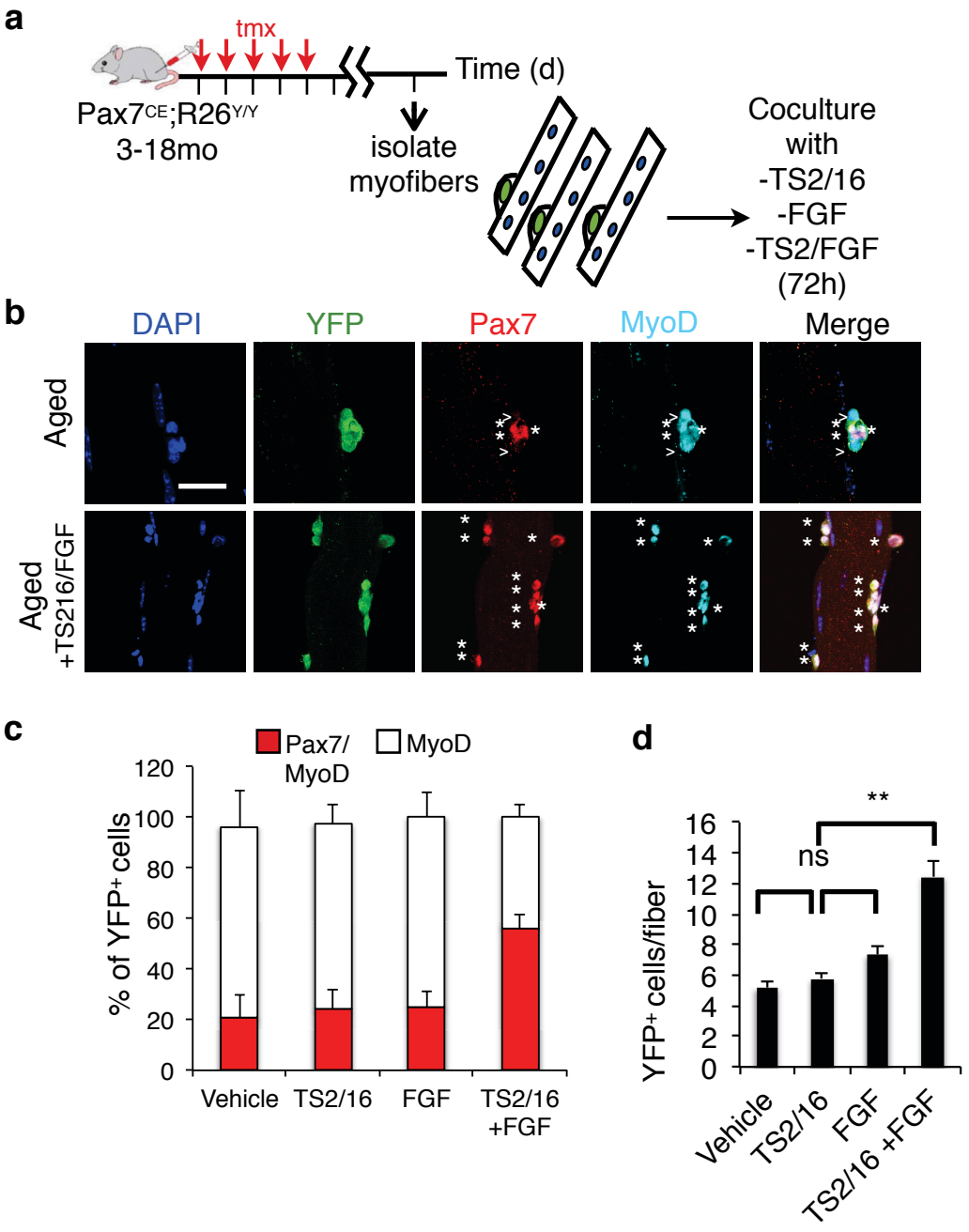
a
tmx
Time (d)
Pax7CE;R26Y/Y
3-18mo
isolate
myofibers
Coculture
with
-TS2/16
-FGF
-TS2/FGF
(72h)
b
DAPI
YFP
Pax7
MyoD
Merge
Aged
Aged
+TS216/FGF
c
Pax7/
MyoD
MyoD
% of YFP+ cells
120
100
80
60
40
20
0
Vehicle
TS2/16
FGF
TS2/16
+FGF
d
**
ns
YFP+ cells/fiber
16
14
12
10
8
6
4
2
0
Vehicle
TS2/16
FGF
TS2/16 +FGF

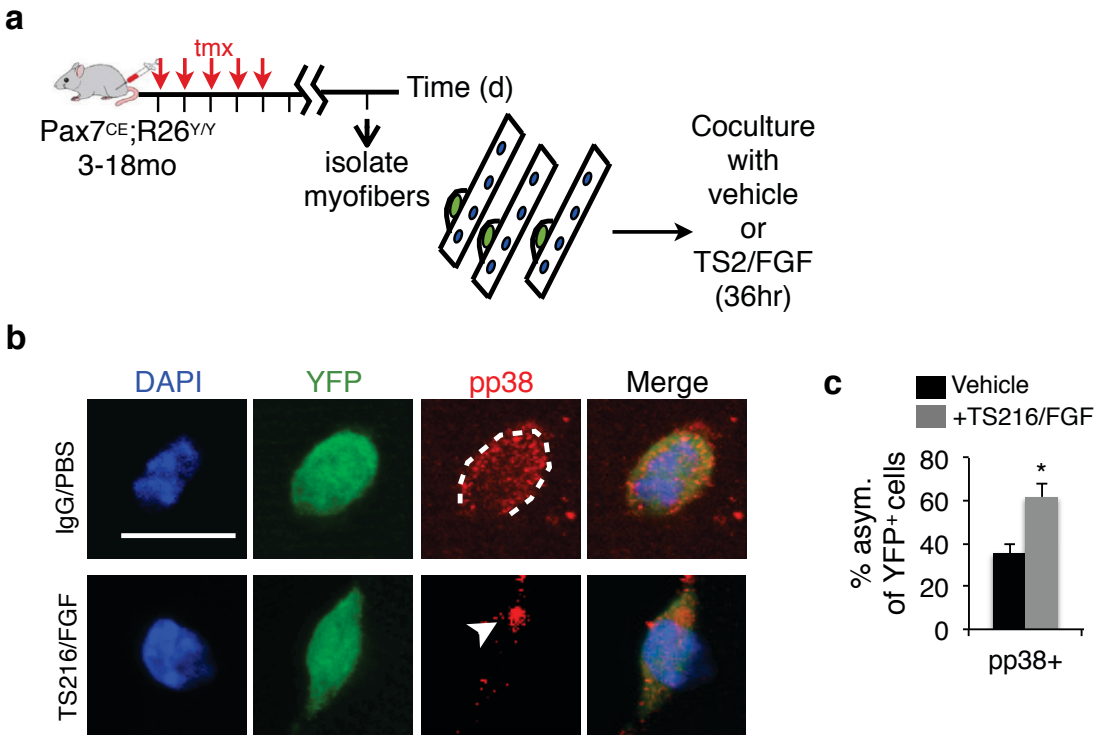

Figure 3.11. Activating β1-integrin in aged SCs restores responsiveness to FGF to rescue the asymmetric localization of pp38. a, Schematic of tamoxifen (tmx) regimen and myofiber harvest. **b,c,** Myofiber-associated YFP$^+$ SCs from young and aged mice cultured for 36 h with vehicle or TS2/16 (10 μg/ml) and FGF-2 (1 ng/ml) and stained for pp38 (asymmetric, arrowhead) (**b**) and the percentages of asymmetric pp38 were plotted in (**c**); * = p<0.05, Student's t-test; n = 3 experiments, ≥ 25 myofibers each.

for stem cell biology.

The positive effect of TS2/16 on regeneration in aged muscle environment led us to test whether it may also benefit in another scenario of impaired muscle regeneration: dystrophic muscles. For this, we employed the *mdx* mouse model, which lacks dystrophin due to a non-sense mutation. A single dose of TS2/16 to these mice was sufficient to promote the expansion of myogenic cells, as shown by increased EdU incorporation 3 d after treatment (Figure 3.12a-c). Furthermore, multiple applications resulted in dramatic increases of muscle fiber cross sectional area and diameter when compared to vehicle-treated mice (Figure 3.12d-j). As α7β1-integrin binds to laminin, an ECM component that also engages with the dystrophin complex, activating β1-integrin likely also enhances muscle fiber integrity in *mdx* mice via improved connection to the ECM. Thus, activating β1-integrin also has therapeutic potential to improve muscle repair in diseased conditions.

Figure 3.12. Activating β1-integrin improves the pathology of muscular dystrophy. **a,** Schematic of short-term integrin activating treatment in TA muscle of 3-month-old *mdx* mice. **b,** Representative images of EdU^+ nuclei 5 d after integrin activation as compared to vehicle. **c,** Percentage of EdU^+ nuclei ($Pax7^+/MyoD^+$, labeled with arrowhead, or centrally located in regenerating myofibers, labeled with asterisk); $n = 3$ animals per treatment; 10 sections per animal. **d,** Schematic of long-term integrin activating treatment in skeletal muscle of 3 mo old *mdx* mice. **e,** Representative images of H&E staining of muscle of *mdx* mice treated with TS2/16 or vehicle control at 28 d; scale bar = 25 μm. Quantification of average cross-sectional area (CSA) (**f**) and diameter (**g**) at 28 d; $n = 3$ animals per treatment, 10 sections per animal. Numerical data are expressed as mean ± s.e.m.; Student's *t*-test: *= $p < 0.05$, **= $p < 0.01$.

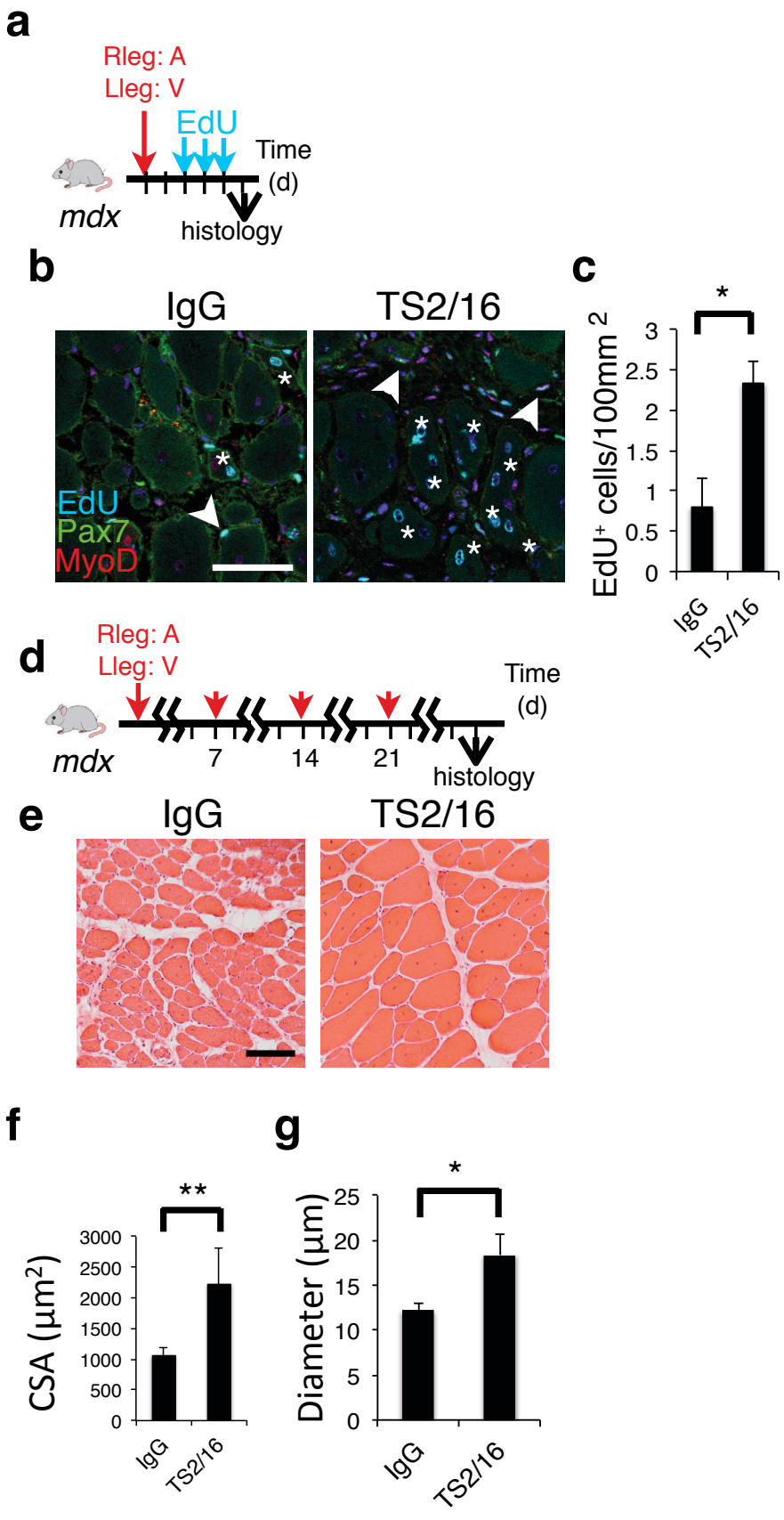
a
Rleg: A
Lleg: V
EdU
Time
(d)
mdx
histology
b
IgG
TS2/16
EdU
Pax7
MyoD
c
*
EdU+ cells/100mm 2
3
2.5
2
1.5
1
0.5
0
IgG
TS2/16
d
Rleg: A
Lleg: V
Time
(d)
mdx
7
14
21
histology
e
IgG
TS2/16
f
**
CSA (μm2)
3000
2500
2000
1500
1000
500
0
IgG
TS2/16
g
*
Diameter (μm)
25
20
15
10
5
0
IgG
TS2/16

DISCUSSION

Skeletal muscle deteriorates upon aging leading to the impairment of movement, which greatly affects the quality of life in all elderly people. This age-related muscle wasting, called sarcopenia, is characterized by loss of muscle mass as well as muscle integrity. Additionally, satellite cell function declines upon aging, leading to deficiencies in aged muscle regeneration. This reduction in regenerative capacity has been linked to 1) decrease in overall SC number, 2) cell-intrinsic changes, notably elevated growth factor signaling through increased phospho-p38α/β MAPK activity, and 3) cell extrinsic changes in systemic cues as well as the local microenvironment, especially the increased stiffness and changes in composition of the extracellular matrix (Wood et al., 2014).

Integrins function to connect the outside of the cell to the inside, both structurally and contextually, through modulating growth factor signaling and affecting gene transcription. Given that these processes are defective in aged SCs, we theorized that integrin integrity, presentation, or activity becomes misregulated upon aging to induce muscle dysfunction. Furthermore, perhaps in correcting these defects we could positively impact SC function and muscle pathology and provide potentially new therapeutic targets.

Our results together frame a model in which β1-integrin acts as a major sensor of the young adult SC niche for maintenance of quiescence and for responsiveness to injury-released FGF, and that the dysfunction in integrin activity is one of the main cause(s) of age-associated decline of regeneration and FGF sensitivity (Figure 3.13).

We utilized a satellite cell specific driver of Cre recombinase in order to inactivate β1-integrin specifically in this stem cell. These SCs (*Itgb1*-KO SCs) display

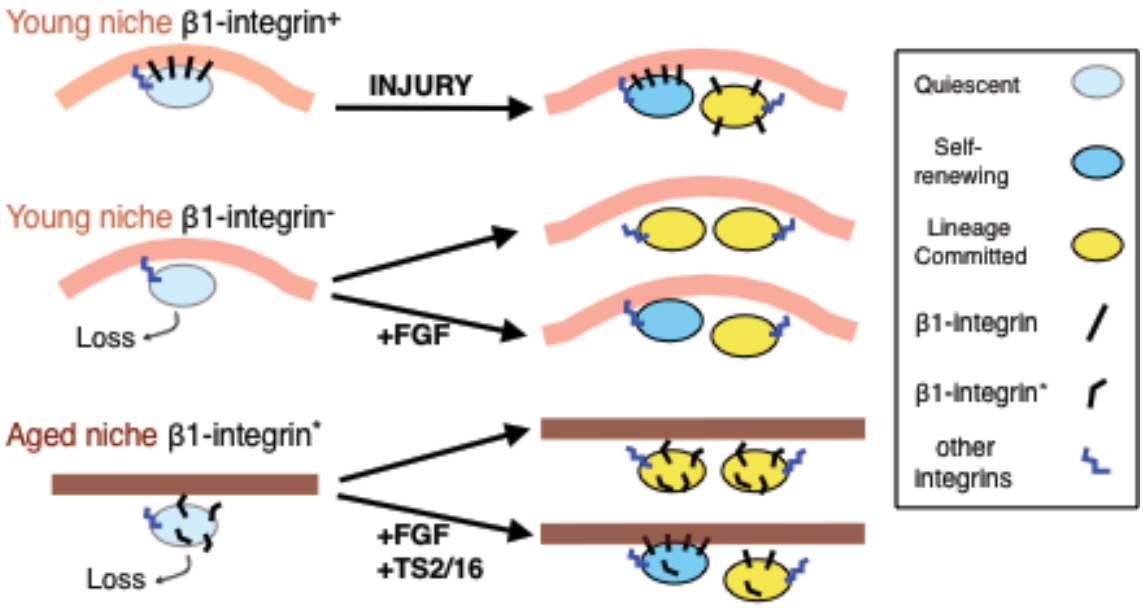

Figure 3.13. Integrin acts as a sensor of the SC niche to mediate responsiveness to FGF for self-renewal.

hallmarks of aged SCs: they 1) lose quiescence and 2) are defective in self-renewal. However, as they reside in a young environment and given the compensatory ability of integrins demonstrated in other systems, it is likely that *Itgb1*-KO SCs retain some connection to the ECM (Mercurio, 2002). These other integrins coordinate with FGF to rescue appropriate segregation of phospho-p38 for asymmetric divisions (Figure 3.8). Blocking all RGD-recognizing integrins abolishes this rescue (Figure 3.9). Because RGD-binding integrins and their cognitive ECM components are numerous and SCs express almost all α- and β-integrins (Figure 1.1), defining the precise contribution of each of them in this context may take considerable efforts. Despite this complexity, our findings help to explain why ECM implantation can enhance muscle regeneration (Merritt et al., 2010).

Aged SCs display sporadically localized activated β1-integrin (Figure 3.2), suggesting that the ECM becomes disorganized upon aging, either by wear and tear of muscle fibers or erroneous deposition by interstitial fibrotic cells. The resulting ECM disorganization inhibits proper alignment of integrin and its activation along the basal membrane in aged SCs. Without proper connection to the niche, aged SCs cannot sense FGF therefore generate predominately lineage-committed daughters (Figure 3.10). Increasing β1-integrin activity restores sensitivity to FGF, to asymmetrically localize phospho-p38 for SC self-renewal.

Additionally, enhancing integrin activity *in vivo* (by treatment with TS2/16) restores muscle regeneration in aged animals (Figure 3.5). We surmise that muscle damage releases a sufficient amount of FGF2 to coordinate with activated β1-integrin *in vivo*, in contrast to *in vitro* assays where additional FGF2 was needed. In contrast,

treatment of young animals with the RGD peptide, results in an 'aged' phenotype, repressing muscle regeneration to a level comparable to the aged mice. Synthetic peptides containing the RGD motif have been extensively used to inhibit integrin and ligand interactions, although in certain contexts they can induce integrin's 'high-affinity' confirmation (Buckley et al., 1999; Ye et al., 2012). Additional examination of these RGD-treated animals will be necessary to assess how the peptide affects integrin presentation or activity, however the results demonstrate unequivocally that mechanical sensing of the SC to its niche via integrin is critical.

Defining the ligand for β1-integrin and how it may become disorganized or improperly presented upon aging should be an area of future consideration. As mentioned, previous studies on integrin trafficking demonstrated that the net endocytosis rate of the active β1 integrins is higher than inactive, where is counteracted by rapid recycling back to the plasma membrane (Arjonen et al., 2012). This finding correlates with our observation that active β1-integrin is found intracellularly in aged SCs. Besides, affecting phospho-p38 localization, however, how this may impact transcription of downstream targets, as well as the identity of those targets remain to be defined. Obvious candidates were not elucidated in the RNA-seq data from *Itgb1I*-KO SCs (Figure 2.15). However, as mentioned these cells may experience compensation by other integrins and also experience a loss of β1-integrin as opposed to a dysregulation of integrin signaling, which may lead to differences between the two populations.

The finding that integrin is the sensor of the SC niche that becomes dysregulated upon aging, may help explain previously published work describing the aged phenotype. It is evident that levels of p38α/β MAPK activity are crucial, and become elevated in

aged SCs. However, the interpretation that SCs are insensitive to FGF signaling, and therefore mount an attenuated FGR1 response to attempts of activation by FGF ligand may be secondary to defects in integrin activity. Restoring proper integrin activity in SCs *in vivo* reestablishes the response to endogenous FGF ligands in order to properly segregate pp38, without any additional manipulations. Other signaling pathways that have been shown to become disregulated upon aging may also be downstream of integrin in the SC. Previous work demonstrated that integrin controls Wnt and Notch pathway activation in somites, which is the site of myogenic precursors that will later give rise to satellite cells (Gros et al., 2005; Rallis et al., 2010). It is possible that these signaling pathways remain linked throughout development and into adulthood in the muscle. Finally, two groups have recently demonstrated that the JAK-STAT pathway becomes elevated in SCs upon aging; inhibiting the signaling cascade is another way to restore function to aged muscle (Price et al., 2014; Tierney et al., 2014). This phenotype may also be downstream of the integrin defect I report here. Given that integrin signaling has been shown to activate the JAK-STAT pathway, and that we visualize active β1-integrin intracellularly in aged SCs, my finding of integrin dysregulation may cause spurious activation of the integrin signaling and downstream targets, like JAK-STAT to additionally contribute to the aging phenotype (Brizzi et al., 1999; Xie et al., 2001). Parsing out the effect that misregulation of β1-integrin has on individual genes and networks will require additional exploration, especially given the wealth of signaling axes that are derived from integrin activity.

Future investigation into how the integrin-FGF axis intersects with other signaling pathways to regulate SC function in the young and aged niche should build a better

understanding for muscle stem cell biology. Importantly, my findings provide a treatment that restores aged SC function *in vivo*, in contrast to previous *ex vivo* treatments. Given the role of integrin in other stem cells, principles derived from this study will likely have direct implications for aging and decline of function in other somatic stem cells.

REFERENCES

Allbrook, D. B., Han, M. F., and Hellmuth, A. E. (1971). Population of muscle satellite cells in relation to age and mitotic activity. *Pathology*, *3*(3), 223–243.

Allen, R. E., Dodson, M. V., and Luiten, L. S. (1984). Regulation of skeletal muscle satellite cell proliferation by bovine pituitary fibroblast growth factor. *Experimental Cell Research*, *152*(1), 154–160.

Andersson, E. R., Sandberg, R., and Lendahl, U. (2011). Notch signaling: simplicity in design, versatility in function. *Development*, *138*(17), 3593–3612.

Argraves, W. S., Suzuki, S., Arai, H., Thompson, K., Pierschbacher, M. D., and Ruoslahti, E. (1987). Amino Acid Sequence of the Human Fibronectin Receptor. *The Journal of Cell Biology*, *105*(3), 1183–1190.

Arjonen, A., Alanko, J., Veltel, S., and Ivaska, J. (2012). Distinct recycling of active and inactive β1 integrins. *Traffic*, *13*(4), 610–625.

Äärimaa, V., Rantanen, J., Best, T., Schultz, E., Corr, D., and Kalimo, H. (2004). Mild eccentric stretch injury in skeletal muscle causes transient effects on tensile load and cell proliferation. *Scandinavian Journal of Medicine & Science in Sports*, *14*(6), 367–372.

Bazzoni, G., Shih, D.-T., Buck, C. A., and Hemler, M. E. (1995). Monoclonal Antibody 9EG7 Defines a Novel β1 Integrin Epitope Induced by Soluble Ligand and Manganese, but Inhibited by Calcium. *Journal of Biological Chemistry*, *270*(43), 25570–25577.

Behringer, R., Gertsenstein, M., Nagy, K. V., and Nagy, A. (2014). *Manipulating the Mouse Embryo*.

Belmokhtar, C. A., Hillion, J., and Ségal-Bendirdjian, E. (2001). Staurosporine induces apoptosis through both caspase-dependent and caspase-independent mechanisms. *Oncogene*, *20*(26), 3354–3362.

Bentzinger, C. F., Wang, Y. X., Maltzahn, von, J., Soleimani, V. D., Yin, H., and Rudnicki, M. A. (2013). Fibronectin regulates Wnt7a signaling and satellite cell expansion. *Cell Stem Cell*, *12*(1), 75–87.

Berkes, C. A., and Tapscott, S. J. (2005). MyoD and the transcriptional control of myogenesis. *Seminars in Cell & Developmental Biology*, *16*(4-5), 585–595.

Bernet, J. D., Doles, J. D., Hall, J. K., Kelly Tanaka, K., Carter, T. A., and Olwin, B. B. (2014). p38 MAPK signaling underlies a cell-autonomous loss of stem cell self-renewal in skeletal muscle of aged mice. *Nature Medicine*, *20*(3), 265–271.

Bintliff, S., and Walker, B. E. (1960). Radioautographic study of skeletal muscle regeneration. *American Journal of Anatomy*, *106*(3), 233–245.

Bischoff, R. (1975). Regeneration of single skeletal muscle fibers in vitro. *The Anatomical Record*, *182*(2), 215–235.

Bjornson, C. R. R., Cheung, T. H., Liu, L., Tripathi, P. V., Steeper, K. M., and Rando, T. A. (2012). Notch signaling is necessary to maintain quiescence in adult muscle stem cells. *Stem Cells (Dayton, Ohio)*, *30*(2), 232–242.

Blanco-Bose, W. E., Yao, C. C., Kramer, R. H., and Blau, H. M. (2001). Purification of mouse primary myoblasts based on alpha 7 integrin expression. *Experimental Cell Research*, *265*(2), 212–220.

Blaschuk, K. L., and Holland, P. C. (1994). The regulation of alpha 5 beta 1 integrin expression in human muscle cells. *Developmental Biology*, *164*(2), 475–483.

Blaveri, K., Heslop, L., Yu, D. S., Rosenblatt, J. D., Gross, J. G., Partridge, T. A., and Morgan, J. E. (1999). Patterns of repair of dystrophic mouse muscle: studies on isolated fibers. *Developmental Dynamics : an Official Publication of the American Association of Anatomists*, *216*(3), 244–256.

Brack, A. S., Conboy, M. J., Roy, S., Lee, M., Kuo, C. J., Keller, C., and Rando, T. A. (2007). Increased Wnt signaling during aging alters muscle stem cell fate and increases fibrosis. *Science*, *317*(5839), 807–810.

Brakebusch, C., and Fässler, R. (2005). beta 1 integrin function in vivo: adhesion, migration and more. - PubMed - NCBI. *Cancer and Metastasis Reviews*, *24*(3), 403–411.

Brennan, K. J., and Hardeman, E. C. (1993). Quantitative analysis of the human alpha-skeletal actin gene in transgenic mice. *Journal of Biological Chemistry*, *268*(1), 719–725.

Brien, P., Pugazhendhi, D., Woodhouse, S., Oxley, D., and Pell, J. M. (2013). p38α MAPK Regulates Adult Muscle Stem Cell Fate by Restricting Progenitor Proliferation During Postnatal Growth and Repair. *Stem Cells (Dayton, Ohio)*, *31*(8), 1597–1610.

Brizzi, M. F., Defilippi, P., Rosso, A., Venturino, M., Garbarino, G., Miyajima, A., et al. (1999). Integrin-mediated adhesion of endothelial cells induces JAK2 and STAT5A activation: role in the control of c-fos gene expression. *Molecular Biology of the Cell*, *10*(10), 3463–3471.

Bronner-Fraser, M., Artinger, M., Muschler, J., and Horwitz, A. F. (1992). Developmentally regulated expression of alpha 6 integrin in avian embryos.

Development, *115*(1), 197–211.

Brooks, S. V., and Faulkner, J. A. (1994). Skeletal muscle weakness in old age: underlying mechanisms. *Medicine and Science in Sports and Exercise*, *26*(4), 432–439.

Buckingham, M. (2006). Myogenic progenitor cells and skeletal myogenesis in vertebrates. *Current Opinion in Genetics & Development*, *16*(5), 525–532.

Buckley, C. D., Pilling, D., Henriquez, N. V., Parsonage, G., Threlfall, K., Scheel-Toellner, D., et al. (1999). RGD peptides induce apoptosis by direct caspase-3 activation. *Nature*, *397*(6719), 534–539.

Byron, A., Humphries, J. D., Askari, J. A., Craig, S. E., Mould, A. P., and Humphries, M. J. (2009). Anti-integrin monoclonal antibodies. *Journal of Cell Science*, *122*(Pt 22), 4009–4011.

Cachaço, A. S., Chuva de Sousa Lopes, S. M., Kuikman, I., Bajanca, F., Abe, K., Baudoin, C., et al. (2003). Knock-in of integrin beta 1D affects primary but not secondary myogenesis in mice. *Development*, *130*(8), 1659–1671.

Calderwood, D. A., Shattil, S. J., and Ginsberg, M. H. (2000). Integrins and actin filaments: reciprocal regulation of cell adhesion and signaling. *Journal of Biological Chemistry*, *275*(30), 22607–22610.

Carlson, M. E., Hsu, M., and Conboy, I. M. (2008). Imbalance between pSmad3 and Notch induces CDK inhibitors in old muscle stem cells. *Nature*, *454*(7203), 528–532.

Casola, S. (2010). Mouse models for miRNA expression: the ROSA26 locus. *Methods in Molecular Biology (Clifton, N.J.)*, *667*, 145–163.

Chakkalakal, J. V., Jones, K. M., Basson, M. A., and Brack, A. S. (2012). The aged niche

disrupts muscle stem cell quiescence. *Nature*, *490*(7420), 355–360.

Chargé, S. B. P., and Rudnicki, M. A. (2004). Cellular and Molecular Regulation of Muscle Regeneration. *Physiological Reviews*, *84*(1), 209–238.

Chen, Y.-W., Zhao, P., Borup, R., and Hoffman, E. P. (2000). Expression Profiling in the Muscular Dystrophies: Identification of Novel Aspects of Molecular Pathophysiology. *The Journal of Cell Biology*, *151*(6), 1321–1336.

Cheung, T. H., and Rando, T. A. (2013). Molecular regulation of stem cell quiescence. *Nature Reviews. Molecular Cell Biology*, *14*(6), 329–340.

Cheung, T. H., Quach, N. L., Charville, G. W., Liu, L., Park, L., Edalati, A., et al. (2012). Maintenance of muscle stem-cell quiescence by microRNA-489. *Nature*, *482*(7386), 524–528.

Collins, C. A., Olsen, I., Zammit, P. S., Heslop, L., Petrie, A., Partridge, T. A., and Morgan, J. E. (2005). Stem Cell Function, Self-Renewal, and Behavioral Heterogeneity of Cells from the Adult Muscle Satellite Cell Niche. *Cell*, *122*(2), 289–301.

Conboy, I. M. (2003). Notch-mediated restoration of regenerative potential to aged muscle. *Science*, *302*(5650), 1575–1577.

Conboy, I. M., Conboy, M. J., Wagers, A. J., Girma, E. R., Weissman, I. L., and Rando, T. A. (2005). Rejuvenation of aged progenitor cells by exposure to a young systemic environment. *Nature*, *433*(7027), 760–764.

Conley, K. E., Cress, M. E., Jubrias, S. A., Esselman, P. C., and Odderson, I. R. (1995). From muscle properties to human performance, using magnetic resonance. *The Journals of Gerontology. Series a, Biological Sciences and Medical Sciences*, *50*

Spec No, 35–40.

Cosgrove, B. D., Gilbert, P. M., Porpiglia, E., Mourkioti, F., Lee, S. P., Corbel, S. Y., et al. (2014). Rejuvenation of the muscle stem cell population restores strength to injured aged muscles. *Nature Medicine*, *20*(3), 255–264.

Cosgrove, D., Meehan, D. T., Delimont, D., Pozzi, A., Chen, X., Rodgers, K. D., et al. (2008). Integrin α1β1 Regulates Matrix Metalloproteinases via P38 Mitogen-Activated Protein Kinase in Mesangial Cells : Implications for Alport Syndrome. *The American Journal of Pathology*, *172*(3), 761–773.

Crawley, S., Farrell, E. M., Wang, W., Gu, M., Huang, H. Y., Huynh, V., et al. (1997). The alpha7beta1 integrin mediates adhesion and migration of skeletal myoblasts on laminin. *Experimental Cell Research*, *235*(1), 274–286.

Cree, M. G., Newcomer, B. R., Katsanos, C. S., Sheffield-Moore, M., Chinkes, D., Aarsland, A., et al. (2004). Intramuscular and liver triglycerides are increased in the elderly. *The Journal of Clinical Endocrinology and Metabolism*, *89*(8), 3864–3871.

Crist, C. G., Montarras, D., and Buckingham, M. (2012). Muscle satellite cells are primed for myogenesis but maintain quies... - PubMed - NCBI. *Cell Stem Cell*, *11*(1), 118–126.

d'Albis, A., Couteaux, R., Janmot, C., Roulet, A., and Mira, J. C. (1988). Regeneration after cardiotoxin injury of innervated and denervated slow and fast muscles of mammals. Myosin isoform analysis. *European Journal of Biochemistry / FEBS*, *174*(1), 103–110.

D'Souza, S. E., Ginsberg, M. H., and Plow, E. F. (1991). Arginyl-glycyl-aspartic acid (RGD): a cell adhesion motif. *Trends in Biochemical Sciences*, *16*, 246–250.

Day, K., Shefer, G., Shearer, A., and Yablonka-Reuveni, Z. (2010). The depletion of skeletal muscle satellite cells with age is concomitant with reduced capacity of single progenitors to produce reserve progeny. *Developmental Biology*, *340*(2), 330–343.

Dellavalle, A., Sampaolesi, M., Tonlorenzi, R., Tagliafico, E., Sacchetti, B., Perani, L., et al. (2007). Pericytes of human skeletal muscle are myogenic precursors distinct from satellite cells. *Nature Cell Biology*, *9*(3), 255–267.

Echtermeyer, F., Schöber, S., Pöschl, E., Mark, von der, H., and Mark, von der, K. (1996). Specific induction of cell motility on laminin by alpha 7 integrin. *Journal of Biological Chemistry*, *271*(4), 2071–2075.

Einsiedel, L. J., and Luff, A. R. (1992). Alterations in the contractile properties of motor units within the ageing rat medial gastrocnemius. *Journal of the Neurological Sciences*, *112*(1-2), 170–177.

Elabd, C., Cousin, W., Upadhyayula, P., Chen, R. Y., Chooljian, M. S., Li, J., et al. (2014). Oxytocin is an age-specific circulating hormone that is necessary for muscle maintenance and regeneration. *Nature Communications*, *5*.

Fässler, R., and Meyer, M. (1995). Consequences of lack of beta 1 integrin gene expression in mice. *Genes & Development*, *9*(15), 1896–1908.

Feil, R., Brocard, J., Mascrez, B., LeMeur, M., Metzger, D., and Chambon, P. (1996). Ligand-Activated Site-Specific Recombination in Mice. *Proceedings of the National Academy of Sciences of the United States of America*, *93*(20), 10887–10890.

Feil, R., Wagner, J., Metzger, D., and Chambon, P. (1997). Regulation of Cre recombinase activity by mutated estrogen receptor ligand-binding domains. *Biochemical and Biophysical Research Communications*, *237*(3), 752–757.

Fre, S., Huyghe, M., Mourikis, P., Robine, S., Louvard, D., and Artavanis-Tsakonas, S. (2005). Notch signals control the fate of immature progenitor cells in the intestine. *Nature*, *435*(7044), 964–968.

Fukada, S.-I., Uezumi, A., Ikemoto, M., Masuda, S., Segawa, M., Tanimura, N., et al. (2007). Molecular signature of quiescent satellite cells in adult skeletal muscle. *Stem Cells (Dayton, Ohio)*, *25*(10), 2448–2459.

Giresi, P. G., Stevenson, E. J., Theilhaber, J., Koncarevic, A., Parkington, J., Fielding, R. A., and Kandarian, S. C. (2005). Identification of a molecular signature of sarcopenia. *Physiological Genomics*, *21*(2), 253–263.

Graus-Porta, D., Blaess, S., Senften, M., Littlewood-Evans, A., Damsky, C., Huang, Z., et al. (2001). Beta1-class integrins regulate the development of laminae and folia in the cerebral and cerebellar cortex. *Neuron*, *31*(3), 367–379.

Gros, J., Manceau, M., Thomé, V., and Marcelle, C. (2005). A common somitic origin for embryonic muscle progenitors and satellite cells. *Nature*, *435*(7044), 954–958.

Grounds, M. D. (1998). Age-associated changes in the response of skeletal muscle cells to exercise and regeneration. *Annals of the New York Academy of Sciences*, *854*, 78–91.

Hall, J. K., Banks, G. B., Chamberlain, J. S., and Olwin, B. B. (2010). Prevention of muscle aging by myofiber-associated satellite cell transplantation. *Science Translational Medicine*, *2*(57), 57ra83–57ra83.

Hellmuth, A. E., and Allbrook, D. B. (1971). Muscle satellite cell numbers during the postnatal period. *Journal of Anatomy*, *110*(Pt 3), 503.

Hershko, A. (1999). Mechanisms and regulation of the degradation of cyclin B.

Philosophical Transactions of the Royal Society of London. Series B, Biological Sciences, *354*(1389), 1571–5– discussion 1575–6.

Humphries, J. D., Byron, A., and Humphries, M. J. (2006). Integrin ligands at a glance. *Journal of Cell Science*, *119*(Pt 19), 3901–3903.

Hynes, R. O. (1992). Integrins: Versatility, modulation, and signaling in cell adhesion. *Cell*, *69*(1), 11–25.

Hynes, R. O. (2002). Integrins: bidirectional, allosteric signaling machines. *Cell*, *110*(6), 673–687.

Iezzi, S., Di Padova, M., Serra, C., Caretti, G., Simone, C., Maklan, E., et al. (2004). Deacetylase inhibitors increase muscle cell size by promoting myoblast recruitment and fusion through induction of follistatin. *Developmental Cell*, *6*(5), 673–684.

Ivaska, J., and Heino, J. (2010). Interplay between cell adhesion and growth factor receptors: from the plasma membrane to the endosomes. *Cell and Tissue Research*, *339*(1), 111–120.

Jaffredo, T., Horwitz, A. F., Buck, C. A., Rong, P. M., and Dieterlen-Lievre, F. (1988). Myoblast migration specifically inhibited in the chick embryo by grafted CSAT hybridoma cells secreting an anti-integrin antibody. *Development*, *103*(3), 431–446.

Järvinen, T. A. H., Kääriäinen, M., Äärimaa, V., Järvinen, M., and Kalimo, H. (2008). Skeletal Muscle Repair After Exercise-Induced Injury. In *Skeletal Muscle Repair and Regeneration* (Vol. 3, pp. 217–242). Dordrecht: Springer Netherlands.

Jones, N. C., Tyner, K. J., Nibarger, L., Stanley, H. M., Cornelison, D. D. W., Fedorov, Y. V., and Olwin, B. B. (2005). The p38alpha/beta MAPK functions as a molecular switch to activate the quiescent satellite cell. *The Journal of Biophysical and*

Biochemical Cytology, *169*(1), 105–116.

Kablar, B., Krastel, K., Ying, C., Asakura, A., Tapscott, S. J., and Rudnicki, M. A. (1997). MyoD and Myf-5 differentially regulate the development of limb versus trunk skeletal muscle. *Development*, *124*(23), 4729–4738.

Kanatsu-Shinohara, M., Takehashi, M., Takashima, S., Lee, J., Morimoto, H., Chuma, S., et al. (2008). Homing of mouse spermatogonial stem cells to germline niche depends on beta1-integrin. *Cell Stem Cell*, *3*(5), 533–542.

Konhilas, J. P., Widegren, U., Allen, D. L., Paul, A. C., Cleary, A., and Leinwand, L. A. (2005). Loaded wheel running and muscle adaptation in the mouse. *American Journal of Physiology - Heart and Circulatory Physiology*, *289*(1), H455–H465.

Konigsberg, U. R., Lipton, B. H., and Konigsberg, I. R. (1975). The regenerative response of single mature muscle fibers isolated in vitro. *Developmental Biology*, *45*(2), 260–275.

Kragstrup, T. W., Kjaer, M., and Mackey, A. L. (2011). Structural, biochemical, cellular, and functional changes in skeletal muscle extracellular matrix with aging. *Scandinavian Journal of Medicine & Science in Sports*, *21*(6), 749–757.

Krans, J. L. (2010). The Sliding Filament Theory of Muscle Contraction. *Nature Education*, *3*(9), 66.

Kuang, S., Chargé, S. B., Seale, P., Huh, M., and Rudnicki, M. A. (2006). Distinct roles for Pax7 and Pax3 in adult regenerative myogenesis. *The Journal of Biophysical and Biochemical Cytology*, *172*(1), 103–113.

Kuang, S., Kuroda, K., Le Grand, F., and Rudnicki, M. A. (2007). Asymmetric self-renewal and commitment of satellite stem cells in muscle. *Cell*, *129*(5), 999–1010.

Le Grand, F., Jones, A. E., Seale, V., Scimè, A., and Rudnicki, M. A. (2009). Wnt7a activates the planar cell polarity pathway to drive the symmetric expansion of satellite stem cells. *Cell Stem Cell*, *4*(6), 535–547.

Legate, K. R., Montañez, E., Kudlacek, O., and Füssler, R. (2005). ILK, PINCH and parvin: the tIPP of integrin signalling. *Nature Reviews. Molecular Cell Biology*, *7*(1), 20–31.

Lepper, C., and Fan, C.-M. (2010). Inducible lineage tracing of Pax7-descendant cells reveals embryonic origin of adult satellite cells. *Genesis (New York, N.Y. : 2000)*, *48*(7), 424–436.

Lepper, C., Conway, S. J., and Fan, C.-M. (2009). Adult satellite cells and embryonic muscle progenitors have distinct genetic requirements. *Nature*, *460*(7255), 627–631.

Lepper, C., Partridge, T. A., and Fan, C.-M. (2011). An absolute requirement for Pax7-positive satellite cells in acute injury-induced skeletal muscle regeneration. *Development*, *138*(17), 3639–3646.

Li, F., Redick, S. D., Erickson, H. P., and Moy, V. T. (2003). Force measurements of the alpha5beta1 integrin-fibronectin interaction. *Biophysical Journal*, *84*(2 Pt 1), 1252–1262.

Liu, L., Cheung, T. H., Charville, G. W., Hurgo, B. M. C., Leavitt, T., Shih, J., et al. (2013). Chromatin modifications as determinants of muscle stem cell quiescence and chronological aging. *Cell Reports*, *4*(1), 189–204.

Lluís, F., Perdiguero, E., Nebreda, A. R., and Muñoz-Cánoves, P. (2006). Regulation of skeletal muscle gene expression by p38 MAP kinases. *Trends in Cell Biology*, *16*(1), 36–44.

Loulier, K., Lathia, J. D., Marthiens, V., Relucio, J., Mughal, M. R., Tang, S.-C., et al. (2009). beta1 integrin maintains integrity of the embryonic neocortical stem cell niche. *PLoS Biology*, *7*(8), e1000176.

Luisa Boldrin, J. E. M. (2012). Human satellite cells: identification on human muscle fibres. *PLoS Currents*, *3*, RRN1294.

MacIntosh, B. R., Gardiner, P. F., and McComas, A. J. (2006). *Skeletal Muscle*. Human Kinetics.

Madaro, L., Marrocco, V., Fiore, P., Aulino, P., Smeriglio, P., Adamo, S., et al. (2011). PKCθ signaling is required for myoblast fusion by regulating the expression of caveolin-3 and β1D integrin upstream focal adhesion kinase. *Molecular Biology of the Cell*, *22*(8), 1409–1419.

Mauro, A. (1961). Satellite Cell of Skeletal Muscle Fibers. *The Journal of Biophysical and Biochemical Cytology*, *9*(2), 493–495.

Mayer, U. (2003). Integrins: redundant or important players in skeletal muscle? *Journal of Biological Chemistry*, *278*(17), 14587–14590.

Mayer, U., Saher, G., Fässler, R., Bornemann, A., Echtermeyer, F., Mark, von der, H., et al. (1997). Absence of integrin alpha 7 causes a novel form of muscular dystrophy. *Nature Genetics*, *17*(3), 318–323.

Meeson, A. P., Hawke, T. J., Graham, S., Jiang, N., Elterman, J., Hutcheson, K., et al. (2004). Cellular and molecular regulation of skeletal muscle side population cells. *Stem Cells (Dayton, Ohio)*, *22*(7), 1305–1320.

Melcon, G., Kozlov, S., Cutler, D. A., Sullivan, T., Hernandez, L., Zhao, P., et al. (2006). Loss of emerin at the nuclear envelope disrupts the Rb1/E2F and MyoD pathways

during muscle regeneration. *Human Molecular Genetics*, *15*(4), 637–651.

Menko, A. S., and Boettiger, D. (1987). Occupation of the extracellular matrix receptor, integrin, is a control point for myogenic differentiation. *Cell*, *51*(1), 51–57.

Mercurio, A. M. (2002). Lessons from the alpha2 integrin knockout mouse. *The American Journal of Pathology*, *161*(1), 3–6.

Merritt, E. K., Hammers, D. W., Tierney, M., Suggs, L. J., Walters, T. J., and Farrar, R. P. (2010). Functional assessment of skeletal muscle regeneration utilizing homologous extracellular matrix as scaffolding. *Tissue Engineering. Part A*, *16*(4), 1395–1405.

Metzger, D., Clifford, J., Chiba, H., and Chambon, P. (1995). Conditional site-specific recombination in mammalian cells using a ligand-dependent chimeric Cre recombinase. *Proceedings of the National Academy of Sciences of the United States of America*, *92*(15), 6991–6995.

Miller, K. J., Thaloor, D., Matteson, S., and Pavlath, G. K. (2000). Hepatocyte growth factor affects satellite cell activation and differentiation in regenerating skeletal muscle. *American Journal of Physiology. Cell Physiology*, *278*(1), C174–81.

Mitchell, K. J., Pannérec, A., Cadot, B., Parlakian, A., Besson, V., Gomes, E. R., et al. (2010). Identification and characterization of a non-satellite cell muscle resident progenitor during postnatal development. *Nature Cell Biology*, *12*(3), 257–266.

Moreno-Layseca, P., and Streuli, C. H. (2014). Signalling pathways linking integrins with cell cycle progression. *Matrix Biology : Journal of the International Society for Matrix Biology*, *34*, 144–153.

Mori, S., and Takada, Y. (2013). Crosstalk between Fibroblast Growth Factor (FGF)

Receptor and Integrin through Direct Integrin Binding to FGF and Resulting Integrin-FGF-FGFR Ternary Complex Formation. *Medical Sciences*, *1*(1), 20–36.

Mori, S., Tran, V., Nishikawa, K., Kaneda, T., Hamada, Y., Kawaguchi, N., et al. (2013). A Dominant-Negative FGF1 Mutant (the R50E Mutant) Suppresses Tumorigenesis and Angiogenesis. *Plos One*, *8*(2), e57927.

Mourikis, P., Sambasivan, R., Castel, D., Rocheteau, P., Bizzarro, V., and Tajbakhsh, S. (2012). A critical requirement for notch signaling in maintenance of the quiescent skeletal muscle stem cell state. *Stem Cells (Dayton, Ohio)*, *30*(2), 243–252.

Patapoutian, A., Yoon, J. K., Miner, J. H., Wang, S., Stark, K., and Wold, B. (1995). Disruption of the mouse MRF4 gene identifies multiple waves of myogenesis in the myotome. *Development*, *121*(10), 3347–3358.

Pellinen, T., Tuomi, S., Arjonen, A., Wolf, M., Edgren, H., Meyer, H., et al. (2008). Integrin trafficking regulated by Rab21 is necessary for cytokinesis. *Developmental Cell*, *15*(3), 371–385.

Price, F. D., Maltzahn, von, J., Bentzinger, C. F., Dumont, N. A., Yin, H., Chang, N. C., et al. (2014). Inhibition of JAK-STAT signaling stimulates adult satellite cell function. *Nature Medicine*, *20*(10), 1174–1181.

Quach, N. L., Biressi, S., Reichardt, L. F., Keller, C., and Rando, T. A. (2009). Focal adhesion kinase signaling regulates the expression of caveolin 3 and beta1 integrin, genes essential for normal myoblast fusion. *Molecular Biology of the Cell*, *20*(14), 3422–3435.

Raghavan, S., Bauer, C., Mundschau, G., Li, Q., and Fuchs, E. (2000). Conditional ablation of beta1 integrin in skin. Severe defects in epidermal proliferation, basement

membrane formation, and hair follicle invagination. *The Journal of Biophysical and Biochemical Cytology*, *150*(5), 1149–1160.

Rallis, C., Pinchin, S. M., and Ish-Horowicz, D. (2010). Cell-autonomous integrin control of Wnt and Notch signalling during somitogenesis. *Development*, *137*(21), 3591–3601.

Rantanen, J., Ranne, J., Hurme, T., and Kalimo, H. (1995). Denervated segments of injured skeletal muscle fibers are reinnervated by newly formed neuromuscular junctions. *Journal of Neuropathology and Experimental Neurology*, *54*(2), 188–194.

Rathbone, C. R., Yamanouchi, K., Chen, X. K., Nevoret-Bell, C. J., Rhoads, R. P., and Allen, R. E. (2011). Effects of transforming growth factor-beta (TGF-β1) on satellite cell activation and survival during oxidative stress. *Journal of Muscle Research and Cell Motility*, *32*(2), 99–109.

Relaix, F., Rocancourt, D., Mansouri, A., and Buckingham, M. (2005). A Pax3/Pax7-dependent population of skeletal muscle progenitor cells. *Nature*, *435*(7044), 948–953.

Reverte, C. G., Benware, A., Jones, C. W., and LaFlamme, S. E. (2006). Perturbing Integrin Function Inhibits Microtubule Growth from Centrosomes, Spindle Assembly, and Cytokinesis. *The Journal of Cell Biology*, *174*(4), 491–497.

Rocheteau, P., Gayraud-Morel, B., Siegl-Cachedenier, I., Blasco, M. A., and Tajbakhsh, S. (2012). A subpopulation of adult skeletal muscle stem cells retains all template DNA strands after cell division. *Cell*, *148*(1-2), 112–125.

Rooney, J. E., Welser, J. V., Dechert, M. A., Flintoff-Dye, N. L., Kaufman, S. J., and Burkin, D. J. (2006). Severe muscular dystrophy in mice that lack dystrophin and

alpha7 integrin. *Journal of Cell Science*, *119*(Pt 11), 2185–2195.

Rosen, G. D., Sanes, J. R., LaChance, R., Cunningham, J. M., Roman, J., and Dean, D. C. (1992). Roles for the integrin VLA-4 and its counter receptor VCAM-1 in myogenesis. *Cell*, *69*(7), 1107–1119.

Ryall, J. G., Schertzer, J. D., and Lynch, G. S. (2008). Cellular and molecular mechanisms underlying age-related skeletal muscle wasting and weakness. *Biogerontology*, *9*(4), 213–228.

Sacco, A., Doyonnas, R., Kraft, P., Vitorovic, S., and Blau, H. M. (2008). Self-renewal and expansion of single transplanted muscle stem cells. *Nature*, *456*(7221), 502–506.

Sambasivan, R., Yao, R., Kissenpfennig, A., Van Wittenberghe, L., Paldi, A., Gayraud-Morel, B., et al. (2011). Pax7-expressing satellite cells are indispensable for adult skeletal muscle regeneration. *Development*, *138*(17), 3647–3656.

Sampaolesi, M., Torrente, Y., Innocenzi, A., Tonlorenzi, R., D'Antona, G., Pellegrino, M. A., et al. (2003). Cell therapy of alpha-sarcoglycan null dystrophic mice through intra-arterial delivery of mesoangioblasts. *Science*, *301*(5632), 487–492.

Schwander, M., Leu, M., Stumm, M., Dorchies, O. M., Ruegg, U. T., Schittny, J., and Müller, U. (2003). β1 Integrins Regulate Myoblast Fusion and Sarcomere Assembly. *Developmental Cell*, *4*(5), 673–685.

Seale, P., Sabourin, L. A., Girgis-Gabardo, A., Mansouri, A., Gruss, P., and Rudnicki, M. A. (2000). Pax7 is required for the specification of myogenic satellite cells. *Cell*, *102*(6), 777–786.

Serrano, A. L., Baeza-Raja, B., Perdiguero, E., Jardí, M., and Muñoz-Cánoves, P. (2008). Interleukin-6 is an essential regulator of satellite cell-mediated skeletal muscle

hypertrophy. *Cell Metabolism*, *7*(1), 33–44.

Shattil, S. J., Kim, C., and Ginsberg, M. H. (2010). The final steps of integrin activation: the end game. *Nature Reviews. Molecular Cell Biology*, *11*(4), 288–300.

Shea, K. L., Xiang, W., LaPorta, V. S., Licht, J. D., Keller, C., Basson, M. A., and Brack, A. S. (2010). Sprouty1 regulates reversible quiescence of a self-renewing adult muscle stem cell pool during regeneration. *Cell Stem Cell*, *6*(2), 117–129.

Sheehan, S. M., and Allen, R. E. (1999). Skeletal muscle satellite cell proliferation in response to members of the fibroblast growth factor family and hepatocyte growth factor. *Journal of Cellular Physiology*, *181*(3), 499–506.

Siegel, A. L., Atchison, K., Fisher, K. E., Davis, G. E., and Cornelison, D. (2009). 3D Timelapse Analysis of Muscle Satellite Cell Motility. *Stem Cells (Dayton, Ohio)*, *27*(10), 2527–2538.

Siegel, A. L., Kuhlmann, P. K., and Cornelison, D. D. W. (2011). Muscle satellite cell proliferation and association: new insights from myofiber time-lapse imaging. *Skeletal Muscle*, *1*(1), 7.

Smeeton, J., Zhang, X., Bulus, N., Mernaugh, G., Lange, A., Karner, C. M., et al. (2010). Integrin-linked kinase regulates p38 MAPK-dependent cell cycle arrest in ureteric bud development. *Development*, *137*(19), 3233–3243.

Snow, M. H. (1977a). Myogenic cell formation in regenerating rat skeletal muscle injured by mincing. I. A fine structural study. *The Anatomical Record*, *188*(2), 181–199.

Snow, M. H. (1977b). The effects of aging on satellite cells in skeletal muscles of mice and rats. *Cell and Tissue Research*, *185*(3), 399–408.

Song, W. K., Wang, W., Sato, H., Bielser, D. A., and Kaufman, S. J. (1993). Expression

of alpha 7 integrin cytoplasmic domains during skeletal muscle development: alternate forms, conformational change, and homologies with serine/threonine kinases and tyrosine phosphatases. *Journal of Cell Science*, *106 (Pt 4)*, 1139–1152.

Soriano, P. (1999). Generalized lacZ expression with the ROSA26 Cre reporter strain. *Nature Genetics*, *21*(1), 70–71.

Srinivas, S., Watanabe, T., Lin, C. S., William, C. M., Tanabe, Y., Jessell, T. M., and Costantini, F. (2001). Cre reporter strains produced by targeted insertion of EYFP and ECFP into the ROSA26 locus. *BMC Developmental Biology*, *1*, 4.

Stephens, L. E., Sutherland, A. E., Klimanskaya, I. V., Andrieux, A., Meneses, J., Pedersen, R. A., and Damsky, C. H. (1995). Deletion of beta 1 integrins in mice results in inner cell mass failure and peri-implantation lethality. *Genes & Development*, *9*(15), 1883–1895.

Tajbakhsh, S., and Buckingham, M. (2000). The birth of muscle progenitor cells in the mouse: spatiotemporal considerations. *Current Topics in Developmental Biology*, *48*, 225–268.

Takagi, J., and Springer, T. A. (2002). Integrin activation and structural rearrangement. *Immunological Reviews*, *186*(1), 141–163.

Tanentzapf, G., Devenport, D., Godt, D., and Brown, N. H. (2007). Integrin-dependent anchoring of a stem-cell niche. *Nature Cell Biology*, *9*(12), 1413–1418.

Tario, J. D., Humphrey, K., Bantly, A. D., Muirhead, K. A., Moore, J. S., and Wallace, P. K. (2012). Optimized staining and proliferation modeling methods for cell division monitoring using cell tracking dyes. *Journal of Visualized Experiments : JoVE*, (70), e4287.

Thompson, L. V. (2009). Age-related muscle dysfunction. *Experimental Gerontology*, *44*(1-2), 106–111.

Tierney, M. T., Aydogdu, T., Sala, D., Malecova, B., Gatto, S., Puri, P. L., et al. (2014). STAT3 signaling controls satellite cell expansion and skeletal muscle repair. *Nature Medicine*, *20*(10), 1182–1186.

Troy, A., Cadwallader, A. B., Fedorov, Y., Tyner, K., Tanaka, K. K., and Olwin, B. B. (2012). Coordination of satellite cell activation and self-renewal by Par-complex-dependent asymmetric activation of p38α/β MAPK. *Cell Stem Cell*, *11*(4), 541–553.

Tsuchida, J., Ueki, S., Saito, Y., and Takagi, J. (1997). Classification of "activation" antibodies against integrin beta1 chain. *FEBS Letters*, *416*(2), 212–216.

Urciuolo, A., Quarta, M., Morbidoni, V., Gattazzo, F., Molon, S., Grumati, P., et al. (2013). Collagen VI regulates satellite cell self-renewal and muscle regeneration. *Nature Communications*, *4*, 1964.

Walker, J. L., and Assoian, R. K. (2005). Integrin-dependent signal transduction regulating cyclin D1 expression and G1 phase cell cycle progression. *Cancer and Metastasis Reviews*, *24*(3), 383–393.

Wang, Y., and Jaenisch, R. (1997). Myogenin can substitute for Myf5 in promoting myogenesis but less efficiently. *Development*, *124*(13), 2507–2513.

Warren, G. L., Hayes, D. A., Lowe, D. A., Williams, J. H., and Armstrong, R. B. (1994). Eccentric contraction-induced injury in normal and hindlimb-suspended mouse soleus and EDL muscles. *Journal of Applied Physiology*, *77*(3), 1421–1430.

Weintraub, H. (1993). The MyoD family and myogenesis: Redundancy, networks, and thresholds. *Cell*, *75*(7), 1241–1244.

Wen, Y., Bi, P., Liu, W., Asakura, A., Keller, C., and Kuang, S. (2012). Constitutive Notch activation upregulates Pax7 and promotes the self-renewal of skeletal muscle satellite cells. *Molecular and Cellular Biology*, *32*(12), 2300–2311.

Whalen, R. G., Harris, J. B., Butler-Browne, G. S., and Sesodia, S. (1990). Expression of myosin isoforms during notexin-induced regeneration of rat soleus muscles. *Developmental Biology*, *141*(1), 24–40.

Wood, L. K., Kayupov, E., Gumucio, J. P., Mendias, C. L., Claflin, D. R., and Brooks, S. V. (2014). Intrinsic stiffness of extracellular matrix increases with age in skeletal muscles of mice. *Journal of Applied Physiology*, *117*(4), 363–369.

Xie, B., Zhao, J., Kitagawa, M., Durbin, J., Madri, J. A., Guan, J. L., and Fu, X. Y. (2001). Focal adhesion kinase activates Stat1 in integrin-mediated cell migration and adhesion. *Journal of Biological Chemistry*, *276*(22), 19512–19523.

Xiong, J.-P., Stehle, T., Zhang, R., Joachimiak, A., Frech, M., Goodman, S. L., and Arnaout, M. A. (2002). Crystal structure of the extracellular segment of integrin alpha Vbeta3 in complex with an Arg-Gly-Asp ligand. *Science*, *296*(5565), 151–155.

Yamada, K. M., and Even-Ram, S. (2002, April). Integrin regulation of growth factor receptors. *Nature Cell Biology*, pp. E75–6.

Yang, J. T., Rando, T. A., Mohler, W. A., Rayburn, H., Blau, H. M., and Hynes, R. O. (1996). Genetic analysis of alpha 4 integrin functions in the development of mouse skeletal muscle. *The Journal of Biophysical and Biochemical Cytology*, *135*(3), 829–835.

Yao, C.-C., Ziober, B. L., Squillace, R. M., and Kramer, R. H. (1996). α7 Integrin Mediates Cell Adhesion and Migration on Specific Laminin Isoforms. *Journal of*

Biological Chemistry, *271*(41), 25598–25603.

Ye, F., Kim, C., and Ginsberg, M. H. (2012). Reconstruction of integrin activation. *Blood*, *119*(1), 26–33.

Yu, J.-G., Carlsson, L., and Thornell, L.-E. (2004). Evidence for myofibril remodeling as opposed to myofibril damage in human muscles with DOMS: an ultrastructural and immunoelectron microscopic study. *Histochemistry and Cell Biology*, *121*(3), 219–227.

Zammit, P. S., Golding, J. P., Nagata, Y., Hudon, V., Partridge, T. A., and Beauchamp, J. R. (2004). Muscle satellite cells adopt divergent fates: a mechanism for self-renewal? *The Journal of Biophysical and Biochemical Cytology*, *166*(3), 347–357.

Zammit, P. S., Partridge, T. A., and Yablonka-Reuveni, Z. (2006). The skeletal muscle satellite cell: the stem cell that came in from the cold. *The Journal of Histochemistry and Cytochemistry : Official Journal of the Histochemistry Society*, *54*(11), 1177–1191.

Zou, L., Cao, S., Kang, N., Huebert, R. C., and Shah, V. H. (2012). Fibronectin induces endothelial cell migration through β1 integrin and Src-dependent phosphorylation of fibroblast growth factor receptor-1 at tyrosines 653/654 and 766. *Journal of Biological Chemistry*, *287*(10), 7190–7202.

CURRICULUM VITALE

MICHELLE E. ROZO, Ph.D.
5/31/1987. Chicago, Illinois.
(814) 880 2119 / michelle.e.rozo@gmail.com

EDUCATION

PH.D. Cell, Molecular, Developmental Biology and Biophysics, Johns Hopkins University. May 2015.

Thesis: *The function of β1-integrin in the adult skeletal muscle stem cell*. Adviser: Dr. Chen-Ming Fan. GPA 3.88/4.0

B.A. in **Biological Sciences,** Minor in Global Health, **Northwestern University.** May 2009. GPA 3.4/4.0

EXPERIENCE

Research Assistant, UPMC Center for Health Security, Baltimore, MD, 9/2014 – Present

- Work focusing on the role of scientists in biosecurity and biodefense, specifically how they can contribute to an effective response against a biological weapon or natural epidemic
- Contributed to projects in multiple health security arenas; exploring appropriate communication of medical countermeasures, creating a synopsis of international biosafety legislation, determining the factors and technological advances contributing to adherence to tuberculosis treatment
- Developed and co-wrote 2 grant proposals; Improving Security through International Biosafety Norms and Evaluating the Effectiveness of the Biosecurity Training Program's Efforts in the BMENA Region
- Editor for the Center's peer-reviewed journal, *Health Security (*formerly *Biosecurity and Bioterrorism)*
- Contributor to the Center's daily newsletter *Health Security Headlines*

Doctoral Student, Carnegie Institute of Embryology, Baltimore, MD, 9/2009 – Present

- One first author publication submitted, one review and one group project published
- Trained two graduate students
- Presented research at group meetings and departmental seminars, ~6 talks/year
- Won an NIH Ruth L. Kirschstein National Research Service Award Grant for Predoctoral Fellows

Independent Researcher, Federation of American Scientists (FAS), Washington, DC, 6/2013-12/2013

- Developed an independent research project in coordination with Dr. Dave Franz and Dr. Charles Ferguson to carry out country-specific case studies of biosecurity engagement programs

- Interviewed over 35 individuals from government agencies (DOS, DOD, USDA, OSTP), their non-governmental partners (AAAS, NAS, CRDF Global and Metabiotia), and international scientists
- Created a Strategic Framework based on these interviews to restructure engagement programs by utilizing qualitative metrics of success in order to prioritize global health security
- Published the results of the project in a FAS Issue Brief in May 2014

Undergraduate Researcher, Biological Sciences, Northwestern University, Evanston, IL, 3/2007 – 6/2009

- Recipient of Northwestern Undergraduate and Weinberg Research Grants, 2007, 2008

Honorary Visiting Fellow, University of Stellenbosch, Stellenbosch, South Africa, spring 2008

- Researched recidivism of tuberculosis patients undergoing the Directly Observed Treatment, Short-course (DOTS) plan
- Presented findings to ~100 Global Health students and faculty upon returning to Northwestern

SCIENTIFIC PUBLICATIONS AND PRESENTATIONS

Rozo, M., Li, L., and CM Fan. Coordination of β1-integrin and FGF Drives Muscle Regeneration During
Aging. Presentation at Gordon Conference for Myogenesis. Myogenesis: Molecular and Cellular Networks; 2015; June 21-26; Lucca, Italy.

Rozo, M. and CM Fan. Coordination of β1-integrin and FGF Drives Muscle Regeneration During
Aging. *Submitted and out for review at Nature Medicine.*

Southard, S., Low, S., **Rozo, M.,** Li, L., Harvey, T., Fan, CM., Lepper, C. 2014 A series of Cre-ERT2 drivers
for manipulation of the skeletal muscle lineage. Genesis. 52(8):759-70.

Fan C-M., **Rozo, M.E.,** Li, L., Lepper, C. 2012. Making skeletal muscle from progenitor and stem cells:
development versus regeneration. Wiley Interdiscip Rev Dev Biol, 1(3):315-327.

OTHER PUBLICATIONS

Rozo, M. and Gigi Kwik Gronvall. 1977 influenza: Biosafety lapse with global consequences or a vaccine trial
gone wrong? *Submitted and out for review at mBio.*

Rozo, M. 2014. Placing global biosecurity engagement programs under the umbrella of global health security.
Federation of American Scientists, Issue Brief.
http://fas.org/wp-content/uploads/2014/05/bio-engagement-final-may-2014.pdf

LEADERSHIP ACTIVITIES

Maryland Therapeutic Riding Center, Crownsville, MD. **Professional Association of Therapeutic Horsemanship (PATH) certified International Riding Instructor**, 9/2012-present

- Develop and teach weekly therapeutic and hippotherapy riding lessons
- Provide support to riders; from age 8-45, with physical or emotional disabilities
- 2011 Annapolis and Anne Arundel County Non-Profit of the Year

Mentoring to Inspire Diversity in Science (MInDS), Johns Hopkins University, **President** (2011-2012),

Treasurer (2010-2011), member (2009-present)

- Led weekly meetings of graduate students to further the group's aims to mentor students within Johns Hopkins as well as within the greater Baltimore community
- Taught monthly science lessons to all 10th grade students, 4-6 classes/visit, at Baltimore Talent Development High School (BTDHS)
- Coordinated meetings between BTDHS teachers and JHU faculty to start annual campus visits (2011-present) designed to encourage the students to apply to college
- Persuaded the Dean of the School of Arts and Sciences and the Dean of the Biology Department to co-fund the outreach in 2010-2011
- Secured the Graduate Community Small Grant: Expanding MInDS in Biology from the Johns Hopkins Urban Health Institute for 2011-2012
- Outstanding Graduate Student Organization Award from the Office of Student Activities 2010-2011

CAMPUS and ACADEMIC ACTIVITIES

Teaching

- DuPont Teaching Award, Johns Hopkins University, 2010-2011
- Graduate Teaching Assistant, *Immunology*, *Biochemistry,* and *General Biology,* 2010-2012
- School and Community Integrated Pest Management Assistant, *BugMobile!*, Pennsylvania State University, 2003-2005, educated the community on proper removal of pests – usually while "wearing" a live Madagascar hissing cockroach

Environmental Concerns Chair, Graduate Representative Organization (GRO), JHU, 2010-2011

- Hosted and planned a variety of "green" events; including, a "Toxic Tour" of Baltimore, a worm composting event, a tree planting party with TreeBaltimore, and a trash cleanup in Wyman Park
- Wrote the Clean Living section in the 2011 issue of the GRO Guide to Living in Baltimore, which is distributed to all incoming graduate students every year

Class Representative, Graduate School Representative Council, 2009-2012

- Responsible for communicating the concerns of CMDB graduate students to program chairs

- Organized the 2010 and 2011 CMDB recruitment programs; coordinated student transport and meals, planned and executed student demonstrations and tours of the facilities, and spoke on the student panel